ABSTRACT

ANYA, ABSEEN RIFA. Application of AIMSUN Micro Simulation Model in Estimating Emissions on Signalized Arterial Corridors. (Under the direction of Dr. Nagui Rouphail).

Tailpipe emissions are affected by several factors including driver behavior, road characteristics and traffic conditions. Microscopic simulation models are able to generate large amounts of synthetic vehicle activity that can be used to estimate emissions on any facility. Vehicles on arterial roads typically accelerate, decelerate and change lanes frequently in response to various traffic control strategies, traffic entering or leaving the facility and the activity of multi-modal traffic. For accurate estimation of the emissions from an arterial facility, it is necessary to ensure that the simulated vehicle activity closely represents field observed vehicle activity. This thesis demonstrates the improvement in emissions estimations on an urban arterial corridor with signalized intersection, by calibrating the internal behavioral model parameters in the AIMSUN micro-simulation program from field observed vehicle activity data at high temporal resolution.

Simulated and field-observed vehicle activity data were characterized by Vehicle Specific Power (VSP), defined as the power per unit mass of vehicle. Emissions were estimated based on the VSP modal emission rates and the time spent by vehicles in each VSP mode. The emissions were compared for routes along an urban arterial and for shorter segments within each route. At both spatial scales, the emissions from calibrated simulation vehicles having the same average number of stops and travel time distribution as field-observed vehicles were closer to real-world emissions than the simulation vehicles under default model parameters. The calibrated simulation model was also able to capture emissions hotspots along the routes more accurately than the model with default parameters.

The calibration process presented in this thesis is supplemental to existing micro-simulation calibration techniques because it focuses specifically on improving vehicle activity for better emissions estimates. Future applications of the AIMSUN model once it is properly calibrated for emissions estimation on arterials, include evaluating the emissions impacts of different traffic management strategies.

Application of AIMSUN Micro Simulation Model in Estimating Emissions on Signalized Arterial Corridors

by
Abseen Rifa Anya

A thesis submitted to the Graduate Faculty of
North Carolina State University
in partial fulfillment of the
requirements for the degree of
Master of Science

Civil Engineering

Raleigh, North Carolina

2013

APPROVED BY:

_____	_____
Dr. Nagui M. Rouphail Committee Chair	Dr. H. Christopher Frey
_____	
Dr. Bastian J. Schroeder	

DEDICATION

To My Parents

BIOGRAPHY

Abseen Anya was born and raised in the busy metropolitan city of Dhaka, Bangladesh. She moved to the United States in 2007 to attend Lafayette College in Easton, PA. She graduated with honors in 2011 receiving a Bachelor of Science degree in Civil Engineering. While working as an undergraduate research scholar at Lafayette College, Anya became interested in research, especially in the areas of sustainability and environmental issues. In 2011 she began her career as a graduate student and research assistant at NC State University. This thesis completes the requirements for her Master of Science degree in Civil Engineering with a concentration in transportation engineering.

ACKNOWLEDGMENTS

The research presented here has been funded by the U.S. Environmental Protection Agency's STAR program through EPA Assistance ID No. RD-3 3 83455001.

I would like to thank Dr. Nagui Rouphail and Dr. H.C. Frey for the opportunity to work on this project and for their guidance throughout my time at NC State University. I would also like to express my gratitude to Dr. Bastian Schroeder for serving on my committee and providing his valuable insight and suggestions.

Many thanks to Dr. Behzad Aghdashi, Dr. Soheil Sajjadi and Briana Phillips for their help and support.

TABLE OF CONTENTS

LIST OF TABLES vii
LIST OF FIGURES ix
Chapter 1 Introduction 1
1.1 Background and Motivation 1
1.2 Problem Statement 3
1.3 Objectives 4
1.4 Scope 5
1.4 Research Contributions 6
1.5 Outline 7
Chapter 2 Literature Review 8
2.1 Integration of Micro-simulation models with emissions modeling 9
2.2 On-board Emissions Measurements using Portable Emissions Measurement System (PEMS) 12
2.3 Vehicle Specific Power based emissions modeling 16
2.4 Calibration of Traffic flow models in Micro-simulation 22
2.5 Summary of Reviewed Literature 25
Chapter 3 Application of Micro-simulation Model 26
3.1 Vehicle Generation in AIMSUN 27
3.2 Internal Behavioral Models 27
3.4 Car Following Model 28
3.5 Selecting Model Parameters for Calibration 31
Chapter 4 AIMSUN Model Development and Field Data Extraction 36
4.1 Study Site 36
4.2 AIMSUN Model 39
4.2.1 Network Geometry 39
4.2.2 Traffic Signal Timing 40
4.2.3 Traffic Demand 40
4.3 Data Extraction from PEMS Field Tests 44
Chapter 5 AIMSUN Parameter Calibration with Field Data 47
5.1 Simulation Parameter Distributions for AIMSUN Model Calibration 47

5.2 Preliminary Assessment of Field-Calibrated Parameters 53
5.3 Detailed AIMSUN Model Calibration with 95th Percentile Parameters 61
5.3.1 Travel-time Based Sampling from Simulation Data 62
5.3.2 Analysis of Vehicle Activity and Emissions of Samples from Simulation 67
5.3.3 Sample Selection Based on Average Number of Complete Stops 91
5.3.4 Controlling for both travel time and avg. no. of stops 98
5.3.5 Summary of Calibration Results 104
5.4 Application of Emissions Estimation Methodology on Eastbound Direction 105
5.4.1 Route level analysis for Eastbound Direction 107
5.4.2 Section level analysis for Eastbound Direction 109
5.4.3 Second-by-second Level Analysis for Eastbound Vehicle Activity 114
5.4.4 Summary of Methodology Application 118
Chapter 6 Conclusions 120
6.1 Major Findings 120
6.2 Recommendations and Future Work 124
Chapter 7 References 127
APPENDICES 133
Appendix A Traffic Demand in the afternoon peak and off peak periods 134
Appendix B Field-tested Vehicles 142
Appendix C Cumulative Probabilities of Field Data and Calibration Parameters 144
Appendix D API Code for extracting second-by-second vehicle activity data 146
Appendix E MS Excel Code to identify total number of stops from second-by-second trajectory data 148
Appendix F Automated Sampling Algorithm 150

LIST OF TABLES

Table 1 Attributes of Data Collection Routes 15
Table 2 Definition of VSP Bins 18
Table 3 Controllable Vehicle Attributes, Local and Global Parameters 32
Table 4 AIMSUN Network Attributes 37
Table 5 Lane Configuration of Intersections on Hillsborough Westbound and Eastbound Routes 39
Table 6 Number of Field Trajectories in the each Direction and Time Period 45
Table 7 KS-Test Results for Parameter Distributions in the Peak and Off-Peak Periods 49
Table 8 Numerical Summary of AIMSUN modeling parameter distributions 52
Table 9 Trajectory Travel Times from Empirical Data and Simulation under Different Parameter Distributions 54
Table 10 Average Vehicle Specific Power (VSP) Modal Emission Factors for 42 Passenger Cars Measured with a Portable Emissions Measurement System (Anya et al., 2013) 55
Table 11 Selected Route-level Emission Rates of CO2 per unit Distance from Empirical Data and Simulation under Different Parameter Distributions 56
Table 12 Selected Route-level Emission Rates of NOx per unit Distance from Empirical Data and Simulation under Different Parameter Distributions 56
Table 13 Number of Seconds of Data to Construct Parameter CDFs 59
Table 14 Sample Sizes for Travel Time Distributions 63
Table 15 Summary of Selected Simulated Samples on Hillsborough Westbound Route 66
Table 16 Route Level Emission Rates per unit Distance from Empirical and Simulated Vehicle Activity Controlled for Travel Time Distribution 71
Table 17 Section Names and Lengths 74
Table 18 Results of the Wilcoxon Rank-Sum Test 81
Table 19 KS-Test Results of Empirical vs. Simulated Speed and Acceleration Distributions on the Hillsborough Westbound Route 90
Table 20 Details of the Sample with Same Average Numbers of Stops as Field Data 94
Table 21 Simulated Route-level Emissions of Samples Controlled for Average Numbers of Stops 96
Table 22 Details of Simulated Sample with Same Average Number of Stops and Travel Time Distribution as Field Sample 98

Table 23 Route-level emissions from simulated sample with same travel time distribution and average number of stops as field data 100
Table 24 Summary route-level emissions on Hillsborough Westbound route from calibration of AIMSUN model and sample selection 105
Table 25 Details of field and simulated-data samples on Hillsborough Eastbound Route 107
Table 26 Route Level Emission Rates per unit Distance from Empirical and Simulated Vehicle Activity on Hillsborough Eastbound Route Based on Samples Controlled for Travel Time Distribution and Average Number of Stops 108
Table 27 Summary of Wilcoxon Rank Sum test for Section Level Emissions Estimates on Hillsborough Eastbound Route 110
Table 28 KS-Test Results of Empirical vs. Simulated Speed and Acceleration Distributions on the Hillsborough Eastbound Route 118

LIST OF FIGURES

Figure 1 Portable Emissions Measurement System (PEMS) Equipment Assembly 14
Figure 2 Data collection routes between NC State University (NCSU), North Raleigh and Research Triangle Park (RTP) 15
Figure 3 Schematic of the Hillsborough Street arterial corridor in AIMSUN 37
Figure 4 Hillsborough Westbound and Eastbound Routes 38
Figure 5 Time table for Wolfline Bus No. 6 in the westbound direction modeled in AIMSUN 43
Figure 6 GPS points on PEMS Routes 45
Figure 7 Field observed vehicle trajectories in the Hillsborough Westbound route during the afternoon off-peak period 46
Figure 8 Truncated normal distributions of AIMSUN modeling parameters 51
Figure 9 VSP Distribution using different simulation parameters for intermediate travel time of 5.72 minutes 57
Figure 10 Relative positions of the range and mean values of empirical maximum, 95th percentile, 85th percentile and AIMSUN default parameter distributions 59
Figure 11 Travel Time Distributions from simulated and empirical trajectories 63
Figure 12 Speed profile of simulated trajectories under calibrated parameters 64
Figure 13 Stratified probability distribution of the field-observed travel times (minutes) 66
Figure 14 VSP Distributions from field data and simulated data under default and calibrated parameters on Hillsborough Westbound Route 68
Figure 15 Cumulative Distribution Functions of VSP from empirical and simulated data 69
Figure 16 Iso-VSP contour plots at 0% road grade 70
Figure 17 Definition of a section 73
Figure 18 Beginning and ending points of 13 sections on Hillsborough Westbound route 74
Figure 19 Average proportions of total emissions released in each section of the Hillsborough Westbound route by simulated and empirical vehicles 76
Figure 20 Speed-acceleration pairs from field data and simulation under Default Parameters with super-imposed iso-VSP lines 83

Figure 21 Speed-acceleration pairs from field data and simulation under Calibrated Parameters with super-imposed iso-VSP lines 84
Figure 22 Positive and negative accelerations from calibrated AIMSUN vehicle activity and field data..... 85
Figure 23 Distribution of empirical and simulated accelerations in 10mph speed bins 88
Figure 24 Distribution of empirical and simulated accelerations in 10mph speed bins 89
Figure 25 Complete stops along a route 93
Figure 26 VSP distributions of travel time and no. of stop controlled simulated samples and field data..... 95
Figure 27 Relationship between average number of stops and average travel time for travel time distribution controlled and average number of stops controlled samples..... 97
Figure 28 VSP distribution of travel time distribution and average number of stops controlled simulated samples and field data 99
Figure 29 Section Level Analysis comparing samples with varying average number of stops to empirical data..... 101
Figure 30 Hillsborough Street corridor and routes 106
Figure 31 VSP Distributions from simulated and field data on Hillsborough Eastbound Route 108
Figure 32 Section-level analysis of emissions on Hillsborough Eastbound Route 111
Figure 33 Distributions of acceleration in 10 mph speed bins for the eastbound vehicle activity from calibration simulation and field data 115
Figure 34 Distributions of acceleration in 10 mph speed bins for the eastbound vehicle activity from calibration simulation and field data 117

Chapter 1 Introduction

1.1 Background and Motivation

The transportation sector is a significant contributor to air quality problems in the United States. Following the Clean Air Act of 1990, the U.S. Environmental Protection Agency (EPA) established the National Ambient Air Quality Standards (NAAQS) for six criteria pollutants, including carbon monoxide (CO), nitrogen dioxide (NO_2) and ozone (US EPA, 2012). In 2012, 61% of the nation's total emissions of carbon monoxide and 35% of total emissions of nitrogen oxides were produced by highway vehicles (US EPA, 2012). Nitrogen oxides are oxidized to nitrogen dioxide in the air, and together with volatile organic compounds (VOC), serve as precursors to ozone. Tropospheric or "ground level" ozone is harmful to the human respiratory system, forms urban smog and has been estimated to reduce $500M in crop yield (US EPA, 2003). Carbon Monoxide (CO) and Carbon Dioxide (CO_2) are produced from combustion of fuel in vehicle engines. CO binds with hemoglobin in in the blood, reduces oxygen in the body and in extreme circumstances causes death. While CO_2 is not directly harmful to human health, it is a greenhouse gas (GHG) that traps heat in the Earth's atmosphere. Given the role of mobile sources in local, regional, national and global air quality, it is imperative that the impacts of vehicle tailpipe emissions on the environment be given sufficient consideration when planning, implementing or evaluating transportation facilities.

Emissions from a vehicle's tailpipe, produced during driving or idling after the engine has warmed up is known as running emissions (US EPA, 1994). The amount of running emissions is affected by several factors, including the size, age, and type of vehicle, driver behavior, characteristics of the road infrastructure and prevailing traffic conditions (Rouphail, 2008). Modern strategies to reduce vehicle emissions cover a wide range of options such as improving traffic operations, reducing traffic congestion and the total number of miles travelled or encouraging smaller and more efficient vehicles with alternative technologies and fueling options (North Carolina State University, 2002). Field tests and computer simulation are both options to assess the effectiveness of such strategies.

Limitations of field tests include the high cost of equipment, time and man power, as well as the inability to directly evaluate alternatives for future projects. Simulation modeling tools can simulate traffic and provide measures of traffic flow and emissions at different levels of spatial and temporal resolution. Microscopic traffic simulation tools provide detailed vehicle trajectories on a road network and are suitable for evaluating local or network-wide improvements in traffic control and management. The marginal cost of repeating simulation runs and setting up different scenarios is low while this is not usually true of field tests.

Detailed vehicle trajectories from a calibrated and validated micro-simulation model can be used as input for microscopic emissions models to estimate emissions at different levels of aggregation. While micro-simulation models can generate large amounts of synthetic vehicle activity for use in fuel use and emissions models, the quality of all subsequent emissions estimates from this data depends largely on how representative the data is of real world vehicle activity at a small temporal and spatial resolution. To ensure the accuracy of simulated data it is typical to use real world data for calibration and validation of the simulated network. The model parameters, including those in the model's driver behavior algorithms, have to be calibrated with values that are appropriate for the facility type and the context or region in which the facility exists or will exist.

Vehicle activity on freeway facilities is very much different from that on arterial roads. Interruptions on arterial road segments such as signalized intersections, affect vehicle activity at the micro-level and aggregate measures of traffic do not fully capture these effects. Simulating second-by-second arterial vehicle activity in a micro-simulation platform allows the transient vehicle operations to be captured and subsequently reflected in the emissions estimates. As opposed to freeways, vehicles on arterial roads accelerate or decelerate and change lanes more frequently in response to various traffic control strategies, traffic entering or leaving the facility and the activity of multi-modal and pedestrian traffic. This is especially apparent when using micro-simulation to model arterial road segments and applying the output to estimate emissions. If the model is not calibrated well, the high natural variation in arterial vehicle activity often leads to overestimating emissions. Calibration methods are needed to minimize the error in emissions estimates on arterial roads. A range of traffic

management strategies, such as signal coordination, can be implemented on arterial corridors to improve traffic flow. Therefore it is important to calibrate simulation models of arterial traffic very well so that the environmental impacts quantified from simulation of different networks and traffic control methods are accurate reflections of what is or can be expected on the field.

1.2 Problem Statement

Based on reviewing previous work on integrating micro-simulation and emissions estimation models, it is hypothesized that the parameters of internal behavioral models within microscopic simulation packages need calibration to better replicate vehicle activity on arterial corridors. Simulated vehicle activity data can be quantified by Vehicle Specific Power (VSP) which is a proxy variable for engine load. VSP-based emissions analysis can be performed easily on simulated vehicle activity. However, simulated vehicles exhibits choppy speed profiles with sharp accelerations and decelerations and an inclination to maximize the time spent cruising with no changes in speed. These differences are more pronounced for arterial road segments than for freeways. Traffic on freeways typically experiences fewer stops, higher speeds and lower accelerations or decelerations when cruising, in contrast to arterial traffic. As a result, the emissions estimated from freeway vehicle activity are close to field-based emissions, while the same has not been observed for arterial traffic (Swidan, 2011).

The inherent differences between real-world driving behavior and the vehicle behavior controlled by strict simulation algorithms lead to differences in VSP distributions and emissions estimates. Therefore the calibration of the internal behavioral parameters can help improving simulated vehicle activity and estimated emissions. The challenges in calibrating the behavioral models in simulation packages for better emissions assessments include the availability of field data. A comprehensive methodology driven by field data is required to calibrate and validate microscopic simulation of traffic so that not only can simulation be used to evaluate existing traffic conditions, but to predict the environmental effectiveness alternative strategies with accuracy.

1.3 Objectives

In recent years, the application of microscopic traffic simulation and emissions modeling tools to study road networks and the impact of traffic on air quality has proliferated. With the increased acceptance and use of the Portable Emissions Measurement System (PEMS), emissions data and vehicle activity data from engine scanners and GPS units accompanying the PEMS unit, are available to analyze measurements under real world conditions. The primary aim of this thesis is to utilize high-resolution empirical vehicle activity collected during PEMS tests to calibrate the driver behavioral models in the AIMSUN micro-simulation software and develop a repeatable methodology to estimate emissions from simulated data with reasonable accuracy. The purpose of developing a methodology that is particularly applicable to arterial traffic is to build a framework for estimating emissions of a wide variety of arterial traffic conditions and management strategies that cannot be empirically tested. The following is a list of specific objectives that will be achieved during the course of the research effort:

- Identify a set of easily controllable parameters in AIMSUN, which can be calibrated to improve second by second vehicle activity and emissions estimates on an interrupted arterial corridor.
- Calibrate parameters in the behavioral sub-models of AIMSUN simulation software using field-collected vehicle activity data on the interrupted arterial corridor
- Demonstrate Vehicle Specific Power (VSP) modal analysis to estimate emissions on the corridor at different spatial scales
- Compare second-by-second speeds and accelerations from the simulation model and field data to explain any trends or unique observations in emissions estimates from the simulation and the field
- Develop and verify a repeatable methodology to compare trajectory-level emissions from simulated data arterial facilities with field-based estimates, such that it can be extended to a framework for evaluating the environmental impacts of different arterial traffic management strategies.

1.4 Scope

In line with the motivation for this research effort, the study is focused on an urban arterial that is interrupted by several signalized intersections. The model will be constructed in AIMSUN with road geometry and traffic conditions as direct input. Empirical vehicle activity data from field tests by NC State University with Portable Emissions Measurement Systems (PEMS) equipped vehicles will be used to calibrate selected model parameters in AIMSUN with respect to reducing differences in emissions between the simulation and field-based estimates. This calibration methodology based on emissions will be supplemental to existing micro-simulation calibration practices. A review of the relevant literature shows that existing calibration procedures do not focus specifically on reducing errors in emissions estimates, but on reducing errors in measures of traffic performance in the field. Existing calibration methodologies are highly relevant to modeling traffic well in the micro-simulation platform and therefore, the calibration procedure developed in this thesis is intended to serve as an addition to existing procedures with a specific application to improving emissions estimates.

The parameters investigated for calibration with field data will be limited to those from the car following model in AIMSUN. The car following model is the main internal behavioral model in AIMSUN that updates the instantaneous speed and acceleration of vehicles. Emissions models based on engine load are highly dependent on instantaneous speeds and accelerations, making the car following model ideal for calibration. Other internal behavioral models such as lane-changing and gap-acceptance are important too in directing vehicle activity in simulation; however, the scope of this research effort is limited to the AIMSUN car following model only. It is worth noting that the parameters in the car following model are shared with a few of the other internal behavioral models in AIMSUN, and calibrating them will have an impact on the other models as well. The impacts on the other models are not explored in this research effort.

Field-based emission factors will be applied to empirical and simulated vehicle activity data to estimate emissions. To identify the context in which vehicle activity and

emission estimates from field data and simulation are comparable, the analysis will be done at three different aggregation levels –

- Route level – average vehicle activity and emissions of vehicles traversing the entire length of the arterial from simulation and field data will be compared
- Section level – average emissions at the each section (mid-block to midblock distances) along the arterial from simulation and field data with will be compared to identify if emissions "hotspots" along a route can be captured in simulation output. A "hotspot" is defined as a local peak in the emissions rate per unit distance relative to upstream and downstream sections.
- Second-by-second level – any variations in second-by-second vehicle activity data between field collected and simulated data will be captured by analysis at this level.

Emission estimates will be completed using the VSP modal approach of North Carolina State University (2002). Second by second emission rates are available from PEMS but will not be used directly for comparison, because typically there is high variation in emissions data collected over short distances. In addition, the available PEMS tests were conducted using both passenger cars and passenger trucks from a range of model years and engine sizes, making it difficult to normalize the emissions data collected directly from all the vehicles.

1.4 Research Contributions

One of the major challenges of research in transportation and air quality is capturing the transient operation of vehicles observed in the real world and reproducing it in computer simulation to estimate emissions. To take advantage of the benefits of simulation tools it is necessary to ensure that the output from simulation is a true reflection of reality. In this thesis, a detailed investigation of micro-scale arterial traffic and emissions rates, on an individual vehicle trajectory basis, is conducted from extensive field data. Based on the field data, a sequence of steps is developed to calibrate the AIMSUN microscopic simulation model of an arterial corridor, such that individual vehicle behavior from simulation is closer to the behavior observed in the field. This calibration process will serve as an addition to existing calibration techniques to help improve simulated activity and the emissions

estimates which depend on the quality of simulated activity. The set of parameter values suggested in this work may be applied to arterial corridors with similar characteristics, or, the method by which field data is used to derive the calibrated parameter values may be utilized in other simulated arterial road networks.

In this research effort, the emissions estimations are based on individual trajectories on a signalized arterial corridor. The impact on emissions estimates of a number of factors that measure traffic flow is investigated in detail. Identification of these factors is an important contribution because future work can focus on improving the calibrated micro-simulation model's ability to reproduce vehicle activity in simulation as measured by these factors. This will set the stage for effectively comparing the environmental impacts of different traffic control strategies on urban arterial segments using a well-calibrated micro-simulation model.

1.5 Outline

The organization of this thesis is as follows: Chapter 2 presents the literature review on the integration of microscopic traffic simulation and emissions models, Vehicle Specific Power (VSP)-based emissions modeling, use of Portable Emissions Measurement Systems (PEMS) and the calibration of traffic flow models in microscopic traffic simulation. Chapter 3 takes an in-depth look at the car-following sub-model in AIMSUN and identifies modeling parameters that will be calibrated using field data. Chapter 4 is a description of the study site and extraction of field data from the PEMS database maintained by NC State University. Chapter 5 outlines the process of calibrating selected simulation modeling parameters and demonstrates the methodology to use simulated trajectories to estimate route-level emissions within a reasonable amount of error. Chapter 6 presents the conclusions based on the findings of the thesis. Chapter 7 is a list of references. Appendices A-E are attached at the end of the document.

Chapter 2 Literature Review

The impacts of the transportation sector on local and regional air quality are significant, and the issue has become a global concern. This has spurred research in the area of transportation and air quality and led to the development of several types of traffic emissions models. Before the1980's emissions modeling was limited to estimating hot running emissions of petrol cars based on certification test data, whereas current models are capable of predicting emissions of a range of pollutants, vehicle types and running modes at various spatial and temporal scales (Smit et al., 2010).

Song et al. (2013) identified three general approaches to today's traffic emission modeling – (1) using aggregate measures of traffic flow models such as average speed, and density in macroscopic traffic models, (2) using slightly more disaggregate measures like average trip speeds and the number of vehicle stops in link-based meso-scopic models, e.g., and (3) using instantaneous vehicle engine, vehicle speed and acceleration data in micro-scopic models. The macroscopic approach typically utilizes average speed or total vehicle miles travelled on a network from transportation planning models such as TRANSPLAN, MINUTP or EMME/2 in the United States and TRIPS or STEMM in Europe (Pronello & André, 2007). The average fuel use and emissions rates are calculated using macroscopic model output in emissions models such as US Federal's MOBILE6 or California's EMFAC in the USA (Yue, 2008) and COPERT II in Europe (Pronello & André, 2007). Macroscopic models cannot capture the transient variation in vehicle emissions under different traffic conditions (Y. Song et al., 2013). In the meso-scopic approach, traffic models such as ITEM, DTA or VT-Meso can generate time dependent link flows and speeds which can serve as input for emissions models. Both the macro-scopic and meso-scopic approaches are applicable to larger traffic networks and are suitable for estimating emissions on a regional scale. The microscopic approach is more suited to operation level analysis where modeling the emissions impacts of individual vehicles, based on instantaneous speed and acceleration levels, is required (Ahn et al., 2002). This approach can be computation-intensive since

traffic microscopic simulation models generate very detailed vehicle activity which can then be coupled with emissions models.

The ability of micro-simulation software to model the activity of individual vehicles in roadway systems in fine detail lends to its extensive application in evaluating traffic operations under various levels of congestions and complex geometries (B. Park & Qi, 2005). It is easy and fast for agencies with access to micro-simulation software to generate high volumes of second-by-second traffic data (Dowling et al., 2004). Collecting the same kind of data in the field can be time-consuming and often infeasible as costs become prohibitive. In addition, micro-simulation models can be used to quantify factors which are be difficult to measure in the field or predict analytically, such as tailpipe emissions, fuel use or toll revenues (B. Park & Qi, 2005).

In a microscopic simulation model, information about each vehicle is updated every second, based on its interaction with other vehicles and the road infrastructure, traffic control and guidance settings. The instantaneous movements of individual vehicles in a road network are governed by microscopic flow theory (Fang, 2010), coded into micro-simulation software in the form of the internal behavioral models for car-following, lane-changing and gap-acceptance. The mathematical algorithms of the internal behavioral models are characterized by several parameters which can be adjusted by the user to reflect the real-world local traffic conditions of each modeled network. During calibration, the changes to model parameters should be based on field data whenever feasible. If it is not possible to collect the required field data or when the necessary guidelines do not exist, best-guessed values may be used to calibrate the traffic simulation model (B. Park & Schneeberger, 2003)

2.1 Integration of Micro-simulation models with emissions modeling

Many micro-scopic traffic simulation models such as NETSIM and INTEGRATION (Ahn, 1998) and AIMSUN (TSS, 2012) have built-in fuel use and emissions estimation models. The working principle behind many of these models is vehicle-acceleration-indexed look up tables, which limit the ability of the models to handle road grades or the vehicle operational history (National Research Council, 2000). Several studies have demonstrated the integration of traffic microscopic simulation models with external emissions models and the

application to evaluating traffic operations. In one study a communication interface between the VISSIM microscopic simulation model and the CMEM modal emissions model was developed to quantify and compare vehicle emissions for two traffic control and management strategies (Kun & Lei, 2007). The VISSIM model was calibrated with road infrastructure data, traffic volumes, signal timing plans and public transport line information.

CMEM (Comprehensive Modal Emissions Model) is a micro-scopic modal emissions model that uses second-by-second vehicle activity data (speeds, accelerations, grades) and vehicle specific parameters (engine displacement, maximum torque etc.) to calculate the vehicle engine demand. It then calculates the instantaneous emissions of HC, CO, NO_x and CO_2 based on the vehicle's operating modes – deceleration, idling, acceleration and cruising (Smit et al., 2010). Kun & Lei (2007) constructed the communication interface between VISSIM and CMEM based on matching vehicle types between the models. The approach was used to show that setting exclusive bus lanes reduced tailpipe emissions of HC, CO and NO_x from buses but increased the emissions of HC and CO for cars and light duty gasoline vehicles. Signal timing optimization improved both traffic operations and emissions.

Stevanovic et al. (2009) sought to integrate VISSIM, CMEM and a stochastic signal optimization tool called VISGAOST were integrated to minimize fuel use and CO_2 emissions on signalized corridors (Stevanovic et al., 2009). In this approach, emissions estimated by CMEM for a particular signal timing plan in VISSIM is fed into VISGAOST and a Genetic Algorithm procedure within VISGAOST is applied to create the optimized signal plan based on results from CMEM. Another study focused on the emissions from a single vehicle and the relationship between emissions and driver aggressiveness (Nam et al., 2003) by coupling VISSIM and CMEM. VISSIM and CMEM were also coupled to observe the changes in short-run emissions and long -run emissions due to induced demand in a network from two traffic-flow improvements (Stathopoulos & Noland, 2003). The traffic flow improvements are a lane addition downstream of a merge between two urban priority arterials and traffic signal coordination along a corridor. The authors found that the traffic flow improvement strategies reduced total emissions in the network, but relatively small increases in demand

after the lane add or signal coordination resulted in emissions quickly returning to the original levels.

VISSIM has been combined with other micro-scopic air pollution models including MODEM and VT Micro. MODEM is a speed-based emissions inventory database (Jost et al., 1992). The database was constructed based on results from chassis dynamometer driving cycle measurements and surveys of operating characteristics of vehicles in an urban environment in Europe. Fuel use and emissions are calculated in MODEM using instantaneous speed and acceleration for different vehicle types. A study conducted in the UK demonstrated the application of VISSIM and MODEM to estimate emissions under different traffic conditions (J. Y. Park et al., 2001). The estimated emissions were found to be similar to the UK's standard macroscopic air pollution model specified in the Department of Transport's Design Manual for Roads and Bridges (DMRB), but in some cases significantly different from measured emissions from roadside pollutant monitors. Ahn et al (2009) studied the emissions impact of a hypothetical change in intersection control by coupling VISSIM with VT Micro and INTEGRATION with CMEM. The simulation models were calibrated with field data and validated with the length of side street queues. Compared to a base case of two-way stop control for a low-speed road intersecting a high-speed road, estimates were made for a replacement signalized intersection and for a roundabout. The results indicated that fuel consumption and emissions increased as a result of either of the replacements, and more so for the roundabout. INTEGRATION and VT-Micro were also used to compare an isolated intersection served by a traffic signal, all-way stop control, two-way stop control and a single-lane roundabout. The intersection was simulated as a simple four-way intersection with single-lane approaches and uniform demand. The roundabout was estimated to have lower emissions of NO_x, HC, CO and CO_2, compared to the other alternatives, under conditions such as low left turns or when demand was 40% to 60% of total demand (Ahn et al., 2009).

A study combining the PARAMICS micro-simulation model with CMEM demonstrated that the Advanced Driver Alert Systems (ADAS) can reduce emissions at signalized intersections (Li et al., 2009) .CMEM and PARAMICS were also coupled to

investigate the impacts on vehicle emissions and air quality from Intelligent Speed Adaptation (ISA) technologies (Servin et al., 2006), High Occupancy Vehicle (HOV) lanes (Boriboonsomsin & Barth, 2008), High Occupancy Toll (HOT) lanes and uphill truck climbing lanes (Barth et al., 2001). The emissions from varying freeway speed limits in Houston, TX were investigated by combining three different emissions models with micro-scale simulation data from TRANSIMS (TRansportation ANalysis SIMulation Systems) – the TRANSIMS emissions module, MOBILE5 and MOBILE5 (Qu et al., 2003). Smit et al. (2010) consider MOBILE to be an "average-speed" model because the inputs for the model are mean travelling speeds and vehicle miles travelled. On the other hand, the TRANSIMS emissions module is based on the CMEM model. The authors found that under congested conditions, the MOBILE suit of models estimate lower emissions than the TRANSIMS emissions module because they are unable to capture the sharp accelerations and decelerations using the average speed approach.

2.2 On-board Emissions Measurements using Portable Emissions Measurement System (PEMS)

Emission factors are the empirical relationships between vehicle activity and the resulting emissions (Franco et al., 2013). Emission factors can be developed from experimental data collected under controlled laboratory conditions or in real-world environments. Several emissions models described earlier, which are integrated with micro-simulation models use emission factors based on data from dynamometer testing in the laboratory. CMEM and MODEM are examples of emissions models which propose emission factors developed from chassis and engine dynamometer testing under controlled conditions. During dynamometer testing, driving cycles are simulated under laboratory conditions to collect instantaneous emissions data. Although this kind of testing is highly standardized and considered to be accurate, the emission factors from on-board measurement data is more representative of actual emissions in the field.

Portable Emissions Measurement Systems (PEMS) are able to capture second-by-second micro-scale emissions under real-world operating conditions (Frey et al., 2006). This

also allows researchers to utilize the data at different levels of aggregation and characterize the variability in emissions on a variety of road types. As part of previous and on-going research projects, NC State University has developed an extensive database of high-resolution vehicle operation and emissions measurements from PEMS equipped vehicles driving on pre-defined test routes between NC State University, North Raleigh and the Research Triangle Park. The research team uses the OEM-2100AX Axion System, which measures tailpipe exhaust concentrations of NO, HC, CO and CO_2 to collect emissions measurements.

The PEMS equipment include a sampling probe that continuously collects tailpipe emissions, a filter bowl to remove water vapor, non-gaseous materials and aerosol droplets and two five-gas analyzers to analyze the emissions. The gas analyzers measure NO (ppm) and O_2 (%) by means of electrochemical sensors and HC (ppm), CO (%) and CO_2 (%) using a non-dispersive infrared (NDIR) optical chamber (Clean Air Technologies International, 2003). Once the sampled tailpipe gas passes through the analyzers, the exhaust and water vapor is removed via exhaust hoses. Along with the PEMS unit, an external engine scanner is used to collect vehicle activity and engine dynamics data from the vehicle's Electronic Controls Unit (ECU) via the vehicle's On-Board Diagnostics (OBD) port. The data includes second by second observations of speed, acceleration, engine RPM, manifold air pressure (MAP) and intake air temperature (IAT). During the PEMS tests, three GPS units are deployed to record the instantaneous positions of the vehicle.

The PEMS equipment, OBD engine scanner and GPS units are easily installed into vehicles as shown in Figure 1. At the start of each testing period, the PEMS unit is calibrated using a calibration gas composed of 0.5% CO, 6% CO_2, 202 ppm HC and 298 ppm NO (Clean Air Technologies International, 2003). To prevent drifting, the PEMS unit is "zeroed" at 15 minute intervals using ambient air which contains negligible levels of NO, HC and CO. The two gas analyzers are never zeroed at the same time, ensuring that no gaps occur in emissions data collection. The computer that is integrated into the PEMS unit provides an interface for users to observe the output from the gas analyzers in real time as well as program the data to be saved to "bags" which can be used to denote a route or a time period.

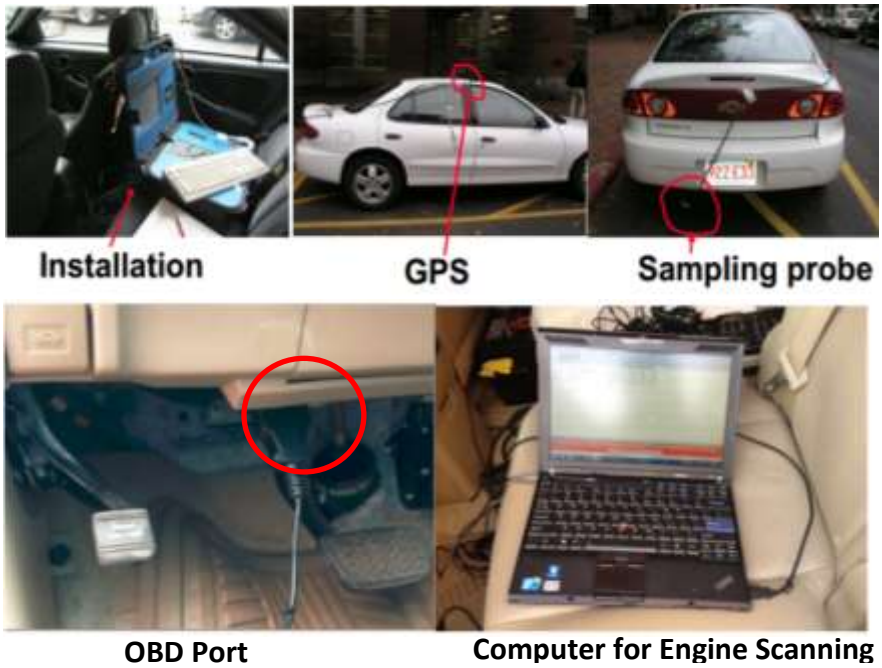

Figure 1 Portable Emissions Measurement System (PEMS) Equipment Assembly

PEMS field tests were conducted by NC State University on a set of test routes between the Research Triangle Park (RTP) and the NC State University Campus in Raleigh, NC. The tests consisted of collecting both instantaneous vehicle activity and tailpipe emissions data. The data were collected repeatedly on two routes between North Raleigh and the RTP and two routes between NCSU and North Raleigh, using light duty gasoline vehicles with a wide range of manufacturers, engine sizes and model years. The routes represent alternative commuting routes between the same origins and destinations, thus covering several facility types including freeways, ramps, local and arterial streets and a range of road grades. Figure 2 shows these routes.

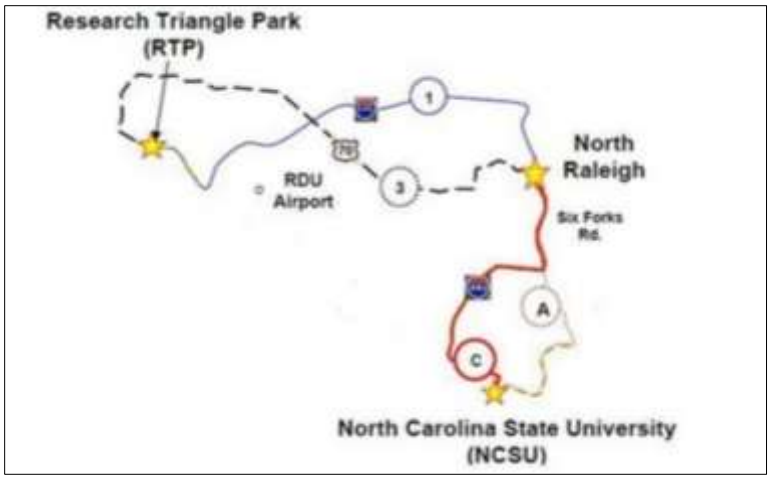

Figure 2 Data collection routes between NC State University (NCSU), North Raleigh and Research Triangle Park (RTP)

During each testing period, a vehicle completed Routes A, C, 1 and 3 by travelling through a total of 36 miles of freeway and 76 miles of arterial streets. The test vehicles encountered different intersection controls along the routes which are summarized in Table 1.

Table 1 Attributes of Data Collection Routes

Routes		Mileage (mi)		Intersection Control (no.)		
No.	Name	Freeway	Arterial	Signal	Stop Sign	Roundabout
1	A In	0	11	43	26	3
2	A Out	0	11	43	26	3
3	C In	5	6	29	16	2
4	C Out	5	6	29	16	2
5	1 In	13	3	4	3	0
6	1 Out	13	3	4	3	0
7	3 In	0	18	26	31	0
8	3 Out	0	18	26	31	0

During each testing period, second-by-second emissions of NO, HC, CO and CO_2 from the tailpipe exhaust are measured and recorded by the PEMS unit. Vehicle activity data are collected via GPS devices recording latitude, longitude and altitude of the test vehicle (Yazdani & Frey, 2012). The On-board Diagnostics (OBD) port in each vehicle acquire the

engine RPM, intake air temperature (IAT), mass air flow (MAF) and second-by-second speed and fuel flow. The internal clocks of each component are independent and need to be synchronized in order to match the data that was collected at the same time. The PEMS, GPS and OBD data were all converted to follow a frequency of 1Hz. Data from a pair of components were then synchronized by means of a "master" parameter and a "slave" parameter, based on the datasets exhibiting correlated trends in their time series (Sandhu, 2010).

After synchronization, the combined datasets are checked for errors. There can be several types of errors in the data, including, but not limited to: unusual engine RPM, engine RPM "freezing" or remaining constant for more than 3 seconds, leakage in and overheating of the gas analyzers, negative emissions values due to random measurement errors, ambient air infiltration into exhaust gas sampling system and loss of power to any component of the PEMS equipment (Sandhu, 2010). Errors in data are identified using quality assurance algorithms in LabView and corrected if possible or removed if the data is found to be invalid.

Once the data from all PEMS equipment are synchronized and quality assured, it is possible to characterize the second-by-second vehicle activity by using Vehicle Specific Power (VSP) and to develop modal emission factors from the instantaneous emissions data. The following section provides examples of integrating micro-simulation models and with VSP-based emissions estimation.

2.3 Vehicle Specific Power based emissions modeling

Jiménez-Palacios (1999) introduced the concept of Vehicle Specific Power (VSP) to develop an instantaneous load-based emissions model. Vehicle Specific Power (VSP) accounts for a vehicle's kinetic energy, rolling resistance, aerodynamic drag and the effects of gravity with road grade. It is a proxy variable quantifying the instantaneous tractive power per unit mass of the vehicle engine. Each value of VSP can be associated with an emission function based on laboratory dynamometer testing or field-based measurements (National Research Council, 2000). Physical power-demand based emissions estimation techniques are able to take into account all factors affecting vehicle operations, including vehicle types,

ages, models, fuel types, road grades etc. Jiménez-Palacios (1999) demonstrated stronger dependence of NO, HC and CO emissions on VSP rather than on parameters such as speed, acceleration, absolute power or fuel rate. The VSP-based approach to emissions modeling is simpler than CMEM (North Carolina State University, 2002). VSP is directly calculated from field-measured parameters for which no assumptions are required, unlike for parameters such as engine speed or fuel rate (Jiménez-Palacios, 1999).

VSP is calculated using second-by-second speed, acceleration and road grade. The relationship in Equation 1 can be used to estimate VSP for light-duty gasoline vehicles (North Carolina State University, 2002).

$$\boldsymbol{VSP = v\,(1.1a + 9.81\,(sin(tan^{-1}(r))) + 0.132) + \ 3.02 * 10^{-4}v^3}$$

$VSP = Vehicle\ Specific\ Power\ (kW/ton)$

$v = velocity\ (m/s)$

$a = acceleration\ (m/s^2)$

$r = road\ grade$

Validation studies by North Carolina State University (2002) showed that it is feasible to group instantaneous VSP into a discrete number of bins called “modes”. The number of bins was selected based on the objective of characterizing the variability in emissions from vehicle activity. Therefore, each of the 14 proposed bins are such that the average emission rate associated with the bin is statistically significantly different from any other bin and no one bin explains more than 10% of total emissions. Table 2 shows the VSP ranges within each of the 14 bins as proposed by North Carolina State University (2002).

Table 2 Definition of VSP Bins

VSP Mode	VSP Range (kW/ton)
1	Below -2
2	-2 – 0
3	0 – 1
4	1 – 4
5	4 – 7
6	7 – 10
7	10 – 13
8	13 – 16
9	16 – 19
10	19 – 23
11	23 – 28
12	28 – 33
13	33 – 39
14	Over 39

US EPA's MOVES (MOtor Vehicle Emissions Simulator) emissions model also uses VSP to determine the amount of time a vehicle spends in each of its 23 operating mode bins. Operating modes are categories that differentiate emissions and are based on combinations of speed and VSP (Koupal et al., 2005). In one study, the emissions on one-way and two-way streets in the peak and off-peak periods were compared using traffic data generated by VISSIM micro-simulation software in the US EPA's MOVES model (Wang et al., 2013).The detailed outputs of instantaneous speed and accelerations from VISSIM were used to calculate instantaneous values of Vehicle Specific Power (VSP). Vehicle emissions were estimated from the distribution of VSP in 23 operating modes. The results indicated that two-way streets produce higher total emissions than one-way streets, especially under peak hour traffic conditions. PARAMICS micro-simulation model was integrated with both CMEM and MOVES emissions models to investigate alternative intersection designs – a 3 legged intersection with pre-timed signal control and a single lane roundabout under light and heavy traffic (Chamberlin et al., 2011).The study showed that both models estimated higher emissions with the roundabout installed under light and heavy traffic. CMEM and MOVES were found to produce similar estimates for NO_x emissions but widely different estimates for

CO because MOVES used a detailed modeling approach with second-by-second speed profiles of vehicles while an average speed based approach was used in CMEM.

One study demonstrated the integration of VSP-based emissions modeling approach with micro-scale vehicle activity from VISSIM to evaluate the environmental performance of coordinated and non-coordinated signalized corridors in Beijing, China (Y. Zhang et al., 2009). It was found that that optimizing signal timing on a coordinated corridor and controlling traffic demand significantly reduces vehicle emissions. The VSP modal emissions analysis was also applied to quantify emissions at single-lane roundabouts in Raleigh, NC and Lisbon, Portugal by means of a hybrid approach based on field data for vehicle activity and an existing emissions model (Coelho et al., 2006). Empirical data showed that vehicles at a roundabout follow one of three possible trajectories: (1) a vehicle travels through the roundabout by slowing down in response to the geometrics without stopping fully; (2) the vehicle comes to a full stop at the entry line of an approach to negotiate a gap in the circulating traffic, accelerate to the circulation speed before eventually accelerating back to original speed; and (3) the vehicle enters a queue and experiences stop-and-go motion until passing the yield line. Complete speed profiles for each possible trajectory through the roundabout were developed using the modeling approach of North Carolina State University (2002) to obtain VSP values. VSP modal emission factors in g/s were then used to estimate emissions per vehicle, which, coupled with the proportion of vehicles following each of the three speed profiles and the approach entry flow rate, was used to determine total hourly emissions at the roundabout.

Use of VSP in estimating emissions was also demonstrated by Swidan (2011) in a study of a regional road network in North Carolina created using the AIMSUN micro-simulation system. This study used the modal emission factors estimated from data collected on the same road network using Portable Emissions Measurement System (PEMS) with the VSP distributions from AIMSUN-simulated data. The study found that for freeway segments of the routes, the total empirical emissions and emissions calculated from the modal model were within ± 10% of each other. The arterial sections did not share the same trend because of greater differences in VSP distributions between simulation and real world data. Swidan

(2011) recommended that for evaluating emissions on arterial segments using the VSP modal approach, the internal behavioral model parameters in AIMSUN should be calibrated appropriately to generate vehicle activity that is more representative of the real world.

Traffic on arterial roads experience larger and more frequent speed fluctuations in comparison to freeway traffic. The highest fuel consumption on arterials is associated with driving in congested traffic, characterized by higher speed fluctuations and frequent stops at intersections (Stevanovic et al., 2009).However, low traffic and continuous progression along streets do not guarantee the lowest fuel consumption and emissions. Stevanovic et al. (2009) suggested that the best flow of traffic on arterial streets in terms of fuel consumption and emissions is the one with the fewest stops, shortest delays, and moderate speeds maintained throughout the commute. To investigate the emissions on existing arterial roads and study the effects of improvements to traffic flow using micro-simulation models, it is necessary to ensure that the simulated traffic on arterial traffic accurately represents what is or can be expected to in the real world. In a study that linked the output from macro-scopic transportation models to the microscopic VSP-based emissions modeling approach, it was shown that arterial speed profiles can be grouped together with respect to the average link speed. Average emission rates increased with average speed for arterials (Zhai, 2007)

A recent study investigated the amount of error in emissions estimates using VSP distributions of vehicle activity data from VISSIM and the sensitivity of VSP distributions to modeling parameters (G. Song et al., 2012). It was observed that second-by-second empirical vehicle activity data and simulated vehicle activity data from a calibrated and validated VISSIM model did not yield the same VSP distributions. The parameters had been calibrated using GPS data and Remote Traffic Microwave Sensors (RTMS) data from freeways or expressways with flat terrain in Beijing and included: (1) Desired Speed distribution, (2) Desired Acceleration Distribution, (3) Maximum Acceleration, (4) Desired Deceleration Distribution, (5) Maximum Deceleration, (6) Maximum Deceleration for Co-operative Braking (7) Safety Distance Reduction Factor and (8) Maximum Look Ahead Distance. The differences between the simulated time-varying speeds and the RTMS-collected field speeds were less 15%, while the differences between traffic flow measures were less than 10%. The

validation was done using the link average speed and flow. Emission rates per unit distance were calculated using MOVES emission factors and the VSP distributions for the simulated activity. The simulated vehicle activity produced high errors, especially for NO_x emissions. Simulation model overestimated emissions for low speed conditions by up to 248% and underestimated emissions for high speed conditions by up to 16%. It was found that these errors were systematic errors in the traffic simulation models because they remained statistically the same when a sensitivity analysis was performed on 8 parameters by increasing and decreasing their values by 10%.

It has been demonstrated that calibrating the distributions of acceleration, deceleration and speed of buses in AIMSUN micro-simulation model affect the emissions estimates from the vehicle activity (J. Zhang et al., 2012). Second-by-second bus performance data was collected automatically by the iBus system in London and used to modify input distributions of the relevant parameters pertaining to the motion of simulated buses. Emissions were estimated using the emissions model developed by Panis et al (2006), which is already embedded in AIMSUN. Emission functions which differ by vehicle, fuel and pollutant types are used to modify the emissions calculated at each simulation step using the same formula for all pollutants (Panis et al., 2006). The study showed that under the calibrated parameters, the buses produced significantly more emissions under heavy traffic flow conditions due to more stop-and-go cycles than under the default parameters. The emissions were less sensitive however, under low flow conditions.

The VSP modal approach was also used to compare numerically simulated data from five car following models - optimal velocity model (OVM), generalized force model (GFM), full velocity difference model (FVDM), Weidemann and Fritzsche models (G. Song et al., 2013). It was observed that the Fritzsche produced more realistic VSP distributions than the other models. VSP distributions from the Weidemann model showed larger differences with the field observed VSP distributions at higher speed and overestimated emission. The FVDM model gave the lowest RMSE when the acceleration distributions were compared between simulated and field data. However, RMSE increased as speeds increased to more than 40 km/h. The Fritzsche model had slightly higher RMSE than the FVDM model. The study

found that speed-specific VSP distributions were highly correlated to the acceleration distribution and therefore, improving the acceleration distribution for certain speed bins is a promising method of improving calibration of car following models for estimating emissions using the VSP modal approach. Popular micro-simulation models, PARAMICS and VISSIM are based on the Fritzsche and Wiedemann models respectively. However, the exact differences between the models that are published in literature and the simulation models are not in the public domain (Olstam & Tapani, 2004).

2.4 Calibration of Traffic flow models in Micro-simulation

Calibration methods have been developed through both trial and error based on engineering judgment and through systematic approaches using modern optimization tools. Literature shows that calibration of micro-simulation models often involve calibrating demand between origins and destinations, route choice models (Chu et al., 2003; Toledo et al., 2004) or the network capacity (Dowling et al., 2004). However, calibration approaches also include calibrating parameters that control simulated driver behavior. Emissions are sensitive to individual vehicle trajectories and as such, this section presents literature concerning the calibration of behavioral parameters that affect the second-by-second vehicle activity within the micro-simulation platform.

Several studies have proposed methods to calibrate sub-models governing traffic flow in micro-simulation software using field data. A technique was developed to calibrate 5 common microscopic traffic flow models using GPS data collected on a one lane approach to a signalized intersection (Brockfeld et al., 2003). The optimal parameter settings for each model were found by optimizing the error function between field-observed and simulated travel times using linear programming. The optimized parameters included maximum velocity, accelerations, decelerations and other unique parameters that control random braking behavior and time delays in driver reaction. The study found that the models were not able to replicate the field-observed data very well and only on a few segments of the simulated road were the travel time errors within 10%. In another study, the methodology was presented to calibrate the parameters of four common car following models – (1) the

simple Newell model (2) the safety-distance based Gipps model, (3) intelligent driver model (IDM) and (4) a stimulus-response based MISTSIM model (Punzo & Simonelli, 2005). The parameters of each model were calibrated using GPS data from four vehicles travelling in a platoon on urban and suburban roads in Italy. Three measures of performance (speed, time headway and inter-vehicle spacing) were used to compare simulation output and field observations. Statistical error tests performed between the simulated and field-observed measures of performance included room mean square (RMSe), root mean square percentage error (RMSPe) and Theil's inequality coefficient.

Link speed has also been chosen as the measure of performance that is matched between simulated and observed data during the calibration of a signalized arterial in PARAMICS (Wee et al., 2002). In this study, the key parameters selected for calibration were based on their role in the car-following and constrained linear motion models in PARAMICS, since these models govern the vehicle speeds. The chosen set of parameters to be calibrated included: (1) link speed limit (2) maximum acceleration rate (3) mean target headway (4) mean reaction time and (5) minimum gap. Along with simulated speed trajectories, empirical trajectories were collected by GPS units. Both synthetic and empirical trajectories were divided into 10m segments and the average absolute error between them was minimized to identify the best set of parameter values. The paper presented a recommended set of values for the calibration parameters and established a repeatable methodology for other networks were empirical speed data may be useful in calibrating a microscopic simulation model. In a study of a freeway in the San Francisco Bay Area, the mean target headway and mean reaction time parameters were calibrated in the PARAMICS micro-simulator (Gardes et al., 2002). The network average speed and maximum vehicle throughput were calculated to identify the best values for the calibration parameters. In another PARAMICS model of the Port Area Network in downtown Toronto, Canada, relevant parameters governing vehicle movement were calibrated using a Genetic Algorithm based parameter optimization program called GENOSIM (Ma & Abdulhai, 2002). The optimization tool helped to identify the parameter values for which the absolute error in percentage between field-observed data and simulation model output is a minimum.

Traffic flow on an expressway in China was modeled on VISSIM and several parameters that affect vehicle behavior were selected for calibration, based on the context and practical experience (Zhizhou et al., 2005). The parameters, which included desired speed in reduced speed area, desired lane-change distance, Wiedemann car-following parameters, the average desired distance between stopped cars, the headway time and safety distance, were optimized using Genetic Algorithm. Calibrating the parameters reduced the absolute differences and RMSe between measured and simulated speeds. The study highlighted that the drivers in Shanghai were more aggressive in car following and lane changing activities than what the default parameter values in VISSIM were modeling. B. Park et al., 2006 also found that default parameter values of VISSIM and CORSIM models did not replicate field-observed travel times which were the chosen measure of effectiveness for an arterial corridor with 12 coordinated actuated traffic signals. 14 calibration parameters with different values were evaluated in 200 parameter sets for each of the two simulation models using Genetic Algorithm. The models were validated using the calibrated parameters and queue lengths as the measure of effectiveness (B. Park et al., 2006).

The studies presented in this section cover a range of simulation parameters and calibration techniques and there is scope for developing general calibration principles based on the collective experience (Hollander & Liu, 2008).Since the amount of field data required to calibrate many simulation parameters can become prohibitive, there exists a trade-off between increasing the number of parameters for a better model and keeping the number of parameters manageable. To narrow down the list of potential parameters, Hollander & Liu (2008) recommend neglecting parameters which are easy to measure (e.g. length of vehicle), already available in literature that apply to the particular model being calibrated, or which are deemed to have negligible effects based on multiple runs of the simulation model over a range of parameter values and those irrelevant to the particular model. Dowling et al. (2004) state that model parameters should be selected if their values are not certain and available data can support their adjustment based on analysis. The parameters that affect the simulation on a global basis should be calibrated first and local parameters used for fine tuning the model.

Calibration of micro-simulation is often done with an optimization technique used to identify the best set of parameters. Two common optimization techniques are the Simplex Method and Genetic Algorithms. Manual methods for finding the feasible combination of parameter are also found in literature, and are appropriate for cases where the automated procedure may not be sensitive enough to the parameters or when the simulation model has limited applicability. Several goodness of fit measures have been used in literature to compare observed data to simulated data during the calibration process and according to Hollander & Liu (2008), should be chosen based on the individual simulation network and model. Once a model is calibrated, it needs to be validated with a new set of input data to confirm its predictive power. The authors stress using data from multiple runs of the simulation model and suggest examining the variation in the simulation output in addition to assessing the mean values of traffic measures.

2.5 Summary of Reviewed Literature

The existing literature show that various micro-simulation models have been used in conjunction with emissions models to estimate the environmental impacts of traffic through different types of facilities and traffic management strategies. Load-based emissions models such as the VSP modal approach provide a platform to directly link vehicle operating modes and the resulting tailpipe emissions. It is essential to calibrate micro-simulation models and ensure that the simulated vehicle activity is an accurate reflection of what takes place in the real world. Several calibration methodologies are available using a variety of simulation parameters and measures of effectiveness. Driver behavior models within micro-simulation software impact the individual vehicle trajectories and should be calibrated with local field data when available. The reviewed literature does not show any consistent methodology to calibrate the behavioral parameters in micro-simulation based on improving emissions estimates. Most of the studies integrating micro-scopic simulation models with emissions modeling apply the simulated activity from models already calibrated based on traffic flow parameters, to an emissions model.

Chapter 3 Application of Micro-simulation Model

In recent years, microscopic traffic simulation has become a widely used tool for modeling traffic on a variety of transportation facilities. There are a variety of micro-scopic simulation models available for use, several of which have been highlighted in Chapter 2. AIMSUN (Advanced Interactive Microscopic Simulation for Urban and Non-Urban Networks) is the core simulation module in the GETRAM (Generic Environment for Traffic Analysis and Modeling) package developed by Transportation Systems Solution (TSS) in Barcelona, Spain. The AIMSUN software can be used to model a road network without a limit on the network size, although simulation speed can be constrained by the memory of the machine on which the program is run. A variety of transportation system characteristics and traffic conditions can be modeled in AIMSUN including, incidents, public transportation lines and common ITS technologies (Cheu et al., 2003). AIMSUN user manual provides detailed review of the internal behavioral models that allow the simulation software to replicate the movement of individual vehicles in the network. Tools such as PARAMICS and VISSIM are developed from behavioral models found in literature; however, the exact models in the simulation packages are not disclosed to the public.

One of the primary steps in using traffic micro-simulation tools such as AIMSUN to simulate road networks is model calibration, i.e. the identification of model parameters and the definition of a range of values for controllable parameters (B. Park & Schneeberger, 2003) The FHWA recommends selecting few parameters for calibration and running the simulation repeatedly to narrow down to the best values for a set of selected parameters. AIMSUN is known to have the smallest number of modeling parameters when compared to popular micro-simulation tools such as VISSIM, PARAMICS and MITSIM (Olstam & Tapani, 2004). In this section, the relevant internal behavioral models of AIMSUN micro-simulation software are studied to identify the range of controllable model parameters for an arterial traffic simulation.

3.1 Vehicle Generation in AIMSUN

Vehicles in AIMSUN are generated at headway values sampled from a user-defined distribution. The default headway model is a negative exponential distribution (TSS, 2012). Each vehicle that is able to enter the network has a specific set of attributes assigned to it, which plays a role in the vehicle's second-by-second activity while it remains in the network, e.g. maximum desired speed. It is possible to assign specific attributes to individual links or sections within the road network, e.g. section speed limits. When a vehicle enters the section, its behavior is constrained by these local parameters. Global parameters, which are separately defined from vehicle or local parameters control the behavior of vehicles everywhere in the road network, e.g. driver reaction time. At every simulation step, the position and speed of every vehicle are updated according to the internal behavioral models of AIMSUN which are characterized by multiple vehicle parameters and local and global parameters. New vehicles are generated in the system only after the statuses of vehicles already in the network are updated during each simulation step (TSS, 2012).

3.2 Internal Behavioral Models

Several sub-models make up the behavioral core models in AIMSUN. Brief descriptions of the functions of each model are presented below:

i. Car-following model – This algorithm serves to estimate a vehicle's speed at each time step based on the performance constraints of the vehicle and/or its driver and the behavior of the preceding vehicle.

ii. Lane-changing model – This algorithm models the decision process by which the necessity, desirability and feasibility of a vehicle to change lanes are determined and the vehicle behavior is adjusted accordingly.

iii. Gap accepting model for lane changing – This model evaluates if a gap is acceptable for a lane change, based on cooperation of the upstream vehicles and calculated values for gap, speeds and the deceleration required to complete the maneuver.

iv. Gap acceptance model for give-way behavior at stops – The decision to allow a lower priority vehicle to cross a stop-controlled intersection is modeled by this algorithm, based on position and speeds of higher priority vehicle and level of risk of each driver.

v. Overtaking maneuver – This algorithm models the decision to change to a faster lane based on the speed and position of the preceding vehicle or to a slower lane based on the driver characteristics.

vi. On-ramp model – This is an extension of the lane changing model with local parameters to distinguish ramps and the need for vehicles to merge into the main traffic stream on a freeway.

vii. Off-ramp model - Similar to the on-ramp model, this algorithm is an application of the lane changing model to allow a vehicle exiting the freeway to diverge from the main traffic stream.

viii. Look-ahead model – This model is applied to avoid situations in which a vehicle is unable to complete a desired turning movement due to not reaching the correct lane in time and is lost from the network when the simulation is run with route-based demand.

In AIMSUN, the position and speed of every vehicle in the network is updated after checking for lane-changing decisions and applying the car-following model (TSS, 2012). The Gipps lane-changing process is used in conjunction with the Gipps car-following model which places limits on the driver's braking ability to maintain a safe distance with the preceding vehicle (Gipps, 1986). The car following model is thus highly relevant to investigating individual vehicle activity along busy urban arterials with signalized intersections. In line with the scope and objectives of this thesis, a detailed look is taken at the car-following model in the next section.

3.4 Car Following Model

As noted earlier, multiple traffic simulation software produced by different agencies are available in today's market to simulate the detailed traffic activity at a microscopic level.

As a result, there is variation in the algorithms used to control individual vehicle behavior across the different software packages. The general intent of car following models is to govern the behavior of a vehicle with respect to the behavior of the preceding vehicle or the "leader" vehicle (May, 1990). The leader is considered to be traveling freely, without any other vehicles affecting its behavior while trying to reach its maximum desired speed. Car-following models can be split into classes based on their differing logic (Olstam & Tapani, 2004).

The most common car-following models can be classified under the Gazis-Herman-Rothery (GHR) family, which are often considered to be "the general car-following models". These models set the acceleration of a follower vehicle to be proportional to its speed, the speed difference between itself and the leader and the space headway. Simulation packages such as MITSIM are embedded with GHR car-following models (Olstam & Tapani, 2004)

Another type of car-following model known as psycho-physical models are able to extend the GHR models with thresholds for driver behavior in order to control how a driver reacts to when the thresholds are reached. Examples of psycho-physical models include VISSIM car-following model and the Fritzsche model utilized in the acceleration algorithm in PARAMICS. A third category of car following models, called safety distance or collision avoidance models, allow vehicles to maintain their desired speeds by accelerating as needed and decelerating to avoid collisions with the lead vehicle (J. Zhang et al., 2012). The car following-model in AIMSUN is a safety distance model developed from the empirical Gipps car following model (TSS, 2012).

A follower is either free or constrained by the leader. The Gipps car following model has two components the first of which controls the acceleration of the follower vehicle when it is not affected by the leader vehicle such as under free-flow conditions. The follower accelerates at an increasing rate with the engine torque, but as the vehicle approaches the maximum desired speed, its acceleration decreases to zero (Olstam & Tapani, 2004).Given these constraints, the following relationship determines the speed of a vehicle as it accelerates during its reaction time (TSS, 2012):

$$V_a(n, t+T) = V(n,t) + 2.5a(n)T\left(1 - \frac{V(n,t)}{V^*(n)}\right)\sqrt{0.0025 + \frac{V(n,t)}{V^*(n)}}$$

Where:
$T = reaction\ time$
$V(n,t) = speed\ of\ vehicle\ n\ at\ time\ t$
$a(n) = maximum\ desired\ acceleration\ of\ vehicle\ n$
$V^*(n) = maximum\ desired\ speed\ of\ vehicle\ n\ on\ a\ section$

NOTE: On a section i or a turning s with speed limit $S_{limit}(s)$ and maximum desired speed $v_{max}(i)$, $V^*(n) = \min\{s_{limit}(i,s), v_{max}(i)\}$.
The speed limit can be set directly by the user for each section, along with a speed acceptance factor $\theta(i)$, such that $s_{limit}(i,s) = S_{limit}(s) * \theta(i)$

The second component of the Gipps model as it appears in the AIMSUN car following logic sets constraints on the speed of a vehicle at time (t+T) by considering the effect of its leader, which becomes important in congested situations where headways are small. The speed that the vehicle can reach at time (t+T) will depend on being able to maintain a safe distance from the lead vehicle in order to avoid collision. This speed is calculated by the following relationship (TSS, 2012):

$$V_b(n, t+T) = d(n)T + \sqrt{d(n)^2\,T^2 - d(n)[2\{x(n-1,t) - s(n-1) - x(n,t)\} - V(n,t)T - \frac{V(n-1,t)^2}{d^*(n-1)}}$$

Where
$d(n) = maximum\ desired\ deceleration\ (d(n) < 0)$
$x(n-1,t) = position\ of\ leader\ vehicle\ (n-1)\ at\ time\ t$
$x(n,t) = position\ of vehicle\ n\ at\ time\ t$
$s(n-1) = effective\ length\ of\ leader\ vehicle\ (n-1)$
$d^*(n-1) = estimation\ of\ the\ desired\ deceleration\ of\ leader\ vehicle\ (n-1)$

Note: The accuracy of $d^*(n-1)$can be controlled by used by means of a global modeling variable known as Sensitivity Factor (a)

As noted earlier, in free flow conditions, the first constraint is likely to prevail while in more congested conditions, the second constraint is more like to prevail. The speed at time (t+T) is therefore determined as:

$$V(n, t+T) = \min\{V_a(n, t+T), V_b(n, t+T)$$

In newer versions of AIMSUN (since v. 6.0), a third constraint is applied to the follower vehicle's speed at time (t+T) such that a minimum headway ($MinHW$) is maintained between itself and the leader. This research was conducted using AIMSUN 7.0. The following relationship presents the constraint on minimum headway:

If $[x(n-1, t+T) - s(n-1)] - [x(n,t) + V(n, t+T)T] < v(n, t+T) * MinHW(n)$

Then, $V(n, t+T) = \frac{[x(n-1,t+T)-s(n-1)]-x(n,t)}{MinHW(n)+T}$

The position of the follower vehicle is updated at time (t+T) with the speed calculated above according to:

$$x(n, t+T) = x(n,t) + V(n, t+T)T$$

3.5 Selecting Model Parameters for Calibration

Table 1 lists a full set of controllable vehicle, local and global modeling parameters and the respective behavioral models and metrics that they affect. Where applicable, the default values for the parameters in AIMSUN are also presented in the table for reference.

Table 3 Controllable Vehicle Attributes, Local and Global Parameters

	Attribute	Values	Influences	Current/Default Value	Unit
Vehicle Attributes	Name	Character string	No influence	-	-
	Length	Mean, deviation, minimum and maximum	Influences effective vehicle length in car following	4, 0.5, 3.40, 4.60	m
	Width	”	No influence	2, 0, 2, 2	m
	Max. Desired Speed	”	Car-following, lane changing, travel time, queue discharge	110, 10, 80, 150	km/h
				68.4, 6.2, 49.7, 93.2	*mph*
	Max. Acceleration	”	Car following, lane changing, travel time, queue discharge	3, 0.2, 2.60, 3.40	m/s^2
				6.71, 0.45, 5.82, 7.61	*mph/s*
	Normal Deceleration	”	Car following, lane changing, travel time, queue discharge	4, 0.25, 3.50, 4.50	m/s^2
				8.95, 0.56, 7.83, 10.1	*mph/s*
	Maximum Deceleration	”	Lane changing, travel time, queue discharge	6, 0.5, 5, 7	m/s^2
				13.4, 1.12, 11.2, 15.7	*mph/s*
	Speed Acceptance	”	Car following, travel time, queue discharge	1.1, 0.1, 0.9, 1.3	-
	Minimum dist. between stopped vehicles	”	Influences effective vehicle length in car following, capacity, queue length	1, 0.3, 0.5, 1.5	m
	Max. give-way time	”	Lane changing, gap acceptance	10, 2.5, 5, 15	s
	Sensitivity Factor	”	Deceleration component of car following; <1 means follower is more aggressive	1, 0, 1, 1	
	Minimum Headway	”	Car following model v.6	0, 0, 0, 0	s
	Overtaking to stay on fast lane	”	Lane changing, overtaking	0	%
	Undertaking cases	”	Lane changing, overtaking	0	%
	Imprudent lane changing cases	”	Lane changing, overtaking	0	%
	Sensitivity for Imprudent lane change	”	Lane changing, overtaking	1	-

Table 3 Continued from previous page

Local Parameters (arterial sections)	Section speed limit	Single value	Car following, lane-changing	57	km/h
				35	mph
	Lane speed limit	”	Car following, travel times	-	km/h
	Turning speed	”	Car following, Influences turning capacity, travel times	-	km/h
	Visibility distance at Junctions	”	Give way	25	m
	Yellow Box Speed	”	Speed of a vehicle approaching a yellow box junction will depend on whether leader vehicle is below this speed; junction capacity	10	km/h
				6.2	mph
	Distance Zone 1 (distance to zone where overtaking can occur)	”	Lane Changing model, turning proportions, blocking situations	388.89	m
	Distance Zone 2 (distance to zone where vehicles look for a gap to closer to the correct side of the road from which the turning movement can be completed.)	”		58.33	m
	Time Distance On-ramp	”	On-ramp model, on-ramp capacity	97.22	m
	Section slope	”	Acceleration in car-following model	0	
	Maximum Give Way Time Variability	”	Gap acceptance/give way	0	s
	Reaction Time Variation	Absolute integer	Local variation of reaction times	0	s

Table 3 Continued from previous page

Global Parameters	No. of vehicles	Single value	2-lane car following model	4	veh
	Maximum Distance ahead	”	2-lane car following model	100	m
	Maximum Speed Difference	”	2-lane car following model	50	km/h
	Maximum Speed Difference On-ramp	”	2-lane car following model	70	km/h
	Percent overtake	”	lane-changing model	90	%
	Distance zone variability	”	lane-changing model	40	%
	Percent recover	”	lane-changing model	95	%
	Road side of vehicle movement	”	lane-changing model	left	
	Simulation step	Single value between 0.1 and 1.5 seconds	Updating of unconditional events scheduling list (e.g. signal phases)	1.00	s
	Reaction Time	Single value (can be "fixed" if equal to simulation time step or "variable" for a vehicle type using a discrete probability model)	All internal models, section and on-ramp capacities	1.00	s
	Reaction Time at Stop	Single value - fixed or variable	Affects all internal models, stop and go capacity, queue measures	1.35	s
	Reaction time for front vehicle at traffic light	”	Affects all internal models	1.35	s
	Queue up speed	Single value	Queue measures	1.00	m/s
	Queue leaving speed	”	Queue measures	4.00	m/s

The global, local and vehicle parameters listed in Table 1 appear in several sub-models in the AIMSUN micro-simulation platform and produce the vehicle activity observed in the simulation. In particular, the parameters of the Car Following Model govern the second-by-second speed and position of each vehicle in the simulation and have a significant impact on individual vehicle behavior at the micro-scale. As such, of the controllable parameters in the AIMSUN micro-simulation environment, the following were chosen for the calibration procedure:

1. Maximum desired speed
2. Maximum desired acceleration
3. Normal deceleration
4. Section speed limit

These parameters influence the AIMSUN car following and lane changing models as well as the travel time and queue discharge behavior in the network. Although other parameters such as the "Speed Acceptance" or the "Minimum Distance between Vehicles" which affect the car following algorithm could be calibrated for the simulated model output to be closer to real world activity, it is anticipated that the data required for the process is beyond the scope of this research. As such, the parameters are limited to those listed above and are calibrated using data collected on a busy urban arterial network in Raleigh, NC. The remaining parameters are left with AIMSUN default values. The next chapter investigates the data available to calibrate the selected parameters.

Chapter 4 AIMSUN Model Development and Field Data Extraction

This chapter presents the details of the study area and how it was modeled in AIMSUN microscopic simulation software. The main inputs for the model were the road geometry, signal timing information and traffic demand on the arterial. The simulation model is able to generate and record detailed trajectories of vehicles in the study site. Second-by-second field-observed vehicle activity data were also available from the extensive PEMS database maintained by NC State University. The description of field data collection and quality assurance procedures for the PEMS database are presented in Chapter 2. This chapter outlines the steps taken to extract individual vehicle trajectories from the PEMS database. The individual field-collected vehicle trajectories on the arterial studied in the thesis will be used for AIMSUN model calibration and field-based emissions estimation.

4.1 Study Site

The study site is approximately a 2 mile-long stretch of an arterial corridor called Hillsborough Street, in the City of Raleigh in North Carolina. Hillsborough Street runs in both east- and westbound directions between downtown Raleigh and the Interstate 40 and serves 15,000 vehicles per day (North Carolina Department of Transportation, 2012). The extent of the corridor analyzed in this research effort begins in the area adjacent to NC State University's main campus and continues to the west until the on- and off-ramps for the I-440.

While Hillsborough Street carries commuter traffic to and from the downtown area to the interstate, it also serves local traffic generated by the university campus, supporting commercial establishments and residential neighborhoods in the area. There are 14 coordinated signalized intersections in the study site, with several of the intersections being concentrated in the eastern end of the corridor in the study site, which is adjacent to the university campus with inter-signal distances ranging from 270 to 1,825 feet. The selected site is appropriate for the evaluating emissions on signalized facilities since it is an urban arterial interrupted by signalized intersections. A schematic of the corridor in the AIMSUN simulation platform is shown in Figure 3. The network attributes are presented in Table 4 and are discussed in detail in the Section 4.2.

Figure 3 Schematic of the Hillsborough Street arterial corridor in AIMSUN

Table 4 AIMSUN Network Attributes

No. of Junctions (Signalized intersections)	15
Arterial Road Speed Limit	45 mph
Simulation advance step	1.00 second
Number of Vehicle types	Car, Bus
Signal Control Plan	Coordinated
Time Periods Modeled	Afternoon peak (5-6pm) Afternoon off-peak (1-3.30pm)

The through traffic on Hillsborough Street corridor is served by single lane towards the eastern end of the corridor, and by dual lanes in the western end of the corridor. The significance of the number of through lanes in the corridor lies in that the AIMSUN lane changing model may be applied to through vehicles in these sections. In the westbound direction, Hillsborough Street is a single lane arterial starting from the beginning of the study site, just before the intersection of Enterprise Street, until the intersection of Faircloth Street. After Faircloth Street there are two through lanes of traffic until the On-ramp to I-440 East.

Going eastbound, there are two through lanes on Hillsborough Street until the intersection with Faircloth Street where the number of through lanes drops by one from

Faircloth Street to Dixie Trail. There are 2 through lanes between Dixie Trail and Dan Allen Drive. Just after Dan Allen Drive, the rightmost through lane becomes a right turn lane. Hillsborough Street remains one lane until the end of the corridor in the study site.

Two routes were defined in the study site for the analysis in this thesis – (1) Hillsborough Westbound and (2) Hillsborough Eastbound. The Hillsborough Westbound route began just before the intersection with Enterprise Street and continued until the beginning of the on-ramp to I440 East. The Hillsborough Westbound route began just after the off-ramp from I-440 and ended just past the intersection with Enterprise Street. Each route is shown in Figure 4.

Figure 4 Hillsborough Westbound and Eastbound Routes

The lengths of the westbound and eastbound routes were 1.82miles and 2.01 miles respectively. There are 13 intersections within the lengths of both routes. The lane configuration of the westbound and eastbound approaches at each intersection is summarized in Table 5 for reference.

Table 5 Lane Configuration of Intersections on Hillsborough Westbound and Eastbound Routes

Intersection	Westbound Approach	Eastbound Approach
Beryl Rd.	1L, 2T	1T, 1TR
Meredith St.	1L, 1T, 1TR	1L, 1T, 1TR
Faircloth St.	1L, 1T, 1TR	1L, 1T, 1TR
Shepherd Ave.	1LT, 1TR	1LTR
Dixie Tr.	1L, 1T, 1TR	1LT, 1TR
Dan Allen Dr.	2T, 1L	2T, 1R, 1TWLTL
Brooks Ave.	1L, 1T, 1TR	1T, 1R, 1TWLTL
Gardner St.	1TR	1L, 1T
Pogue St.	1TR	1L, 1T
Horne St.	1T	1TR
Chamberlain St.	1TR	1T (signal for crosswalk)
Logan Ct.	1TR	1L, 1T
Enterprise St.	1TR	1L, 1T

4.2 AIMSUN Model

The stretch of Hillsborough Street with side streets and intersections controlled by traffic signals were modeled in the AIMSUN micro-simulation environment. The network was populated with traffic count data made available by the City of Raleigh, the North Carolina Department of Transportation (NCDOT) and the Triangle Transit Authority (TTA). The following sections outline the main steps taken to replicate the study site in AIMSUN.

4.2.1 Network Geometry

The physical road network was replicated by use of sections and nodes in AIMSUN. Sections were joined together to form the street segments between nodes serving as the intersections. Imagery from Google Earth was used to draw the sections with appropriate lengths and correct number of lanes. Various geometric details such as lane-drops, lane-adds and reserved bus lanes were entered with reference to the imagery in Google Earth from the year 2012.

Sections were joined according to the turning movements at each intersection to form nodes or junctions. Google Earth's aerial views of the intersections along the arterial and the intersections signal plans provided by the City of Raleigh were used to check that the

sections had been connected properly so as to allow all necessary turning movements to occur. All sections in this model were assigned a road type "arterial" with a speed limit of 45 mph (72 km/h).

4.2.2 Traffic Signal Timing

AIMSUN facilitates different types of traffic control including traffic signals and give-way signs. The intersections along Hillsborough Street are controlled by traffic signals. The signal control plans for each of the 14 intersections in the study area were provided by the City of Raleigh and entered into AIMSUN. All signals in the study area operate within a coordinated system with a common cycle length of 100 seconds. The signal control plans also provided the size and location of detectors at the approaches of each intersection, which were entered in the AIMSUN network accordingly and assigned to the appropriate movements.

At each node in the AIMSUN network, signal groups were created as sets of turning movements that follow the same indications of traffic lights. The signal control plans from the City of Raleigh were used to assign signal groups to the phases within the cycle length at each intersection. The signal control in AIMSUN follows NEMA (National Electrical Manufacturers Association) standards. The phasing information entered into AIMSUN from the control plans included the maximum and minimum green times, yellow and red times, passage times and offsets. For the coordinated phases, a "Coordinated Recall" setting was assigned. The signal control at each intersection was checked by simulating different volumes of traffic on the main and side streets and visually ensuring the vehicles cleared each intersection as expected.

4.2.3 Traffic Demand

Traffic demand data may be loaded onto a network in AIMSUN in two ways – (1) by means of an Origin/Destination (O/D) Matrix and (2) by entering traffic flows and turning percentages. The route-based demand model requires defining origin and destination centroids. Vehicles travel on paths between the centroids based on either the probability of

taking that path or on the AIMSUN-defined "best path". This methodology was not chosen for loading demand into the network because of two main reasons. Firstly, only a single arterial corridor with side streets is modeled in AIMSUN, rather than the detailed road network around the study site for which O/D matrices would be more appropriate. Secondly, demand loading through O/D matrices would require validating the AIMSUN assigned link volumes with reference to actual traffic counts. This is a time consuming task that is not directly in line with the objectives of this research initiative. However, populating the network by entering traffic flows and turning percentages is a simpler and easier approach to populating the simulation network.

Turning movement counts at intersections along Hillsborough Street were available from the City of Raleigh and NCDOT. These counts were completed between 2010 and 2012 in the morning, lunch and afternoon peak hours. Since more PEMS field tests were conducted between 1.30pm and 8pm, the counts completed in the afternoon peak period (5pm to 6pm) were used to populate the arterial road in AIMSUN. The volumes along the arterial were balanced and the turning percentages at each intersection derived using balanced volumes. The entering flows and turning percentages for the selected vehicle type "car" was considered as the "PM Peak Traffic State". No field collected traffic counts were available for the off-peak hours during the afternoon. As such, the afternoon peak hour traffic volumes were adjusted by factors of 0.74 and 0.83 to derive entering flows in the off-peak hours of the afternoon in the east and westbound directions. These factors were estimated from the Trans CAD-based Triangle Regional Model v.5. The demand in the afternoon off-peak period (1:00-3.30pm) was derived from the peak period counts and the ratio of peak and off-peak volumes from the 2010 Triangle Regional Model v.05.

Appendix A contains the inputs for defining traffic states in the afternoon peak and off-peak periods in AIMSUN.

The traffic on Hillsborough Street includes both private vehicles as well as public transport. Due to the proximity of the arterial to NC State University's main campus, there are several bus routes along Hillsborough Street for university-run and city-run buses. Buses stop in both the east- and westbound directions of the street at bus bays or normal stops on

the side of the road. Information about the exact locations of bus stops, reserved lanes and bus schedules in the afternoon period was gathered from the NC State University Transportation Department, City of Raleigh and Triangle Transit Authority (TTA).

Although buses adhere to set schedules with respect to major stops, there were little data available regarding the times at which buses made stops at all intermediate stops. Dwell times were used to solve this problem. The dwell time refers to the time during which a bus stops to drop off and/or pick up passengers or waits to depart from the stop to maintain the route schedule. The agencies provided data regarding the dwell times for all stops by trip time on the relevant bus routes averaged over weekdays in the month of October 2012. This month was chosen to represent the most "average" values of trip travel times and dwell times on all buses routes since it lies in the middle of the fall semester in the university calendar with no university-wide holidays. The average dwell times varied by trip time and as a result, distributions of dwell times at each stop on the bus route were derived for the peak and off-peak periods. In AIMSUN, the bus timetables were emulated by setting the departures of the buses from the start of the routes to be at intervals, with dwell times at each stop following distributions characterized by a mean and standard deviation value from the data provided. For each trip, the dwell time for a bus at the stops are sampled from the distributions.

In the study area, there are 7 Wolfline bus lines operated by the NC State University Transportation Department, 2 Capital Area Transit (CAT) bus lines operated by the City of Raleigh and 4 regional bus lines operated by the TTA. Figure 5 shows a sample visual of time table of the Wolfline Bus No. 6 operating in the westbound direction on the arterial in AIMSUN during the afternoon peak period from 5pm to 6pm. It appears that the No. 6 buses arrived at each stop every 15 minutes, and waited for longer periods of time at the "Brooks Stop" than at the other stops.

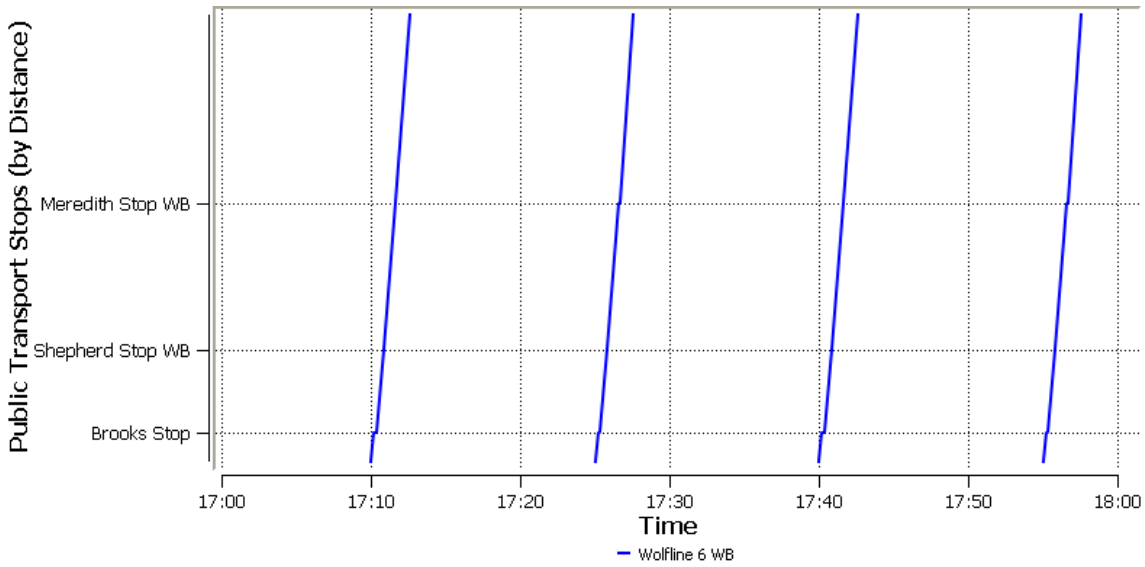

Figure 5 Time table for Wolfline Bus No. 6 in the westbound direction modeled in AIMSUN

The PM Off-peak and PM Peak traffic states were loaded on to the AIMSUN network and assigned different control plans. In the off-peak period between 1 pm and 3.30 pm, the common cycle length was reduced to 95 seconds and the signal phasing was slightly altered according to the information collected from the City of Raleigh. The slight differences in the schedules of some bus routes in the study area during the PM off-peak and peak hours were taken into account when running the simulation with PM Peak and Off-peak traffic states.

Once the AIMSUN model of Hillsborough Street was constructed, populated and checked for any connectivity problems, replications of the simulation could be run under the default vehicle attributes to generate vehicle trajectories on the Hillsborough Westbound and Eastbound routes. Field-observed vehicle trajectories on the same routes were also available from the PEMS database maintained by NC State University. However, the PEMS vehicle activity contains detailed speed traces from several freeway segments and arterial segments besides Hillsborough Street. The field-observed vehicle trajectories in the study site were extracted from the PEMS database using GPS data through a time consuming and labor-intensive process. The following section describes the methodology followed to extract field-observed vehicle trajectories.

4.3 Data Extraction from PEMS Field Tests

The research team at NC State University maintains an extensive database of high-resolution vehicle activity and emissions data collected over several years using vehicles equipped with Portable Emissions Measurement Systems (PEMS). The details of data collection routes and the quality assurance steps are described in Chapter 2. In this thesis, second-by-second vehicle activity and location data of 53 PEMS-equipped vehicles were extracted from the database for the Hillsborough Street corridor modeled in AIMSUN. The vehicle activity included second-by-second observations of speed and acceleration and was used to calibrate the simulation parameters identified in Chapter 3.

The vehicles which were tested between 2010 and 2012 were used in the analysis for this research effort. All vehicles were either passenger cars or passenger trucks and each vehicle was driven by a different driver. The vehicle model years range from 1997 to 2013. The ages of the vehicles ranged from 0 to 14 years at the time of testing. The engine displacements of the vehicle are between 1.4L to 5.4L. The gross weight of the vehicles ranged from 1,720lbs to 7,400lbs. The mileage accumulated by the vehicles was between 615 miles and 282,206 miles. Details of all 53 vehicles can be found in Appendix B.

The activity data in the NC State database were collected directly from each test vehicle's On-board Diagnostics port. The data from GPS units deployed during testing also captured second-by-second speed and acceleration data. However, due to the inherent errors in data from GPS units (Duran & Earleywine, 2012) and the sensitivity of the VSP modal emissions approach to accurate speed and accelerations, only the OBD data were used to define model parameter distributions in the thesis. Therefore there was a need to match the vehicle activity data from the engine scanner with location data from the GPS unit in order to extract the trajectories in the study site.

For each vehicle, the set of GPS points on all routes travelled between NC State University, North Raleigh and the Research Triangle Park were loaded onto Google Earth. Figure 6 shows a sample of GPS data along all the routes in Google Earth. The route is made up of track points, an example of which shown as a blue arrow in Figure 6.

Figure 6 GPS points on PEMS Routes

The latitude and longitude of track points at the beginning and end of the Hillsborough Westbound and Eastbound routes from each vehicle were identified from Google Earth and matched with the same latitude and longitude pairs corresponding to second-by-second speed and acceleration data in the time synchronized and quality assured data files for that vehicle. The time stamps were used to uniquely identify the data that was collected between the beginning and ending pair of track points for each route. These data points made up the eastbound and westbound trajectories in the respective directions. A total of 86 trajectories were extracted from both the Hillsborough Westbound and Eastbound routes from the GPS and OBD data of the 53 vehicles in Appendix B. Due to the nature of the traffic near the NC State University campus where the two routes pass through, the afternoon peak hour was defined as 4.30 – 6 pm and the off peak periods were defined to be between 1 – 4.30pm and 6 – 8.30pm. Table 6 lists the number of field-observed trajectories extracted from the PEMS database in each direction and each time period.

Table 6 Number of Field Trajectories in the each Direction and Time Period

	Time Period	
Route	Afternoon peak	Afternoon off-peak
Hillsborough Westbound	9	20
Hillsborough Eastbound	14	43
Total	23	63

The field trajectories in the Hillsborough Westbound direction in the afternoon off-peak hour are plotted in Figure 7 to show the variation of speed over distance. It is clear from the trajectories that the speeds in the eastern part of the corridor are lower (< 35mph) than on the western end of the corridor (> 35mph). The trajectories in the afternoon off peak hour are shown here since these trajectories are likely to experience less congestion and more free flow conditions on the arterial than trajectories in the peak hour. The 45 mph speed limit placed throughout the arterial in the AIMSUN model is justified as follows. Although the city speed limit is 35mph, the empirical trajectories show that speeds begin to go over the city wide speed limit as early as Brooks Ave. Therefore it seems that the geometry of the road is the constraining factor for the observed lower speeds at the eastern end of the arterial where the intersections are closely spaced. Since in the simulation, second by second speeds are constrained by either the maximum desired speed of the vehicle or the speed limit, putting a speed limit constraint on some sections of the arterial to be below 45 mph may put artificial restrictions on AIMSUN vehicles that field vehicles do not necessarily have i.e. field vehicles can go over the speed limit but AIMSUN vehicles cannot.

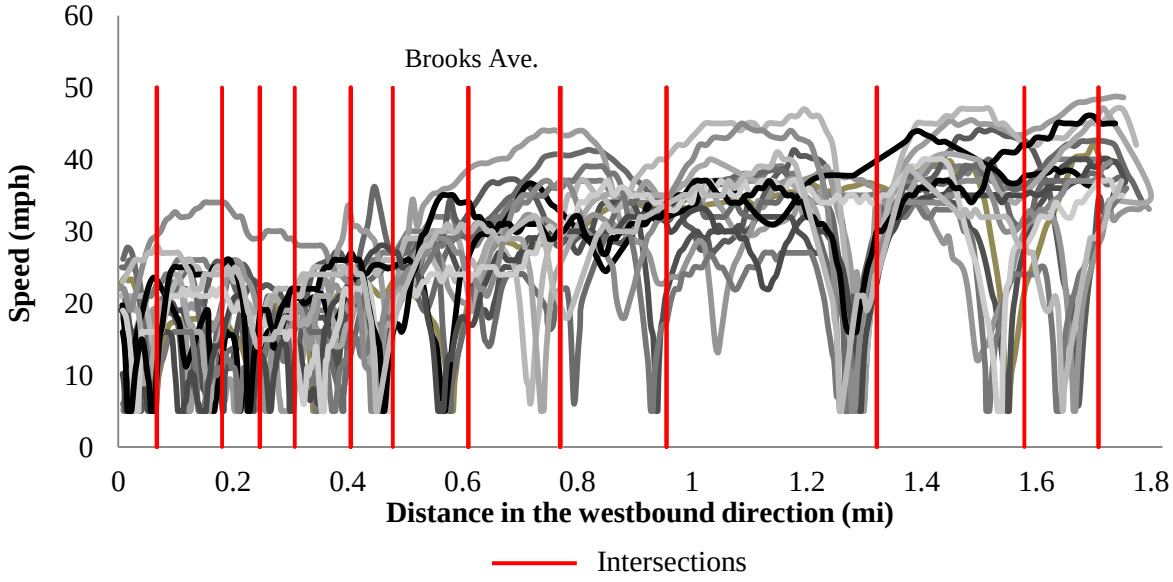

Figure 7 Field observed vehicle trajectories in the Hillsborough Westbound route during the afternoon off-peak period

Chapter 5 AIMSUN Parameter Calibration with Field Data

This chapter describes the calibration of selected parameters in behavioral models using field trajectories on an urban arterial corridor in Raleigh, NC. The effect of calibrating the parameters is demonstrated by comparing the resulting emissions from simulated vehicles on the arterial to emissions from vehicle activity in the field at different spatial scales.

5.1 Simulation Parameter Distributions for AIMSUN Model Calibration

The data collected during PEMS field tests contain second-by-second vehicle speeds, accelerations, decelerations and positions of the vehicle along the tested routes. In order to select the set of values to calibrate each relevant parameter with vehicle activity data, east- and westbound empirical trajectories in the study area were extracted with reference to the vehicle's position data as described in Chapter 4. Measurements from each trajectory were then investigated for parameter calibration in AIMSUN. The following parameters were selected for calibration in Chapter 3:

1. Maximum Desired Speed
2. Maximum Desired Acceleration
3. Normal Deceleration

The fourth calibration parameter identified in Chapter 3, was the "section speed limit". Since this value was set to be the same for all sections and for all simulations of the Hillsborough Street corridor, it is not listed above. The maximum desired speed refers to the maximum speed a vehicle can travel at any point along the network. Similarly, the maximum desired acceleration is the maximum acceleration vehicles achieve on the network under any circumstances. The normal deceleration is the maximum deceleration that a vehicle can achieve under normal circumstances (TSS, 2012). It is different from maximum deceleration, which occurs under special circumstances when severe braking is required. All three parameters follow a truncated normal distribution, defined using the mean, standard deviation, maximum and minimum values for a vehicle type. The values for each parameter are sampled from the distribution for each vehicle that enters the network.

Three sets of values for each parameter were developed from the vehicle activity data collected during PEMS tests along both directions on Hillsborough Street. The following sets of values of each parameter were obtained from each trajectory in the study area:

1. Maximum values – the maximum instantaneous speeds, accelerations and decelerations from each directional vehicle trajectory were identified from PEMS field tests data and the distributions of the maximum values were created. The mean and standard deviation, maximum and minimum values were used to define the truncated normal distribution of each parameter.
2. 95^{th} percentile values – the 95^{th} percentile instantaneous accelerations and decelerations from each directional vehicle trajectory were found and the distributions of 95^{th} percentile values were constructed for each parameter. The mean, standard deviation, maximum and minimum values were used to define the normal truncated distributions of each parameter.
3. 85^{th} percentile values – similar to the previous set of values, the 85^{th} percentile accelerations and decelerations were obtained from individual directional trajectories in the study area. The mean, standard deviation, maximum and minimum of these 86 values were used to define the truncated normal distributions of the three parameters. No distributions of 95^{th} and 85^{th} percentile maximum desired speeds were defined.

It was assumed that the maximum speeds from empirical data sufficiently represent the maximum speeds desired by drivers on the arterial under normal circumstances, while maximum accelerations or decelerations may include events under non-normal circumstances.

As described in Chapter 4, there are a total of 23 directional field trajectories in the afternoon peak hour and 63 directional field trajectories in the afternoon off-peak hour on Hillsborough Street. The second by second speed, acceleration and decelerations were extracted from each trajectory. The maximum, 95^{th} and 85^{th} percentile values of acceleration and deceleration and maximum value of speed were found from each trajectory, resulting in a total of 86 observations of each parameter and measurement value (maximum, 95^{th} or 85^{th} percentile) combination. The observations were separated by the peak or off-peak period in

which the respective trajectories occurred. Kolmogorov-Smirnov (KS) tests were performed on the distribution of observations of each parameter in the afternoon peak and off-peak periods and the results showed no statistically significant differences between the two time periods. The results of the KS-test are shown in Table 7.

Table 7 KS-Test Results for Parameter Distributions in the Peak and Off-Peak Periods

Parameter Values		P-value of KS-Test (H_0: distributions come from the same population)	Hypothesis based on 95% significance level
PM Peak	PM Off Peak		
Max. Acceleration	Max. Acceleration	0.5858	Fail to Reject H_0
Max. Deceleration	Max. Deceleration	0.999	Fail to Reject H_0
Max. Speed	Max Speed	0.2099	Fail to Reject H_0
85^{th} %ile Acceleration	85^{th} %ile Acceleration	0.0836	Fail to Reject H_0
95^{th} %ile Acceleration	95^{th} %ile Acceleration	0.4666	Fail to Reject H_0
85^{th} %ile Deceleration	85^{th} %ile Deceleration	0.9793	Fail to Reject H_0
95^{th} %ile Deceleration	95^{th} %ile Deceleration	0.9996	Fail to Reject H_0

No significant differences were found in the distributions of speeds and accelerations in the east- and westbound directions and in the afternoon peak and off-peak periods. As a result, observations of all 86 trajectories were combined to generate distributions of each parameter value. The same driver did not drive all the PEMS test vehicles and therefore it is assumed that the PEMS vehicle activity database captures a wide range of driver behavior that is representative of the real-world.

The truncated normal distributions of the maximum, 95^{th} percentile and 85^{th} percentile values of the relevant parameters from empirical data are shown in Figure 8 in comparison to the AIMSUN default distribution. The truncation was done at observed maximum and minimum values in each set of values for the parameters. Each distribution of maximum, 95th and 85th percentile acceleration, deceleration and speed was generated from

86 data points, e.g. single observations of the maximum speed were made from 86 trajectories to result in the maximum speed distribution shown in Figure 8 (c).

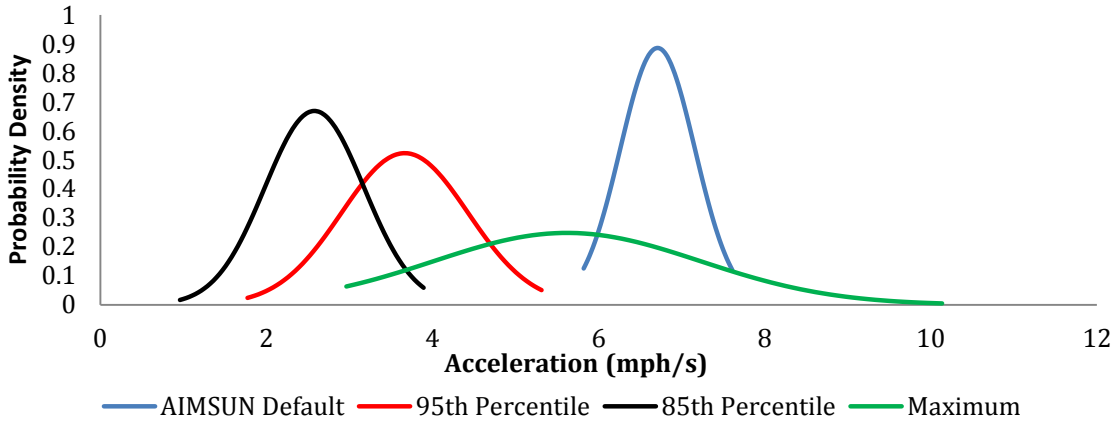

(a) Maximum desired acceleration distribution in mph/s

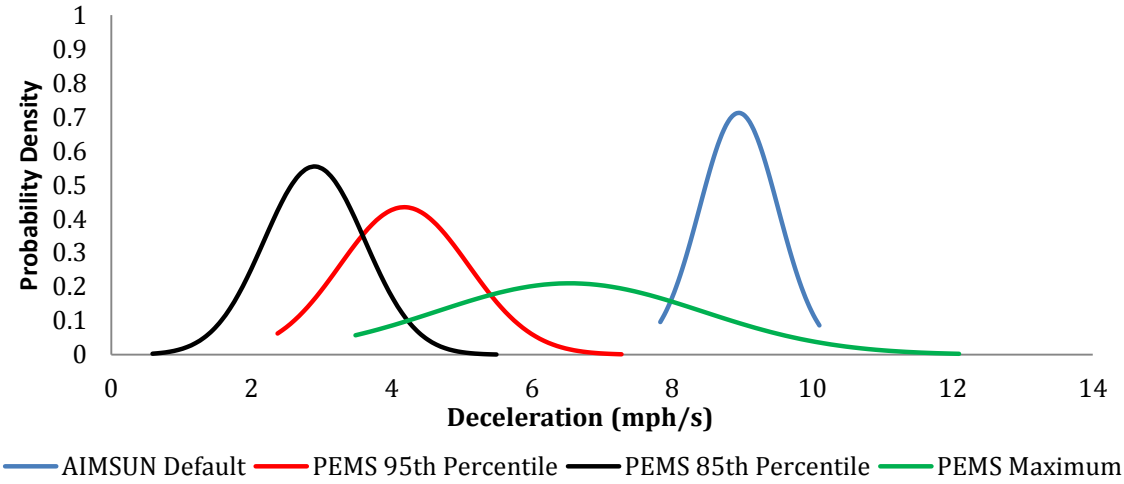

(b) Normal deceleration distribution in mph/s

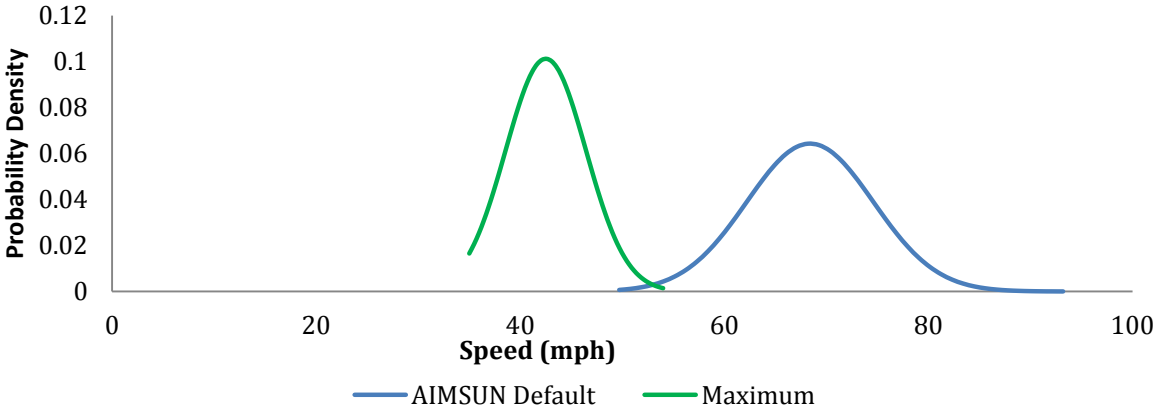

(c) Maximum desired speed distribution in mph

Figure 8 Truncated normal distributions of AIMSUN default modeling and field measured parameters

For all parameters, the AIMSUN default values are higher than the 95th percentile or 85th percentile values. The PEMS maximum distribution is much flatter, indicating more variation. The lowest values are for the PEMS 85th percentile parameter distributions while in comparison, the distribution for the PEMS 95th percentile values is shifted to the right and has a smaller peak and slightly larger variation. Both the peaks of the PEMS 95th and 85th percentile distributions occur far left of the AIMSUN default parameter distribution indicating under default parameters, simulated vehicles can be expected to experience high accelerations to high speeds and high decelerations when slowing down. The default parameters may be more suitable to driving behavior on freeways rather than arterials. Table 8 contains the numerical summary of the distributions.

Table 8 Numerical Summary of AIMSUN modeling parameter distributions

		Distribution Characteristics			
Parameter	**Value**	**Maximum**	**Minimum**	**Mean**	**Std. Dev.**
Max. Desired Speed (mph)	*AIMSUN Default*	*93.2*	*49.7*	*68.4*	*6.20*
	PEMS Maximum	54.0	35.0	42.5	3.94
Max. Desired Acceleration (mph/s)	*AIMSUN Default*	*7.61*	*5.82*	*6.71*	*0.45*
	PEMS Maximum	10.1	2.96	5.62	1.61
	PEMS 95th Percentile	5.31	1.77	3.67	0.76
	PEMS 85th Percentile	3.89	0.96	2.58	0.60
Normal Deceleration (mph/s)	*AIMSUN Default*	*10.1*	*7.83*	*8.95*	*0.56*
	PEMS Maximum	12.1	3.48	6.54	1.90
	PEMS 95th Percentile	7.28	2.37	4.18	0.92
	PEMS 85th Percentile	5.49	0.59	2.90	0.72

Statistical tests of normality showed that the data for each combination of parameter and measurement value were well-modeled by a normal distribution. Appendix C shows the cumulative probability distributions of all second-by-second field observed accelerations, decelerations and speeds used to define the truncated normal distributions of modeling parameters in AIMSUN in Table 8. Figure C1 – C3 show that overall, the truncated normal distributions of parameters represent the distributions of the actual field observations fairly well. Figures C1 shows that the 95th accelerations are modeled fairly well by the truncated normal distributions in AIMSUN – more so than the PEMS 85th percentile or the PEMS

maximum distributions. A similar observation can be made for decelerations in Figure C2. In Figure C3, the distribution of PEMS maximum speeds are modeled well by the truncated normal distribution in AIMSUN. More detailed comparison of field data and parameter distributions are found in Section 5.2

5.2 Preliminary Assessment of Field-Calibrated Parameters

It was hypothesized that the PEMS maximum distributions of acceleration and deceleration may not allow the AIMSUN micro-simulator to closely represent vehicle activity on the arterial. This is because the maximum instantaneous acceleration or deceleration values from the individual empirical trajectories may have occurred during special circumstances such as an emergency stop or due to unique driver behavior given the closely spaced intersections along the arterial. On the other hand, the 85^{th} percentile accelerations and decelerations may be too low for a distribution of the maximum desired acceleration and normal decelerations.

As an initial assessment of calibration parameters, the AIMSUN network was calibrated with the PEMS maximum, 95^{th} and 85^{th} percentile accelerations and decelerations. The speed distribution was developed from PEMS maximum values and kept the same across all simulation runs. The network was loaded with the PM Peak Traffic State and simulated for one hour. Second-by-second vehicle trajectories were extracted from AIMSUN using Application Programming Interface (API) tool which allows customized programs to be written using Python or C++. The API code used by Swidan (2011) was modified to record multiple simulation replications during running the simulation replications in batches and capture observations of vehicle activity on all sections and junctions in the study routes. The API code is provided for reference in Appendix D.

The westbound direction of travel and the afternoon peak hour period were selected for analysis because peak hour volumes were available to populate the AIMSUN network from traffic count data provided by the city of Raleigh, whereas the off-peak period demands were based on factors derived from the Trans CAD-based Triangle Regional Model as described in Chapter 4. During the afternoon peak hour, traffic is progressed in the

westbound direction because this direction serves commuters returning from work in the downtown area. In addition, more empirical trajectories were available in the westbound direction. Four vehicles which travelled in the westbound direction during the PEMS field tests were selected to cover a range of total travel times from low to high.

Trajectories with space mean speeds within a range of 10 km/h can be grouped together (Zhai, 2007). As such four simulated trajectories with space mean speeds within +/- 2.5 mph of average space mean speed of the empirical trajectories in the westbound direction were extracted for analysis. Table 9 presents the travel times of selected empirical and simulated trajectories.

Table 9 Trajectory Travel Times from Empirical Data and Simulation under Different Parameter Distributions

	Travel Times using Different Simulation Parameters (minutes)			
	Low	Intermediate	Intermediate	High
Empirical	4.67	5.42	5.75	7.80
AIMSUN Default	4.68	5.43	5.68	7.13
PEMS Maximum	4.83	5.57	5.77	7.15
PEMS 95th Percentile	4.77	5.23	5.75	7.15
PEMS 85th Percentile	4.98	5.28	5.75	7.47

For both empirical and simulated trajectories, the second-by-second vehicle activities were characterized by VSP distributions. In the VSP modal approach for estimating emissions the emission rates are multiplied with number of seconds in each VSP mode and summed over all modes, to arrive at total emissions for a route or a section of a route.

$$Total\ Emissions_{ki} = \sum_{j=1}^{14} EF_{ij} * t_{kj} \quad for\ i = 1,2,3,4$$

The total emissions are divided by the travel time to arrive at trajectory average emission rates.

$$\boldsymbol{Emission_{ki}\ per\ unit\ time} = \frac{\boldsymbol{Total\ Emissions_{ki}}}{\sum_{j=1}^{14} \boldsymbol{t_{kj}}}$$

Likewise, the total emissions are divided by travel distance to get emissions mass per mile:

$$\boldsymbol{Emission_{ki}\ per\ unit\ distance} = \frac{\boldsymbol{Total\ Emissions_{ki}}}{\boldsymbol{d_k}}$$

$EF_{ij} = Fleet\ average\ emission\ factor\ for\ pollutant\ i\ in\ VSP\ mode\ j\ (mass/s)$
$t_{kj} = time\ spent\ in\ VSP\ Mode\ j\ for\ turning\ movement\ k\ (s)$
$d_k = distance\ between\ origin\ and\ destination\ of\ turning\ movement\ k$

The route-level emissions for each trajectory were calculated using VSP distribution on the route and fleet average modal emission factors used by Anya et al. (2013). The set of fleet average modal emission factors was developed from 42 selected passenger cars from the same PEMS database maintained by NC State University. The modal emission factors are shown in Table 10. Tables 11 and 12 present the results for the emission rates of CO_2 per unit distance and NO_x per unit distance.

Table 10 Average Vehicle Specific Power (VSP) Modal Emission Factors for 42 Passenger Cars Measured with a Portable Emissions Measurement System (Anya et al., 2013)

VSP Mode	VSP Range (kW/ton)	NO as NO_2 (mg/s)	HC (mg/s)	CO (mg/s)	CO_2 (g/s)
1	Below -2	0.31	0.29	2.25	1.04
2	-2 – 0	0.41	0.35	2.88	1.31
3	0 – 1	0.19	0.26	1.79	0.93
4	1 – 4	0.82	0.56	4.96	2.17
5	4 – 7	1.28	0.78	7.43	3.00
6	7 – 10	1.81	0.96	9.30	3.77
7	10 – 13	2.40	1.13	12.23	4.47
8	13 – 16	2.90	1.32	14.38	5.05
9	16 – 19	3.54	1.48	19.54	5.61
10	19 – 23	3.98	1.59	22.31	6.01
11	23 – 28	4.79	1.73	29.14	6.48
12	28 – 33	5.49	1.86	36.73	6.96
13	33 – 39	6.41	2.03	54.38	7.41
14	Over 39	6.06	2.28	128.28	8.06

Table 11 Selected Route-level Emission Rates of CO2 per unit Distance from Empirical Data and Simulation under Different Parameter Distributions

			Estimates using Different Simulation Parameters (g/mi)			
Travel time		Empirical (g/mi)	AIMSUN Default	PEMS Maximum	PEMS 95th Percentile	PEMS 85th Percentile
Low	Rate	304	394	406	368	362
	% Δ*		*29%*	*33%*	*21%*	*19%*
Intermediate	Rate	379	410	437	387	405
	% Δ*		*8%*	*15%*	*2%*	*7%*
Intermediate	Rate	384	436	450	431	416
	% Δ*		*13%*	*17%*	*12%*	*8%*
High	Rate	431	527	512	473	457
	% Δ*		*22%*	*19%*	*10%*	*6%*

*Percent difference between empirical and simulated emissions calculated as: $\frac{simulated-empirical}{empirical} * 100\%$

Table 12 Selected Route-level Emission Rates of NOx per unit Distance from Empirical Data and Simulation under Different Parameter Distributions

			Estimates using Different Simulation Parameters (mg/mi)			
Travel time		Empirical (mg/mi)	AIMSUN Default	PEMS Maximum	PEMS 95th Percentile	PEMS 85th Percentile
Low	Rate	126	199	214	166	152
	% Δ*		*58%*	*70%*	*32%*	*21%*
Low to Intermediate	Rate	157	195	202	163	175
	% Δ*		*24%*	*29%*	*4%*	*12%*
Intermediate to High	Rate	161	214	217	190	171
	% Δ*		*33%*	*35%*	*18%*	*6%*
High	Rate	170	232	217	196	179
	% Δ*		*36%*	*27%*	*15%*	*5%*

Tables 11 and 12 show that the higher absolute percentage differences between the empirical emission rates of CO_2 and NO_x per unit distance occur mostly for the AIMSUN default and PEMS maximum parameter values across the travel times. Similar trends were found for the emission rates of HC and CO but have are not reported here. The 95th percentile values produced closer emissions estimates than either the maximum or the AIMSUN default values for both CO_2 and NO_x. The simulated vehicles with 85th percentile parameter distributions produced estimates with lowest errors rates from the field-based estimates in most cases. However, the emissions analysis does not confirm that the vehicle activity which generated the emissions are representative of the real world. To investigate the differences in vehicle activity, the respective VSP distributions from simulation under different parameters and field data are shown in Figure 9 for the intermediate travel time of 5.72 minutes.

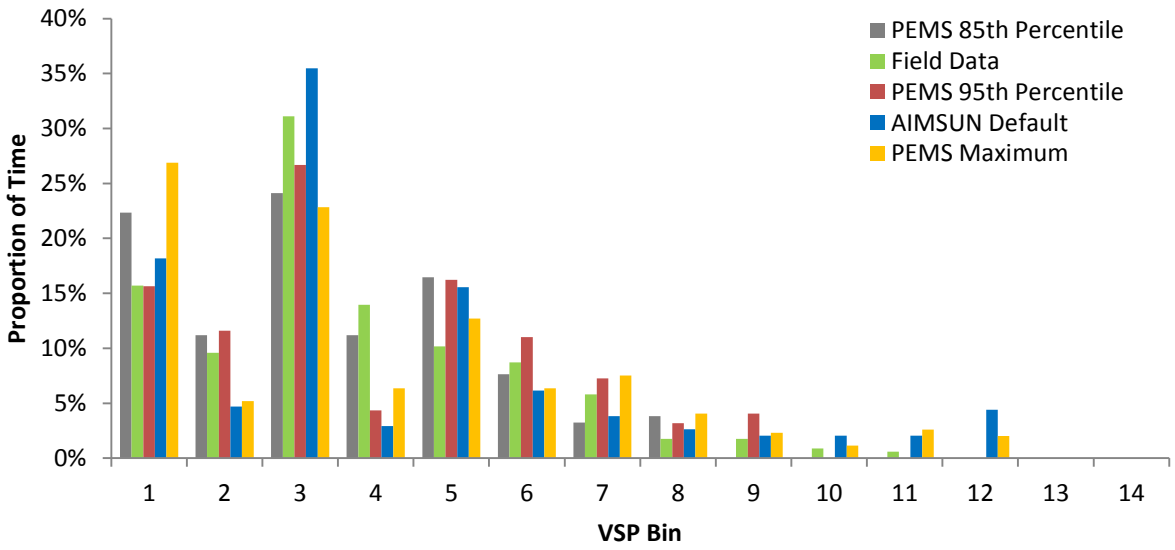

Figure 9 VSP Distribution using different simulation parameters for intermediate travel time of 5.72 minutes

Figure 9 shows that simulations under AIMSUN default and PEMS Maximum parameters produce observations in the larger bins that are not consistent with the field-based VSP distribution. The higher VSP modes are associated with higher emission rates as

described earlier. However, under the 85th percentile parameters, 93% of the simulated vehicle activity occurs in the lower VSP modes (Bins 1 – 6), while the empirical data shows that 11% of the real-world vehicle activity occurs in the higher VSP modes (Bins 7 - 11).

Based on this review of the VSP distribution in Figure 9, the simulated vehicle activity under 85th percentile parameters does not closely represent empirical data although it produces the lowest errors in emissions estimates. To investigate further, the range of the distributions of maximum, 95th percentile, 85th percentile and AIMSUN default values and their relative positions are presented on the cumulative distributions of all instantaneous accelerations and decelerations from 86 empirical trajectories in Figure 10. The total numbers of field observations used to construct the two cumulative distribution functions are listed in Table 13.

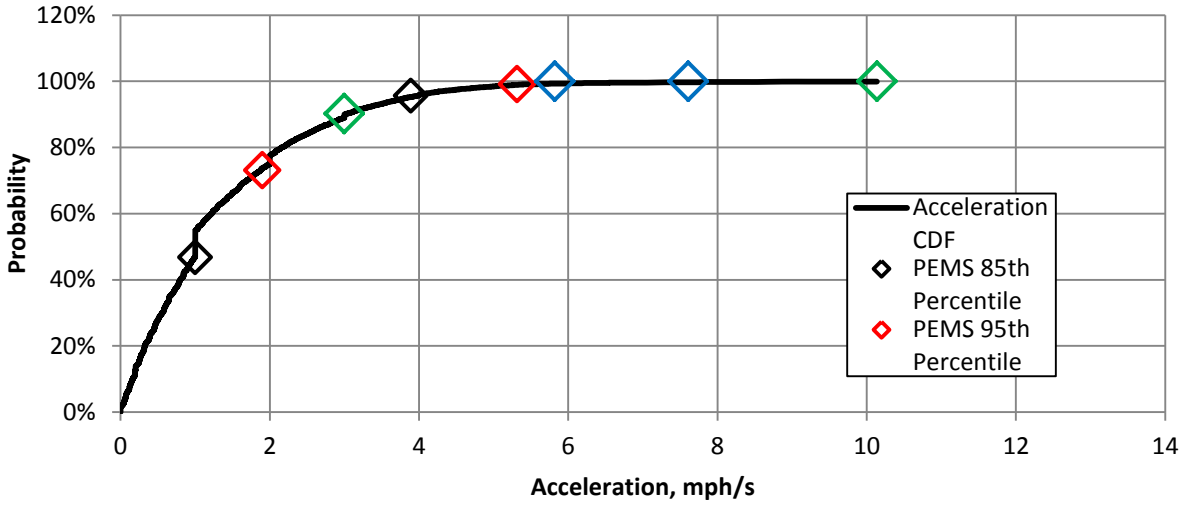

(a) Cumulative Distribution function of empirical instantaneous accelerations in mph/s

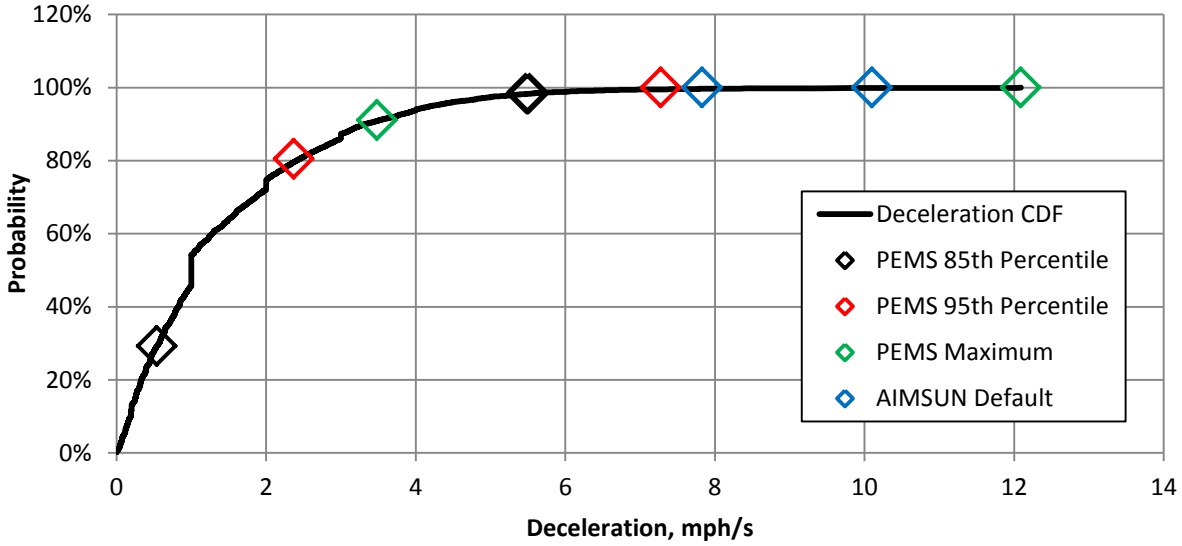

(b) Cumulative Distribution function of empirical instantaneous decelerations in mph/s

Figure 10 Relative positions of the range and mean values of empirical maximum, 95th percentile, 85th percentile and AIMSUN default parameter distributions

Table 13 Number of Seconds of Data to Construct Parameter CDFs

Parameter	Number of seconds of field data
Max. Desired Acceleration (> 0 mph/s)	11,778
Normal Deceleration (< 0 mph/s)	11,309

It is clear from Figure 10 that both AIMSUN default accelerations and decelerations would be observed in less than 1% of empirical vehicle activity data. This further supports the need to calibrate the AIMSUN model for the purposes of this thesis. The range of the PEMS maximum parameters is the largest among the distributions considered. However, most of the PEMS maximum observations appear in 10-15% of the empirical data. These observations suggest that using the PEMS maximum accelerations may not allow simulated vehicle activity to follow empirical vehicle activity closely.

Conversely, the distribution of the 85th percentile accelerations lies between 50% of the empirical observations and deceleration between nearly 70% of the empirical observations. While this distribution is more representative of accelerations and decelerations observed in the field, sampling from this distribution may limit the maximum accelerations or decelerations achievable in simulation. This can be illustrated with an example – 85% of the accelerations observed in field data are below 2.5 mph/s, which is the mean of the distribution of 85th percentile accelerations; however, this may not be representative of driver behavior along the corridor because, if a vehicle entering the simulated network has a maximum achievable acceleration of 2.5 mph/s it cannot exhibit any instantaneous accelerations greater than 2.5 mph/s when travelling below the speed limit and unconstrained by a preceding vehicle, traffic control or road geometry. This is not a realistic scenario.

The 85th percentile parameters do not account for 5% of the high accelerations observed in field data. When maximum desired accelerations are randomly sampled from the 85th percentile distributions some vehicles may be assigned very low *maximum* desired accelerations (< 2 mph/s). On the eastern end of the Hillsborough Street corridor, there are several closely spaced intersections, but towards the west, the spacing increases and vehicles have higher speeds and accelerations. Since the AIMSUN parameters are calibrated for vehicles in all parts of the simulated road network, it may be unrealistic for the constraints on *maximum* desired acceleration to be low. The acceleration mode typically produces higher emissions rates (Rakha & Ding, 2002) and if the simulation model does not allow some portion of the traffic to experience acceleration events of reasonable magnitude, the VSP-based emissions rates may appear to be lower than what would be observed in the real world.

Therefore, for practical concerns with constraining maximum desired accelerations to lower values and thus failing to capture emissions correctly using the VSP approach, the calibration parameters were chosen to reflect 95th percentile values instead of the 85th percentile values. The next section focuses on calibrating the AIMSUN model with PEMS 95th percentile values and making comparisons at the route-, section- and second-by-second levels under PM Peak and Off Peak traffic states.

5.3 Detailed AIMSUN Model Calibration with 95th Percentile Parameters

The previous section demonstrated that vehicle activity from the AIMSUN simulation model with default values of maximum desired speed and acceleration and normal deceleration lead to over-estimating emissions on the Hillsborough Street arterial in the westbound direction. Calibrating the parameters with 95th percentile values was shown to be effective in reducing the errors in emissions estimates and in producing a VSP distribution that is more consistent with the VSP distribution from field-collected vehicle activity. Emissions from simulated and empirical trajectories were compared based on matching the travel time of individual trajectories. It was assumed that simulated or empirical trajectories with the same travel time follow similar driving cycles. This section investigates the impacts of increasing the sample sizes of both simulated and empirical trajectories and basing the comparison of emissions on the samples having the same distributions of travel time and/or the same average number of stops. The research hypothesis is that simulated trajectories following the driving cycles similar to empirical trajectories from a simulation model with properly calibrated behavioral parameters can be used to estimate emissions with a reasonable degree of accuracy. Therefore, the three main research questions addressed in this section based on larger samples of simulated and empirical vehicle activity and emissions data are:

1. Are emissions estimates from individual trajectories improved under calibrated conditions when the comparison is done based on trajectories having similar travel times?

2. Does the number of stops per trajectory present a better basis for comparing emissions from simulation and field-based vehicle activity?
3. Does controlling for both trajectory level travel time and average number of stops in simulated vehicle activity match simulated and field-based driving cycles better than either travel time or average number of stops alone, and therefore present a more fair basis for comparing emissions before and after calibration?

The AIMSUN model was calibrated by setting the vehicle attributes for maximum desired acceleration and normal deceleration to follow the truncated normal distributions of the PEMS 95th percentile values. The maximum desired speed parameter was characterized by the distribution of PEMS maximum values. The network was simulated with PM Peak traffic state. The network was also simulated with all parameters following AIMSUN default distributions to compare with the results from the calibrated model. This section develops a methodology to quantify vehicle activity and emissions from the calibrated model at different spatial scales and a detailed investigation of the differences between empirical and simulated vehicle activity data. The results are presented for the analysis of vehicle trajectories on the Hillsborough Westbound route.

5.3.1 Travel-time Based Sampling from Simulation Data

Once the model was calibrated, the distribution of travel times for simulated vehicles which traversed through the entire length of corridor along the Hillsborough Westbound Route was compared to the distribution of travel times of empirical through vehicles. It was found that the simulated vehicles from both the calibrated and AIMSUN Default models had average travel times which were lower than the field-observed average travel times. The travel time distributions of through vehicles from 10 simulation runs of the calibrated and default models and the field-observed trajectories are presented in Figure 11**.** A summary samples from which the travel time distributions were constructed is presented in Table 14, along with similar information for the Hillsborough Eastbound Route.

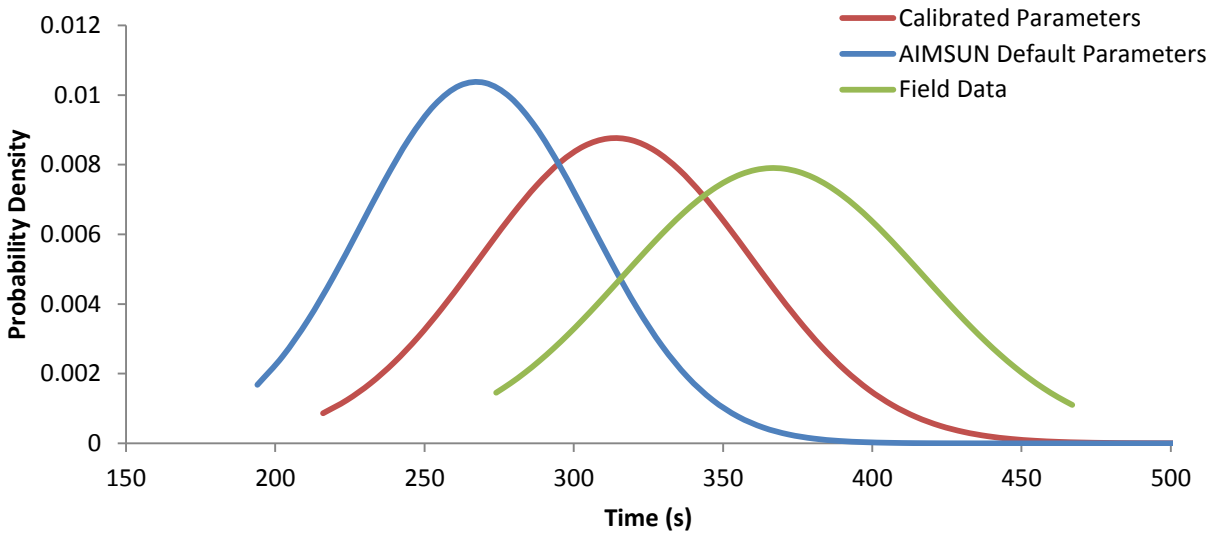

Figure 11 Corridor Travel Time Distributions from all simulated and empirical trajectories

Table 14 Sample Sizes for Travel Time Distributions

Route	Vehicle Activity from	No. of Simulation Replications	Total no. of trajectories	Avg. Travel Time/min (Std. Dev)
Hillsborough Westbound	Field		14	6.11 (0.81)
	Calibrated Simulation	10	2,633	5.23 (0.75)
	Default Simulation	10	2,426	4.46 (0.64)
Hillsborough Eastbound	Field		9	5.93 (1.46)
	Calibrated Simulation	10	1,427	6.00 (0.80)
	Default Simulation	10	1,386	6.32 (1.47)

The lower travel times from the simulation under AIMSUN default parameters may be explained by the maximum desired speeds of vehicles on the corridor. As observed in Chapter 3, the speed limit puts a constraint on the maximum speed that a vehicle can reach. Under AIMSUN default conditions, the desired maximum speed of simulated vehicles is high and the speeds of vehicles through all sections of the corridor are mostly controlled by the speed limit. Under the calibrated parameters, the maximum desired speeds of vehicles are lower and may or may not be constrained by the speed limit. The justification for setting the

speed limit on the corridor at 45 mph is presented in Chapter 4. Therefore, simulated vehicles under default AIMSUN parameters have higher speeds and lower travel times.

Under the calibrated simulation conditions, the vehicles in AIMSUN travel at speeds that are close to field-observed speeds. The eastern end of Hillsborough Street has closely spaced intersections and field-observed trajectories in Chapter 4 show that speeds are lower in this portion of the corridor, but are higher towards the western end of the corridor. Figure 12 shows a random sample of 30 simulated trajectories under calibrated model parameters. The trajectories exhibit lower speeds where the traffic signals are closely spaced and higher speeds as vehicles are able to accelerate over longer distance in the western end of the corridor. A cross section of the trajectories at 520m and 1780m showed the average speeds were 15mph and 39mph respectively. This supports the decision to not place a lower speed limit than 45 mph at the eastern end of the corridor, since simulated vehicle appears to be constrained by the road geometry and signal spacing, rather than maximum desired speeds or the speed limit. Applying a city-wide speed limit of 35mph would not have accurately represented the vehicle behavior observed in the field all throughout the corridor, since simulated vehicles follow the speed limit strictly and would not be able to go over the limit in the western end of the corridor.

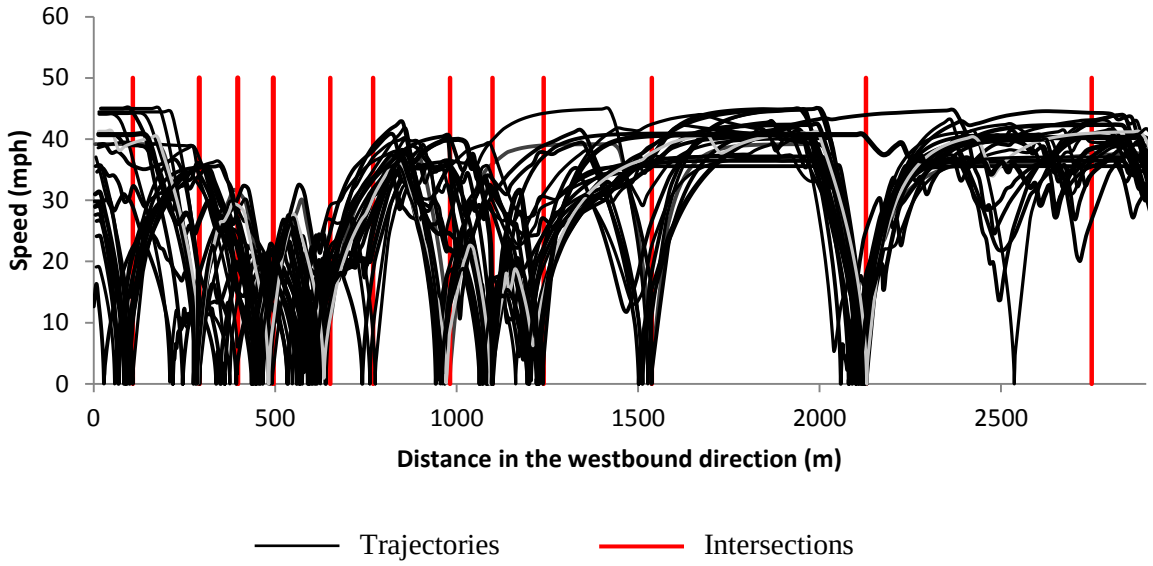

Figure 12 Speed profile of simulated trajectories under calibrated parameters

In the initial analysis of Section 5.1, vehicle activity and emissions from a range of travel times were investigated for simulation under different parameter distributions. For the detailed analysis of the calibrated AIMSUN model, the sample of vehicles for which simulated vehicle activity and emissions will be quantified is increased to 30 so as to ensure that the sample is large enough to detect differences from the empirically calculated emissions. To select simulated vehicles exhibiting activity that is reasonably close to field-observed vehicle activity, the distribution of travel times of selected simulated vehicles were matched with the travel time distribution of empirical vehicles. This was done using the concept of Latin Hypercube Sampling which ensures a range of values of a selected variable is represented in the sampled set (Cheng & Druzdzel, 2000)

The probability distribution of the field-observed travel times was stratified into equal intervals of 0.2 as shown in Figure 13, and the corresponding range of travel times in each of the 5 resulting stratification interval were obtained. Samples of 6 simulated vehicle trajectories were selected randomly such that their travel times fall between the travel time ranges of each stratification interval in the field-observed travel time distribution. A total of 30 vehicle trajectories were selected from each of the calibrated and default simulation datasets. As a result of the sampling technique, the probability distributions of travel times for each sample of 30 vehicles from the simulated datasets were statistically similar to the probability distribution of the field-observed travel times.

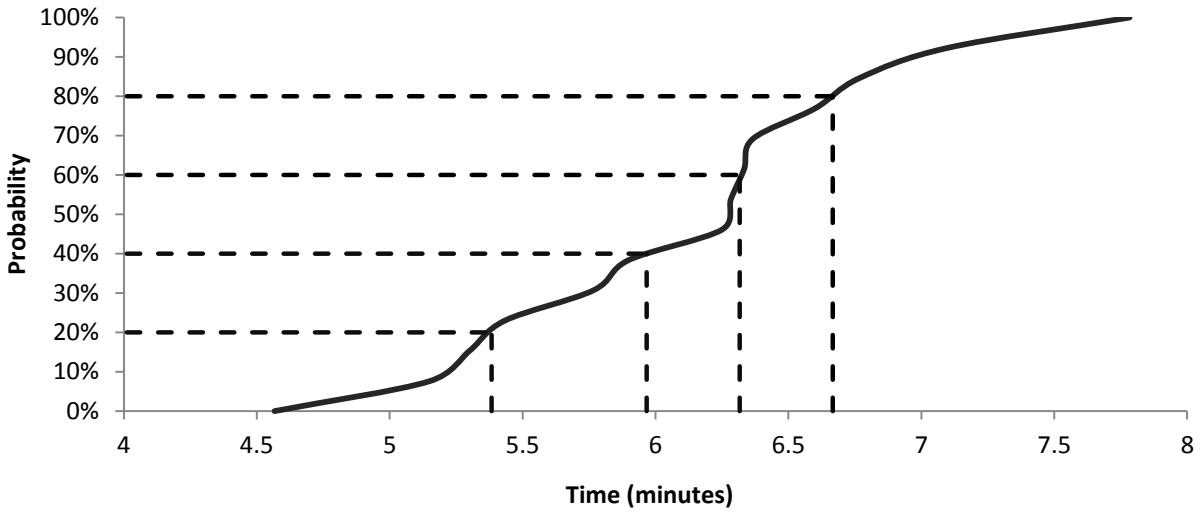

Figure 13 Stratified probability distribution of the field-observed travel times (minutes)

A two-sample t-test showed that the average travel time from field data (T_f) is not statistically different from the average travel times from simulation (T_s). A Kolmogorov-Smirnov Goodness of Fit test was performed to check that the field-observed and simulated samples had the same travel time distributions. A K-S test is a non-parametric statistical test which makes no assumption about the distribution of the data (National Institute for Standards & Technology, 2012).The p-values associated with the K-S tests were based on the maximum differences between two empirical cumulative distribution functions. Table 15 summarizes the selected samples from simulated datasets and the associated statistical tests.

Table 15 Summary of Selected Simulated Samples on Hillsborough Westbound Route

	No. of trajectories	No. of seconds	Avg. Travel Time/min (Std. Error)	Avg. Speed (mph)	P-value of T-test (H_0: $T_f = T_S$)	P-value of KS-Test (H_0: Distribution of T_f = Distribution of T_S)
Field	14	5,119	6.11 (*0.21*)	17.9		
Calibrated Simulation	30	10,802	6.00 (*0.14*)	18.2	0.67 Fail to reject H_0	0.94 Fail to reject H_0
Default Simulation	30	10,870	6.03 (*0.14*)	18.1	0.74 Fail to reject H_0	0.94 Fail to reject H_0

There was no evidence to suggest that the average travel times of the samples from simulated datasets differed significantly from average field-observed travel times. As a result of using the Latin Hypercube sampling method, the distribution of travel times in the field and the simulation samples were also found not to be statistically different.

5.3.2 Analysis of Vehicle Activity and Emissions of Samples from Simulation

The results from westbound trajectories analyzed under the PM peak traffic state are presented in this section. The VSP modal approach of NC State University (2002) and average fleet emission factors of Anya et al. (2013) are applied to empirical and simulated vehicle activity in order to calculate emissions on the route- and section-levels. Vehicle activity was also investigated at the second-by-second level. The previous section presented a methodology to select samples from simulated datasets, based on matching the travel time distributions of field-observed and simulated trajectories. An assumption was made that controlling for the travel times of simulated trajectories in the selected sample such that the travel time distribution matches what is observed in the field, would ensure fair comparisons of emissions and vehicle activity under default and calibrated behavioral model parameters based similar driving cycles.

Route Level Analysis

Vehicle activity data from the 30 simulated trajectories under each of the two simulations conditions were characterized by VSP distributions. The aggregate VSP distributions from simulation were compared to the VSP distribution of vehicle activity from 14 empirical vehicle trajectories. The distributions are shown in Figure 14 and are based on the number of seconds of data highlighted in Table 15 in Section 5.3.1.

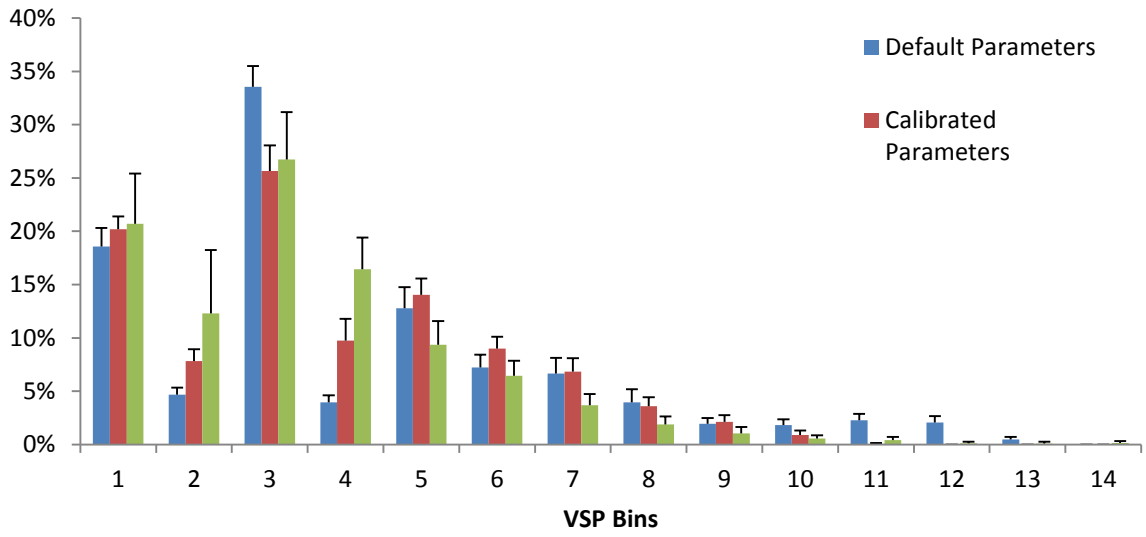

Figure 14 VSP Distributions from field data and simulated data controlled for travel time distribution under default and calibrated parameters on Hillsborough Westbound Route

Figure 14 shows that the VSP distribution under calibrated parameters resembles the VSP distribution from empirical vehicle activity data more closely than the VSP distribution under default parameters. Under the default parameters, the simulated vehicles appear to have spent proportions of time in VSP Bins 11 to 13, which indicate high acceleration events and a higher proportion of time in Bin 3, indicating idling. Under calibrated parameters, simulated vehicles spent 1.0 to 4.7 % more time in VSP bins 5 to 9 than empirical vehicles.

Figure 15 shows the cumulative distributions of VSP values under the 2 simulated conditions and the field tests. There is a clear indication that simulation under default parameter underestimates the proportion of negative VSP values between -2 kw/ton and 0 kw/ton (Bin 2), as compared to the empirical or calibrated simulation's VSP distribution since its CDF shows a flatter slope. However, the fleet average modal emissions rates associated with Bin 2 are low across all four pollutants and the differences in VSP distributions are not very important. Simulation results under default parameters overestimate the number of VSP values in the range between 4 kW/ton to 28 kW/ton (Bins 5-13). Simulation under calibrated parameters provides a slightly closer fit to field-observed values,

although still overestimating the time spent in Bin 2 and virtually spending no time in Bin 10-14. VSP Bin 10-14 have the highest modal emission rates across the pollutants and although the differences in VSP distribution between default parameters and the field data are not very large on an absolute basis, their cumulative effect on emissions is important.

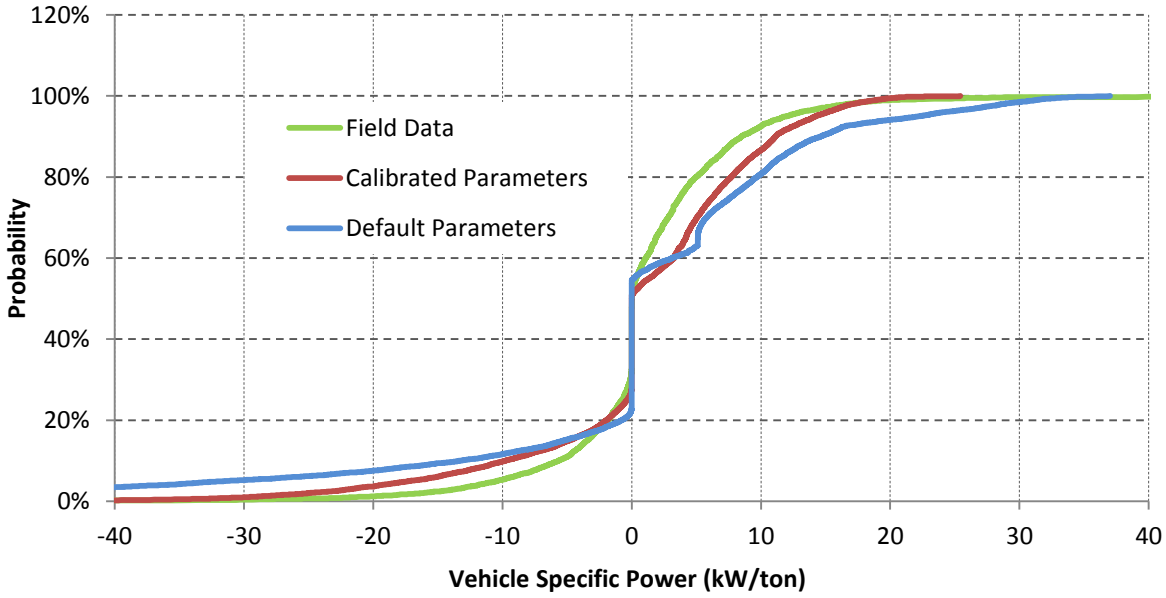

Figure 15 Cumulative Distribution Functions of VSP from empirical and simulated data

Chi-square Goodness of Fit tests were performed on the binned VSP data from simulation and field data. Since a Chi-square test requires a minimum of 5 data points within each bin the high VSP bins needed to be combined together. Further grouping of VSP bins was required to provide physical meaning to the VSP distribution and explain the results from the Chi-Square test better. To help visualize the speed-acceleration combinations that represent the 14 VSP bins, Figure 16 shows an iso-VSP contour plot at a 0% road grade. Each line represents the upper bound of a VSP bin.

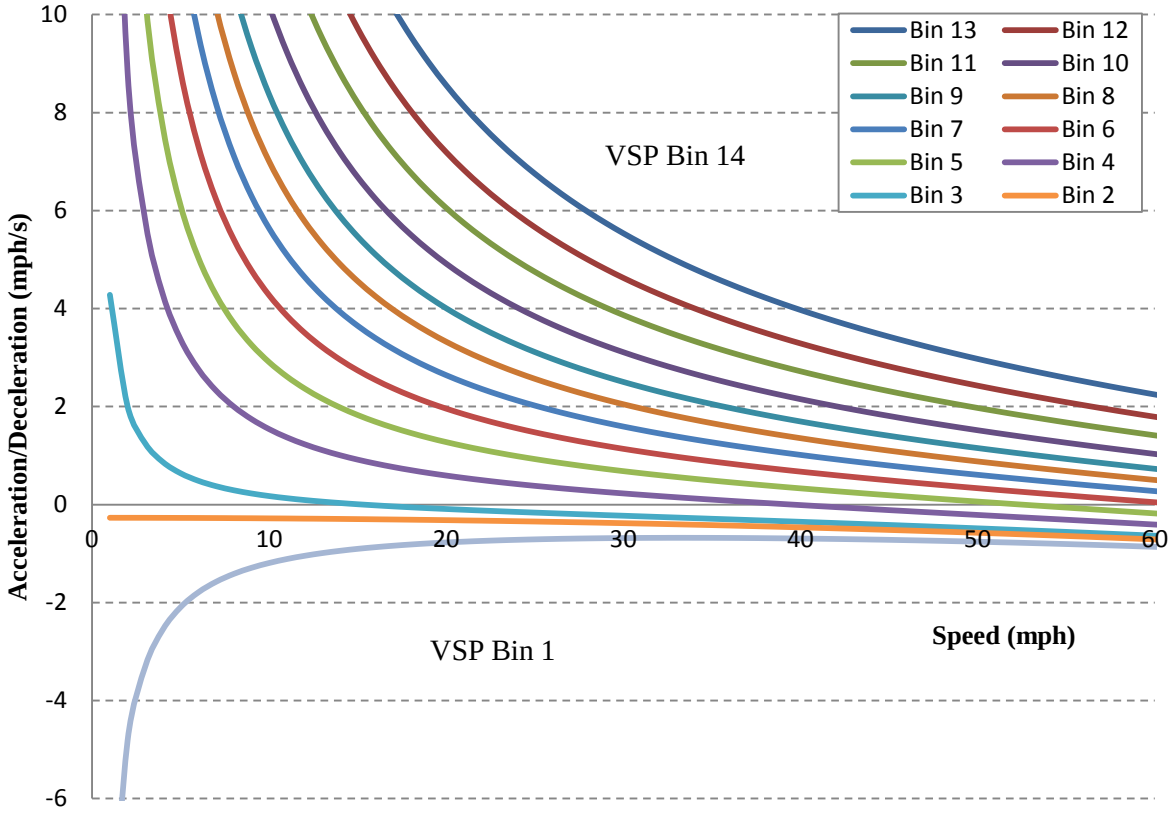

Figure 16 Iso-VSP contour plots at 0% road grade

The negative VSP bins (Bins 1-3) were combined together to represent deceleration or idling events, as were Bins 4-6 to represent accelerating from low speeds. Bins 7-9 were combined to represent acceleration events at slightly higher speeds. VSP values in Bins 10-14 were combined into a single bin such that the minimum number of data points criteria for Chi-Square tests were met and the bin represented high speed-acceleration combinations. The hypotheses of the Chi-square tests take the following form:

H_0: The VSP distribution from simulation under default (or calibrated) parameters is consistent with VSP distribution from empirical data.

H_a: The VSP distribution from simulation under default (or calibrated) parameters is *not* consistent with VSP distribution from empirical data.

The Chi-square tests showed that overall the vehicle activity at the route level is not replicated well by simulation. In both cases, the p-values associated with the tests were very

small (< 2.2E-16) indicating sufficient evidence to reject the null hypotheses (H_0). The Chi-square tests suggested that neither the VSP from simulation with AIMSUN default parameter distributions, nor the VSP from simulation with PEMS 95th percentile parameter distributions for acceleration and deceleration have the same proportion of observations in each bin grouping as the VSP from empirical trajectories.

For the comparison of VSP distribution under default conditions, the higher bin groupings exhibited bigger differences, while the VSP distribution in Bin 1-3 showed very little difference between simulated and field-based activity. The Chi-square test statistic (χ^2) associated with the comparison of the field-observed and calibrated simulation data was much smaller, indicating it yielded a closer fit to the empirical VSP distribution. The biggest differences were observed in VSP Bin grouping 7-8 which represents more acceleration events at speeds starting around 15 mph and increasing to 45 mph in the context of the Hillsborough Street arterial with reference to Figure 16. To keep in line with the objectives of this thesis, the next section investigates whether emissions estimations from the simulated data under calibrated parameters provides a reasonable fit to emissions estimated based on field-data on the corridor at the route level.

Using the fleet average modal emission factors developed by Anya et. al. (2013), the simulated and empirical VSP distributions described above, the average emission rates per unit distance were calculated. The results are presented in Table 16**.**

Table 16 Route Level Emission Rates per unit Distance from Empirical and Simulated Vehicle Activity Controlled for Travel Time Distribution

	Avg. Travel Time/min		**NO (mg/mi)** (Std. Error)	**HC (mg/mi)** (Std. Error)	**CO (mg/mi)** (Std. Error)	**CO_2 (g/mi)** (Std. Error)
Field Data	6.11	Rate	153 (*9.16*)	111 (*4.80*)	894 (*58.5*)	420 (*18.3*)
AIMSUN Default	6.00	Rate	221 (*3.52*)	128 (*2.77*)	1285 (*24.5*)	485 (*10.6*)
		% Difference	**45%**	15%	**44%**	**16%**
Calibrated	6.03	Rate	183 (*3.09*)	118 (*2.33*)	1031 (*20.3*)	448 (8.53)
		% Difference	**20%**	**6%**	**15%**	7%

*Bolded figures indicate differences that are statistically significant at the 5% significance level

Table 16 shows that with the calibrated parameters, the average emission rates of NO, HC, CO and CO_2 per unit time are closer to empirical average rates than under default parameters. The average emission rates from the simulated activity under default parameters are higher than the empirical rates, especially for NO_x and CO. The modal emission factors of NO_x increases monotonically across VSP bins at a sharper rate than HC and CO_2 while for CO the emissions rates are low for VSP bins 1-8 but increase sharply in Bins 9-14 because CO emissions are more sensitive to fuel enrichment at higher VSP values than the other pollutants (North Carolina State University, 2002). As a result, the emission rates of NO_x and CO have higher variation and the observed differences between the simulated and field data are high. The differences in emissions are an artifact of the simulation under default conditions producing more vehicle activity in the higher VSP bins.

Two sample t-tests were performed to determine if there are differences between the emission rates from empirical data and simulated data were statistically significant. The differences in emissions of HC and CO_2 per unit distance in the calibrated model at the route level are below 10% while the differences in emissions rates of NO_x and CO are at or below 20%. Although emission rates of NO, HC and CO_2 are statistically significant the estimates from calibration are more representative of empirical data than the model with default parameters. The above analysis shows that when trajectories from a calibrated AIMSUN model of Hillsborough Street, a busy urban arterial interrupted by several signalized intersections, are compared based on the travel time distribution observed in the field, the estimated emission rates of HC and CO_2 at the route level can be expected to be within a reasonable 10% error rate. CO_2 is directly related to fuel consumption and thus is an important pollutant to study and predict emission rates correctly

Section-level Analysis

The purpose of the section level analysis was to observe whether the emissions hotspots along the route can be captured by applying the VSP modal approach to simulated vehicle activity. The route is composed of links and points as defined by the Highway Capacity Manual 2010. A point is defined as the boundary conditions for links, such as signalized intersections, while a link is defined as the road segment between two points

(Transportation Research Board, 2010). For the section level analysis, the entire route was split into “sections”, where each section is composed of a single point and half of the lengths of the adjacent upstream and downstream links. A diagram of a section is presented in Figure 17.

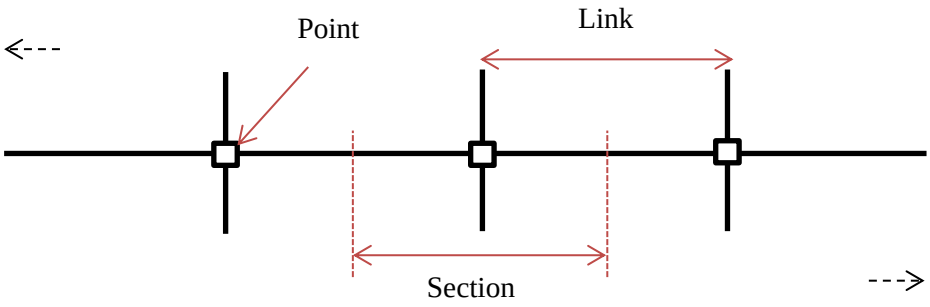

Figure 17 Definition of a section

13 sections were defined along Hillsborough Street and have been named according to the cross street at each intersection within the section. Figure 18 shows the starting and ending points of each section with the westbound route marked along Hillsborough Street. The sections, their respective lengths and starting and ending placemark numbers are presented in Table 17.

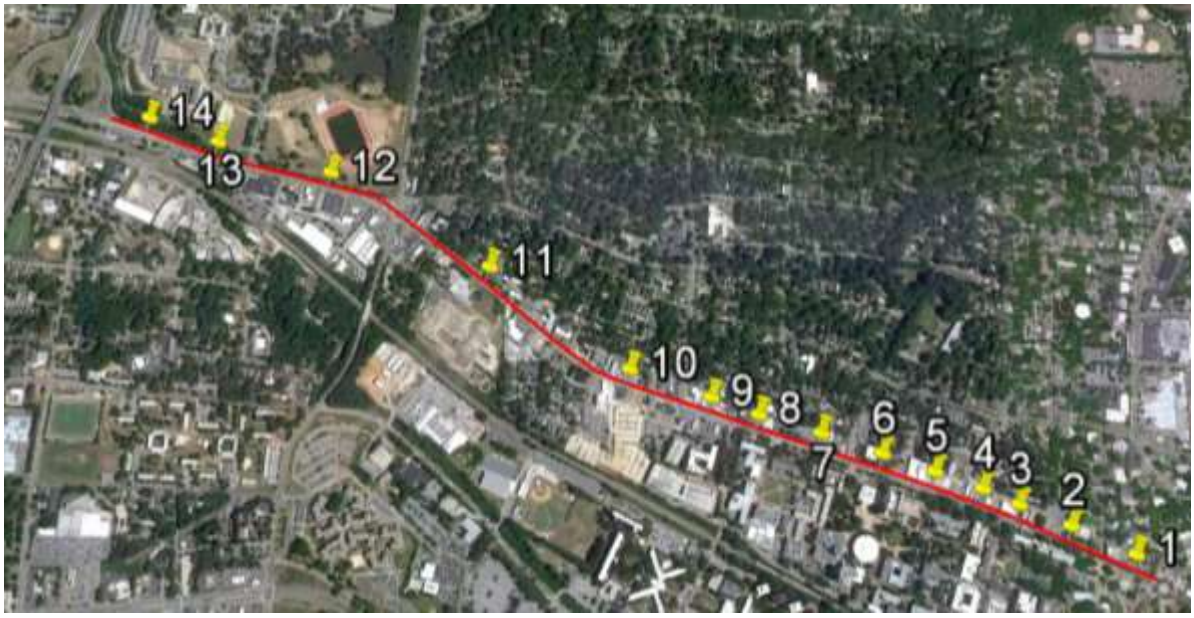

Figure 18 Beginning and ending points of 13 sections on Hillsborough Westbound route

Table 17 Section Names and Lengths

No.	Section Name	Length (mi)	Starting Placemark #	Ending Placemark #
1	Enterprise	0.11	1	2
2	Logan	0.08	2	3
3	Chamberlain	0.06	3	4
4	Horne	0.08	4	5
5	Pogue	0.09	5	6
6	Gardner	0.10	6	7
7	Brooks	0.10	7	8
8	Dan Allen	0.08	8	9
9	Dixie	0.14	9	10
10	Shepherd	0.28	10	11
11	Faircloth	0.31	11	12
12	Meredith	0.20	12	13
13	Beryl	0.13	13	14

The second-by-second vehicle activity along each section within the Hillsborough Westbound route was extracted from each of the 30 empirical and simulated trajectories. The average total emission of NO, HC, CO and CO_2 within the sections were estimated by following the VSP modal approach. The average emissions per unit distance within each

section were used to investigate the empirical emissions hotspots within the route and determine whether the vehicle activity simulated under the default and calibrated parameters were able to replicate what was observed in the field.

Figure 19 shows results the from section-level analysis of NOx, HC, CO and CO_2 emissions along the westbound direction of Hillsborough Street within the study area. The section-level emissions per unit distance are plotted at the location of the intersection contained within each section.

Figure 19 Average proportions of total emissions released in each section of the Hillsborough Westbound route by simulated and empirical vehicles

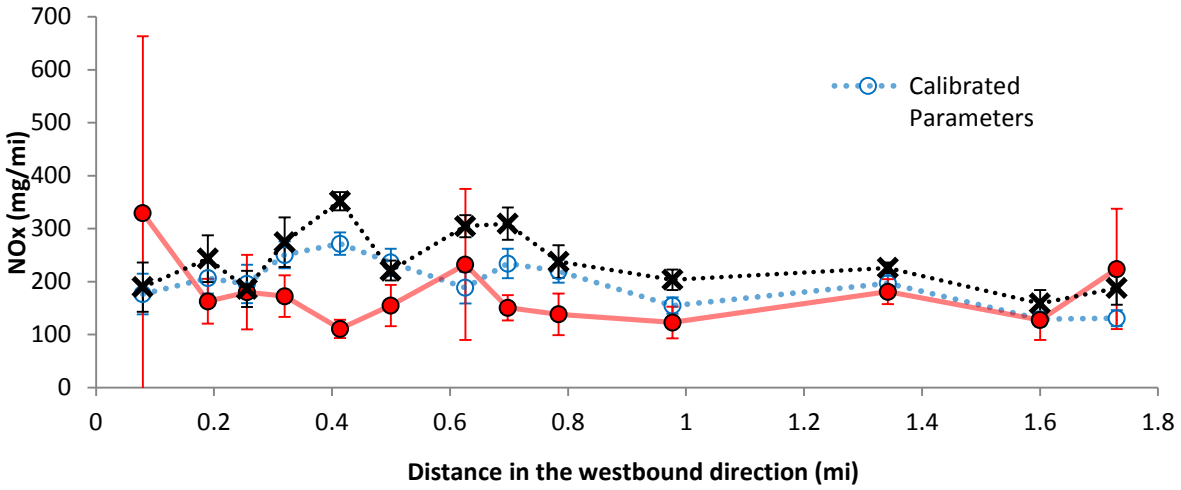

(a) Nitrogen Oxide (NO_x)

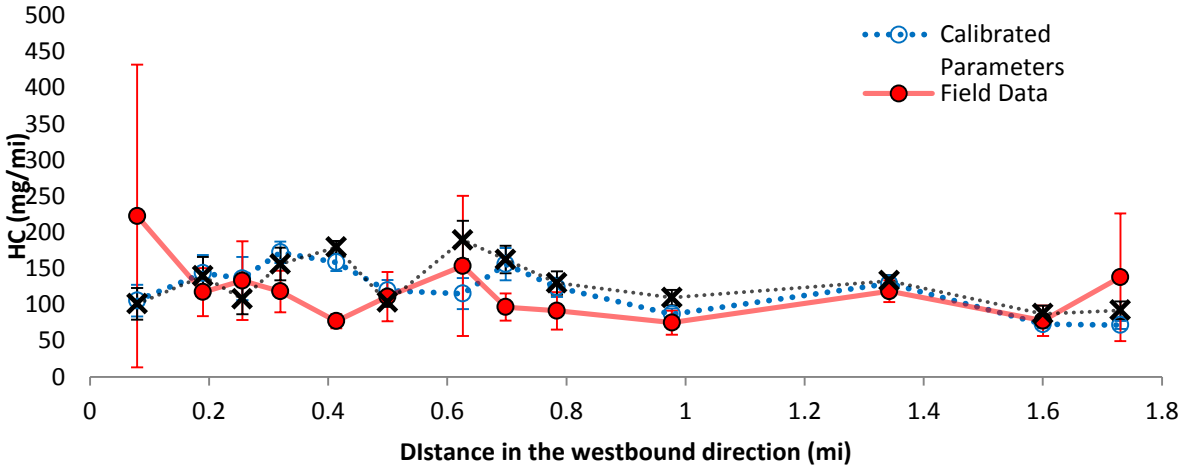

(b) Hydrocarbons (HC)

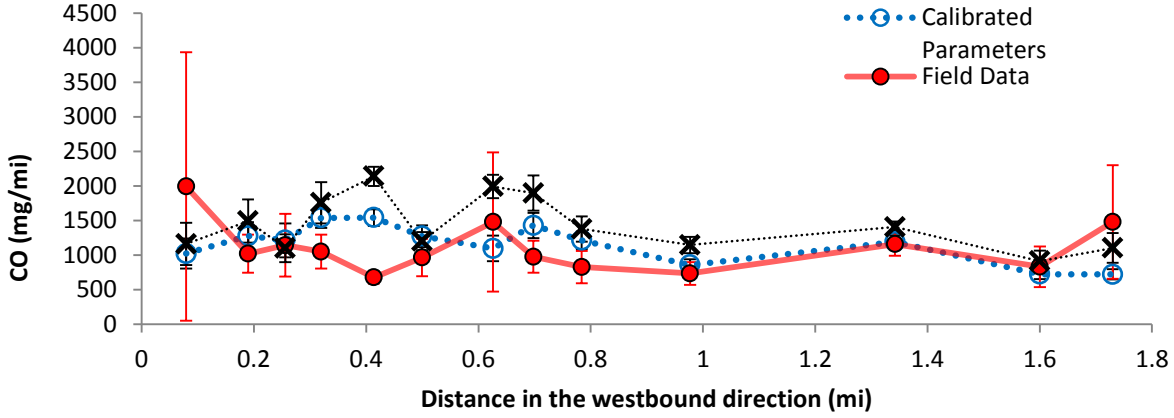

(c) Carbon Monoxide (CO)

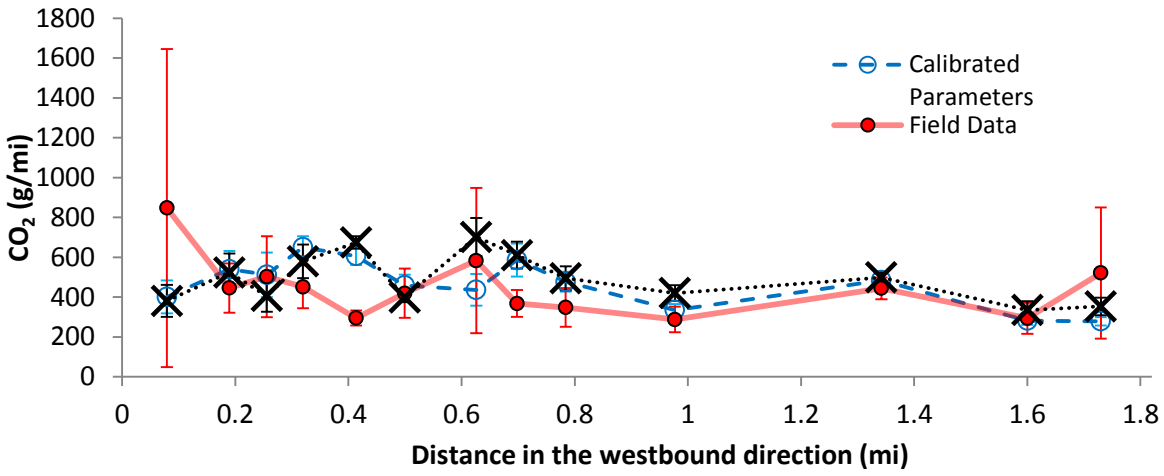

(d) Carbon Dioxide (CO_2)

The section-level emissions per unit distance show that while the calibrated model is not better able to capture the emissions "hotspots" along the Hillsborough Westbound route than the default model, its estimates are closer to field-based estimates across 9 out of 13 sections. Similar trends are seen in the section level analysis across all pollutants. The emissions from field-observed vehicle activity show four peaks along the route – the sections identified as (1) Enterprise (7) Brooks (11) Faircloth and (13) Beryl. Both sets of simulated data capture the peaks at Faircloth across all pollutants, but do not replicate the high emissions rates at Enterprise and Beryl. In addition, the calibrated model fails to capture the peak at (7) Brooks by predicting lower emissions at this section than field data, while the default model is able to detect it.

The largest peak and highest variation in the empirical data is at the section of Enterprise. Simulated data does not reflect the same emission rates in this section as do empirical data. This may be due to this section being modeled as the entrance to the corridor, where vehicles do not need to slow down unless to join a queue or speed up, while in reality, vehicles arriving at that intersection may still be accelerating to higher speeds after being stopped at the previous intersection served by a single lane roundabout, which was not modeled in the simulation. The section of Faircloth is long and can cause vehicles to accelerate and reach higher speeds within the section. Beryl is a short section and does not contain a particularly busy intersection. However, the ramp onto the I-440 East lies just beyond it, an artifact of which is that real-world vehicles tend to speed up after crossing the intersection of Beryl. The combination of higher speeds and accelerations cause higher VSP values and corresponding high emissions, as seen in the empirical data. The emissions from simulated data are not as high, however. This may be due to the fact that the speeds of simulated vehicles are constrained by either the speed limit of the road segment or the maximum desired speeds of each individual vehicle, as sampled from a distribution when the vehicle entered the network. Thus, even if the speed limit on the ramp is high, the vehicle cannot accelerate to more than its maximum desired speed and does not experience any more acceleration once it is at its maximum speed. As a result, VSP values and corresponding emissions are not as high as

those seen in empirical data. The simulation data indicates that the section (5) Pogue is an emissions hotspot, while this was not observed in the field data.

The intersections towards the eastern end of the corridor (between 0mi and 0.8mi) are spaced at smaller distance intervals. The differences between the field-based emissions and simulated emissions of all pollutants are larger in the areas with closely spaced intersections. A visual review of Figure 16 shows that at 9 of the 13 sections presented in the analysis, the calibrated model produced closer estimates to the field-based emission rates of HC and CO_2 than the AIMSUN default model. At 3 sections the calibrated and default models estimated the same emissions per unit distance, while at the remaining section, the default model produced results that were more similar to the field-based estimates. The section-level emissions of NO_x showed that both simulation models produced similar estimates for several of the sections.

Based on these observations a Wilcoxon Rank Sum Test was performed to check whether the calibrated model performed better than the default model, when the estimates from each model were compared to the field-based estimates. A Wilcoxon Rank-Sum Test is a non-parametric test in which the test-statistic is calculated based on the order in which the observations in two samples fall. If one sample is contains larger observations, it will have higher ranks and the test statistic will be higher (Moore & McCabe, 2006). The distribution of the data does not need to be specified for this test. The Wilcoxon rank sum test is used to test the difference between two samples by comparing population medians and thus structure of the test hypotheses is:

H_0: There is no difference between the simulated (calibrated/default) model and field-based emission estimates

H_a: The simulated (calibrated/default) model emissions estimates are higher than field-based estimates

The results of the test are shown in Table 18. There is significant evidence to suggest that the section level emissions estimates of NO_x and CO from the default simulation model are higher than field-based estimates. On the other hand, the section level estimates from the

calibrated simulation model were not found to be statistically different from the field-based estimates for any of the pollutants.

Table 18 Results of the Wilcoxon Rank-Sum Test

Pollutant	Sample 1	Sample 2	P-value of Wilcoxon Rank-Sum Test	Hypothesis (at the 5% significance level)
NO	Default Simulation	Field Data	0.003	Reject H_0
	Calibrated Simulation	Field Data	0.101	Fail to Reject H_0
HC	Default Simulation	Field Data	0.336	Fail to Reject H_0
	Calibrated Simulation	Field Data	0.511	Fail to Reject H_0
CO	Default Simulation	Field Data	0.019	Reject H_0
	Calibrated Simulation	Field Data	0.311	Fail to Reject H_0
CO_2	Default Simulation	Field Data	0.336	Fail to Reject H_0
	Calibrated Simulation	Field Data	0.511	Fail to Reject H_0

At a larger spatial scale, i.e. route level, the emissions from the calibrated model are closer to empirical emissions. At the section level the calibrated model also shows better emissions estimates than the default model. Overall however, the simulation models are not able to capture all the emissions hotspots along the route. The section level emission rates from simulation vary even more from the field-based estimates when the intersections are closely spaced. As a result, a detailed look at instantaneous vehicle activity is taken in the next section, to investigate how second-by-second differences between field data and simulated data can contribute to differences in VSP distributions and the resulting emissions estimates.

Second-by-second Analysis

While it may not be possible to replicate exact instantaneous speeds, accelerations and positions of the field tested vehicles in a computer simulation, it could be expected that in a calibrated model the average vehicle activity would be very similar at the microscopic level. As such, the objective of the second-by-second level analysis is to evaluate if the instantaneous vehicle activity from calibrated simulation provides a reasonable match to the empirical instantaneous vehicle activity data or if any systematic differences exist to

contribute to route-level or section-level differences in VSP distributions and emissions estimation using the modal approach.

In this section, a simple assumption is made that VSP is most sensitive to the product of speed and acceleration. The effect of road grade was not included since the study site is on relatively flat terrain with no steep slopes. As such, scatter plots of speed vs. acceleration for 14 empirical trajectories on the Hillsborough Westbound route and 30 simulated trajectories from default and calibrated simulation models were investigated. Figure 20 and Figure 21 show all speed-acceleration pairs from empirical and simulated trajectories with superimposed iso-VSP curves. The ranges of VSP in each of the 14 VSP bins have been presented earlier in Chapter 4.

Figure 22 shows the acceleration and deceleration events separately for each of the field and calibrated simulation samples to get a clearer picture of the differences at the second-by-second level that remain after calibration.

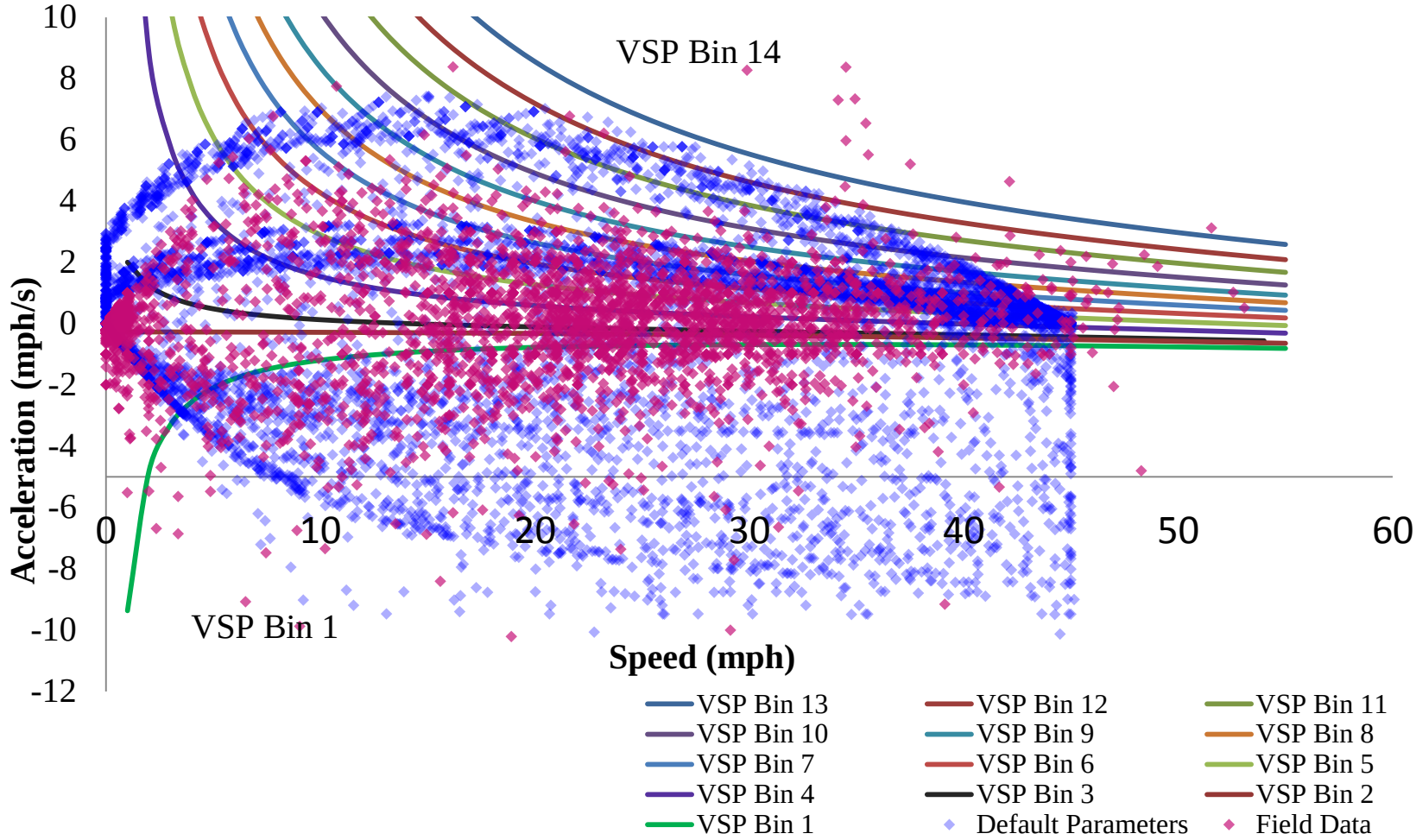

Figure 20 Speed-acceleration pairs from field data and simulation under Default Parameters with super-imposed iso-VSP lines

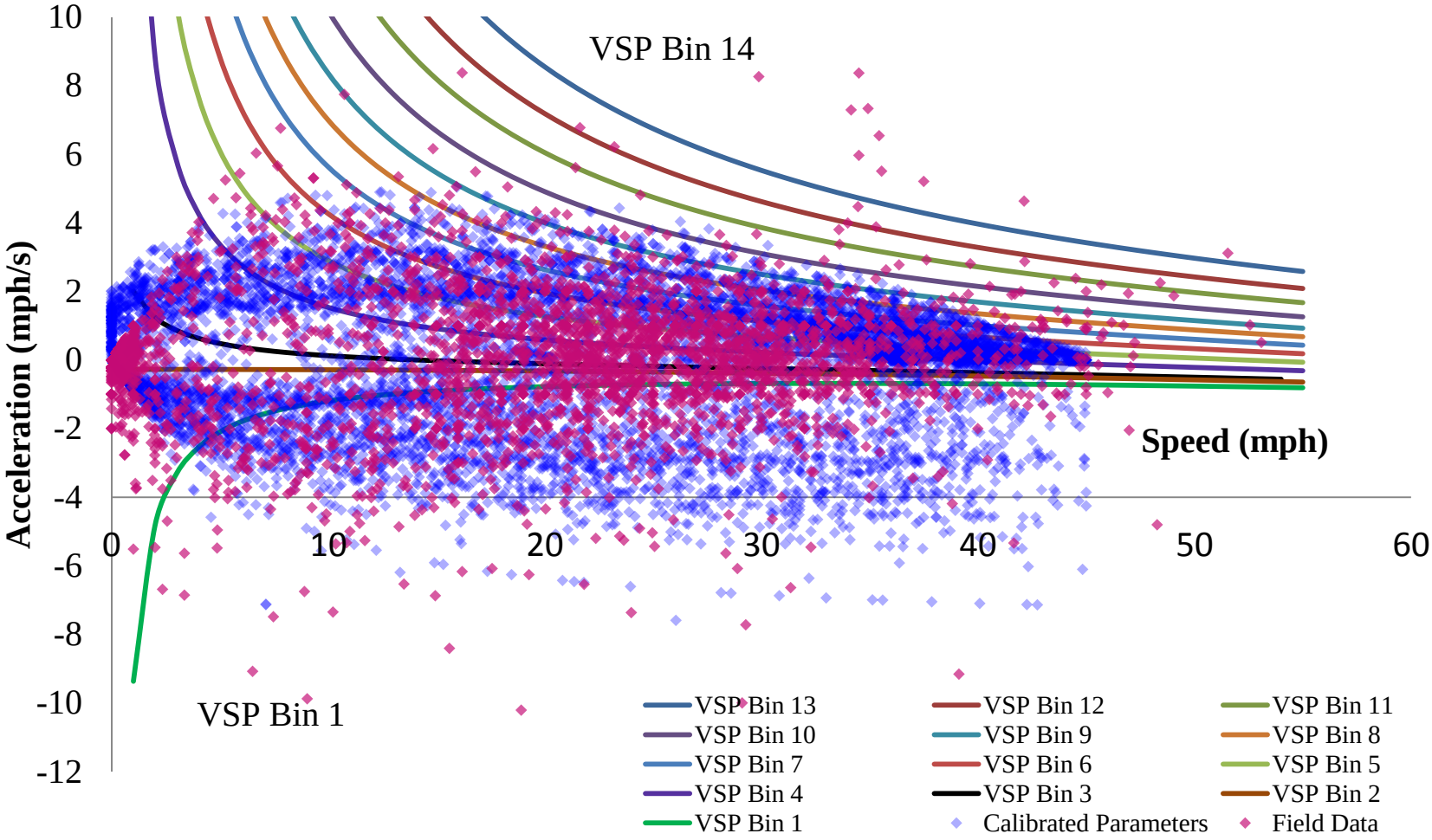

Figure 21 Speed-acceleration pairs from field data and simulation under Calibrated Parameters with super-imposed iso-VSP lines

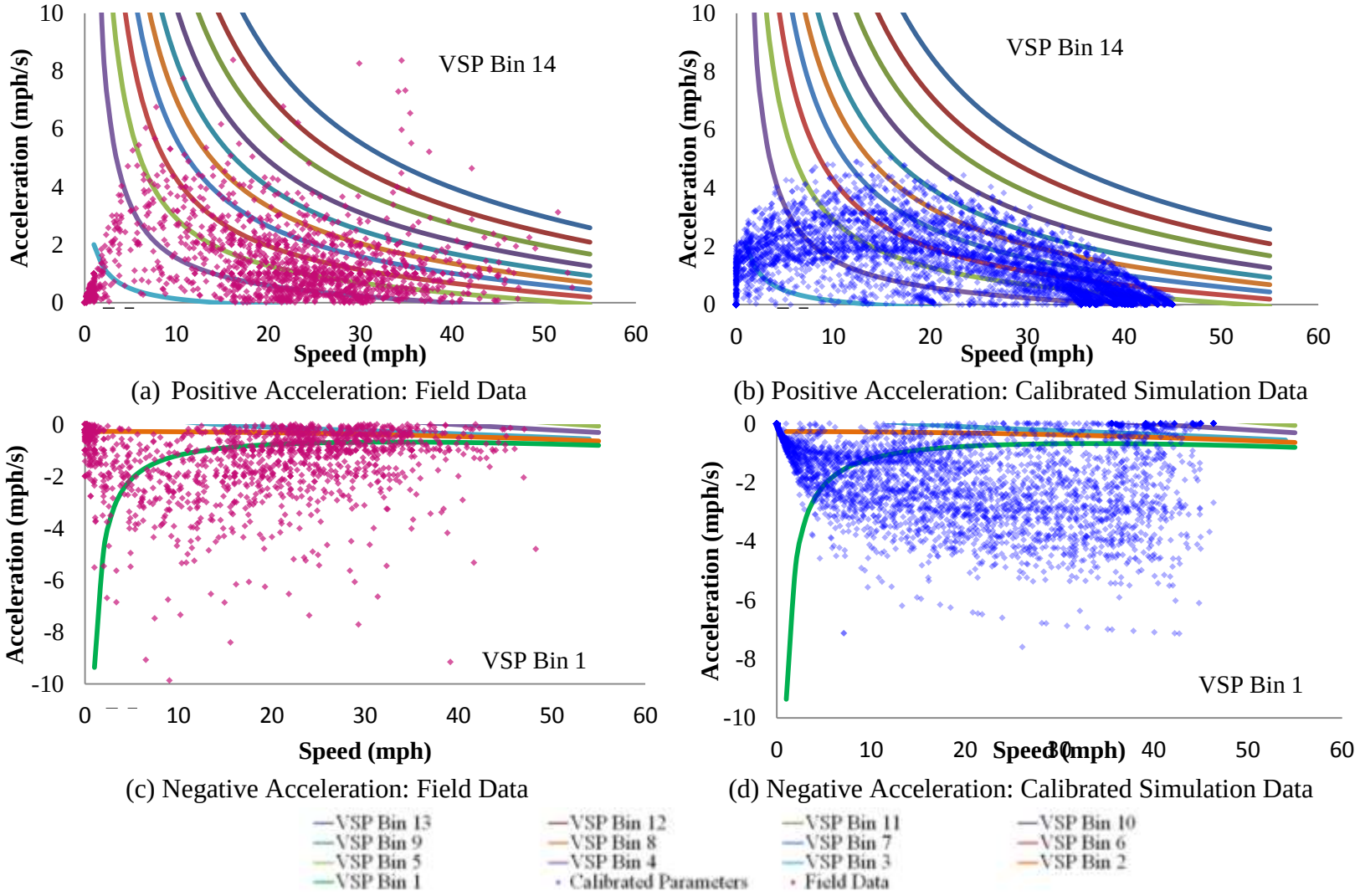

(a) Positive Acceleration: Field Data

(b) Positive Acceleration: Calibrated Simulation Data

(c) Negative Acceleration: Field Data

(d) Negative Acceleration: Calibrated Simulation Data

Figure 22 Positive and negative accelerations from calibrated AIMSUN vehicle activity and field data

Several points may be noted from Figures 20 and 22**:**

1. Between 0-3 mph, the empirical speeds and positive accelerations follow a linear relationship. J. Zhang et al. (2012) observed a similar trend in empirical trajectories of buses in urban networks in London, UK and attributed it to gear changing behavior at very low speeds. This relationship is not observed for the simulated data points where at a speed of 0 mph, accelerations up to up to 2.5 mph/s and 2 mph/s are observed in the default and calibrated models respectively.
2. Between 20-35 mph the empirical speed-acceleration pairs are mostly **concentrated** between VSP Bins 2-7, while the simulated data under default parameters are **spread** between VSP Bins 6-13.
3. Between 30-45 mph, the speed and positive acceleration pairs simulated under default parameters are **concentrated** in Bins 4-9, while empirical speed-acceleration pairs are **scattered** across nearly all the VSP Bins.
4. Between 32-45 mph, the speed and positive acceleration pairs simulated under calibrated parameters are **concentrated** in VSP Bins 5-8.
5. Most of the speed and negative acceleration (deceleration) pairs in simulation activity under both conditions are in VSP 1.

The observations above serve to indicate that although the VSP distribution of simulated activity in a calibrated model is closer to the VSP distribution of field vehicle activity than VSP distribution from the default model, at the second by second level, the proportions in VSP Bins are not due to similarity in the speed-acceleration patterns.

In the simulation model with default parameters, most of the accelerations between 5mph and 35mph were in the range of 4-6 mph/s while empirical accelerations were seldom above 4 mph/s. Between 5-35 mph the positive accelerations from simulation under default parameters appear to be separated into two bands. The lower band ranges between 1.1 mph/s and 3 mph/s while the upper band covers 4.7 mph/s to 7.5 mph/s. An explanation for this could be that the higher band represents the activity during which vehicles which are able to try and achieve their maximum desired speeds by applying higher accelerations. The lower

band may represent activity during which vehicles are constrained by other vehicles, road geometry or signal phasing, allowing vehicles to reach desired speeds by applying lower accelerations.

Once calibrated with the PEMS 95th percentile parameter distributions for acceleration and deceleration, the accelerations between 15 mph and 30 mph are concentrated between 2-4 mph/s while empirical accelerations are concentrated between 0-3 mph/s. In Figure 22(a), the field data clearly shows more scatter with few points of very high acceleration which may an issue with data quality. The field-observed decelerations also show more scatter than the calibrated simulation model. Most of decelerations from the calibrated simulation model are below 4 mph/s. Figure 22(b) shows that low accelerations under calibrated simulations are concentrated between 35-45mph. This is due to the simulated vehicles reaching either their maximum desired speeds or the speed limit and not being able to accelerate further. This behavior is not observed in the field data. The field vehicles experience low accelerations between 20 and 30 mph as shown in Figure 22(a). This is an indication that even if vehicle in the field have high maximum desired speeds, they do not often reach the higher speeds, as shown by the fewer scatter points between 40 mph and 55 mph.

Overall, it is clear from that the second-by-second vehicle activity from simulation under default parameters shows a different pattern from that which is observed in the field. The vehicle activity data from the calibrated model represents the empirical vehicle activity more closely, although still showing differences that contribute to the differences in emissions calculated at the route and section-level analysis. To demonstrate how the distribution of positive and negative accelerations differ between the empirical and simulated data under calibrated parameters, the speeds in each data set were binned into intervals of 10 mph between 0 mph and 50 mph. The distribution of accelerations in each speed range is shown in Figure 23. The distributions of speed within each 10 mph speed bin are shown in Figure 24.

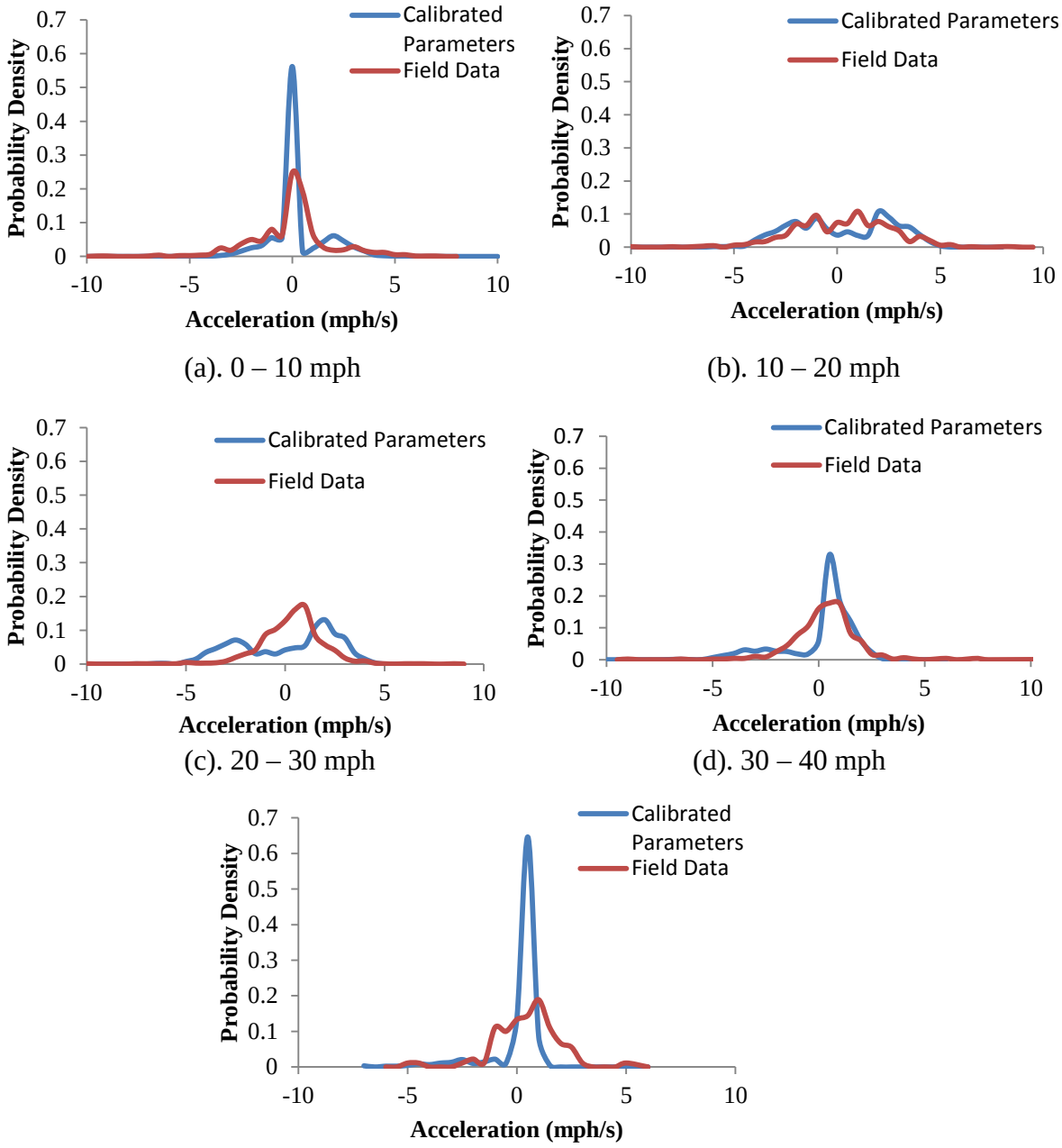

(a). 0 – 10 mph

(b). 10 – 20 mph

(c). 20 – 30 mph

(d). 30 – 40 mph

(e). 40 – 50 mph

Figure 23 Distribution of empirical and simulated accelerations in 10mph speed bins

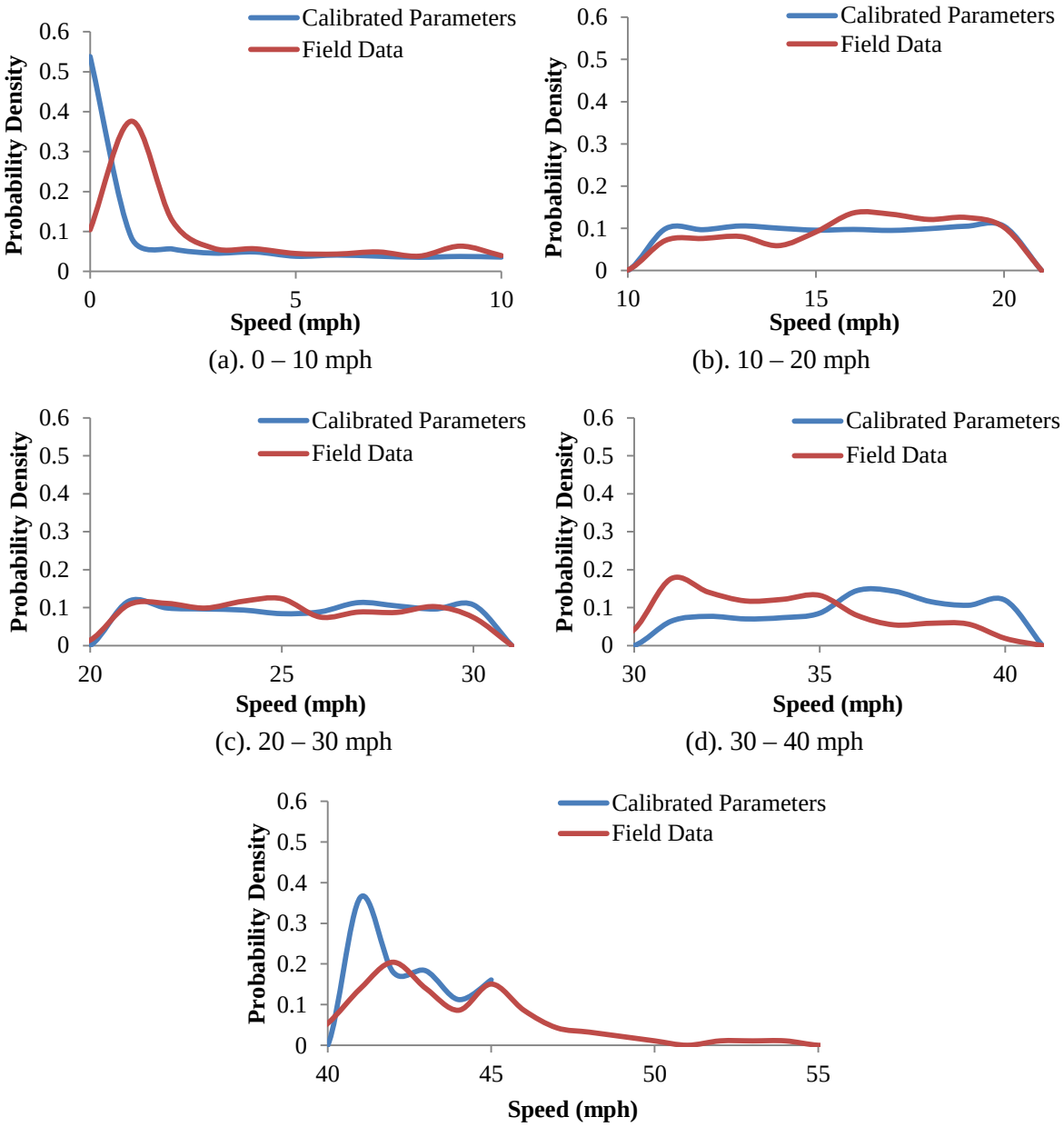

(a). 0 – 10 mph

(b). 10 – 20 mph

(c). 20 – 30 mph

(d). 30 – 40 mph

(e). 40 – 50 mph

Figure 24 Distribution of empirical and simulated accelerations in 10mph speed bins

Based on Figure 23, we can infer that the accelerations within the 10 mph speed bins follow different distributions for empirical and simulated data. Without making any assumptions about the distributions of accelerations within each speed bin, KS-tests were performed to check the null hypothesis that the distributions come from the same populations. KS-tests were also performed on the speed data from the two data sets. The results of the test are reported in Table 19.

Table 19 KS-Test Results of Empirical vs. Simulated Speed and Acceleration Distributions on the Hillsborough Westbound Route

	Speed		**Acceleration**	
Speed bin (mph)	**P-value**	**Hypothesis**	**p-value**	**Hypothesis**
0-10	< 2.26E-16	Reject H_0	< 2.26E-16	Reject H_0
10-20	1.28E-09	Reject H_0	4.57E-05	Reject H_0
20-30	0.0002	Reject H_0	< 2.26E-16	Reject H_0
30-40	< 2.26E-16	Reject H_0	5.87E-11	Reject H_0
40-50	0.0004	Reject H_0	2.57E-10	Reject H_0

The test results confirm that the distributions of accelerations within each speed bin from field data and the simulated data from the calibrated AIMSUN model are different. From Figure 23, we see that between 0 – 10 mph, 30 – 40 mph and 40 – 50 mph, the accelerations and decelerations of simulated vehicles are lower and have less variability than vehicles in the field. For the speed bins 10 – 20 mph and 20 – 30 mph, the simulated data shows that the distributions of positive and negative accelerations are somewhat bi-modal in nature. The speed bin 10- 20 mph indicates stop and go motion. The simulated deceleration behavior in this speed bin appears to be very close to what is observed in the field. The field data shows a higher proportion of observations with lower acceleration values than the simulated data. Between 20 – 30 mph, the field data appears to be uni-modal in nature, centered around low accelerations/decelerations, but with some spread in the data. The simulated data shows that most of the accelerations and decelerations are at the boundary values of the 95^{th} percentile parameter distributions set for the simulation.

Figure 24 shows that the for the speed bins 10-20mph and 20-30mph, the probability densities of simulated speeds is constant, while for empirical data there are more observations of speeds between 15-20 mph and 22-25 mph in the respective speed bins. In the 30-40mph speed bin, the empirical data shows that more observations fall between 30-35 mph while in the simulated data, more observations fall between 35-40mph. Between 40 and 55 mph, there is a peak in simulated speeds around 42 mph, which is the mean of the calibrated maximum desired speed value and 45mph which is the speed limit. The empirical data shows observations beyond 45mph up to 55mph. The KS test results also show that the distributions of speeds within each speed bin from field data and the simulated data from the calibrated AIMSUN model are different.

At the second-by-second level, vehicle activity differs significantly between simulation under calibrated parameters and field tests. The estimation of emissions was improved at the route level when the simulation parameters were calibrated with PEMS 95^{th} percentile values of acceleration and decelerations and PEMS maximum values of speeds. However, the differences in instantaneous speeds and accelerations provide significant clues as to why the simulated VSP distributions and consequently the emissions estimations were not closer to the empirical estimations. It should be noted that these observations from simulated data are made for a sample of simulated vehicles which have the same travel time distribution as the vehicles in the field. The next section presents the VSP modal analysis of vehicles selected from the calibrated AIMSUN model based matching the average number of stops along the route from the field-tested vehicles.

5.3.3 Sample Selection Based on Average Number of Complete Stops

According to Rakha & Ding (2003), the aggressiveness of a vehicle stop has significant impacts on the vehicle's tailpipe emissions, especially for pollutants such as HC and CO. While decelerations associated with stops and cruising at cruise speeds between 5 to 75 mph have relatively lower impact on emissions, acceleration levels can significantly affect emissions. Therefore, accelerations associated with several stop cycles during a trip can increase emissions on the route. It was hypothesized that some of the differences in emission rates between the field-based and calibrated simulation-based estimates in the previous

section may be attributed to a discrepancy in the number of stops between the samples. This section presents the emissions estimates from simulated trajectories that had the same number of stops on average as field-observed vehicles.

For the purposes of this analysis, a complete stop was defined as the cycle of decelerating to a speed below 5 mph followed by accelerating to a speed above 15 mph. If a vehicle advances up the length of queue by stop-and-go motion, without accelerating to a speed beyond 15mph, it will still be considered to have completed one stopping cycle rather than several. The rationale behind selecting a seemingly arbitrary threshold speed of 15 mph when accelerating is that in both simulated and empirical trajectories, there are instances in which vehicles fluctuate above and below 5mph but still travel at low speeds (under 15mph) until accelerating back to a higher desired speed in response to surrounding conditions. To identify complete stops from several hundred simulated vehicles per simulation replication of the route, an automated process is required to make the process of calculating the number of stops from second-by-second trajectory data feasible. In this thesis, since a "complete stop" is defined as a stopping cycle, the threshold speed to which a vehicle must accelerate beyond, to complete the stopping cycle was set as 15 mph to avoid counting the same stop several times and misrepresenting the trajectory data.

A definition of a stopping cycle based on the amount of time spent below 5mph was also considered; however, it was observed that some simulated trajectories spent very little time below 5mph (< 5seconds) before accelerating to speeds as high as 20 or 30 mph in the stopping cycle. On the other hand, some simulated trajectories spent longer time below 5 mph, but also exhibited stop-and-go motion at low speeds, which led to double counting the total number of stops in the automated stop identification macro. Appendix E contains the macro created in Microsoft Excel to identify the number of stops from second-by-second data. The threshold speed of 15 mph can be changed easily in this code if required, but is kept the same for the remainder of the analysis presented in this thesis. It should be noted that stops were counted in the same way from field and simulated data to provide a consistent basis for comparison. Figure 25 depicts 5 complete stops observed in vehicle activity collected in the field.

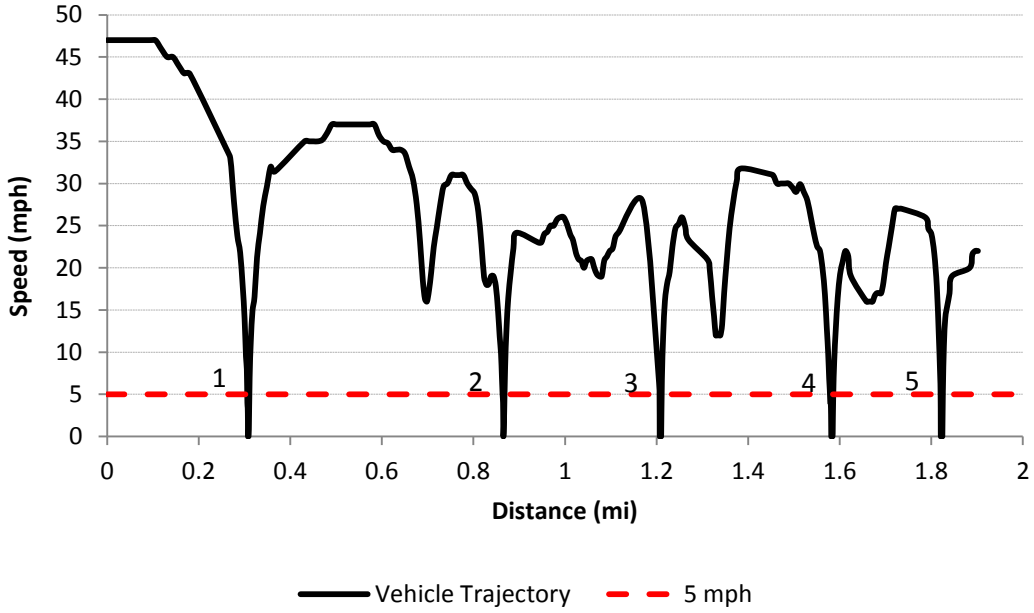

Figure 25 Complete stops along a route

Each of the 14 field-collected trajectories in the Hillsborough Westbound Route was associated a single value of the total number of stops. The average number of stops for the Hillsborough Westbound route was calculated as the average of the total number of stops in each trajectory. The average number of stops from all simulated vehicles on the route was larger than the average number of stops for real-world vehicles under the same conditions. The average number of stops of 2,633 simulated vehicles on the westbound route was 4.41 with a standard error of 1.27 stops while the 14 field-tested vehicles showed 3.86 stops on average with a standard error of 1.46 stops.

Following this, 30 new simulated trajectories were selected from the calibrated AIMSUN simulation model such that the average number of stops of the sample of trajectories was the same as the field-observed average. Since on average, the number of stops in the simulated trajectories was larger, completely random selection of the trajectories would have resulted in most samples having a higher average number of stops. As such, the trajectory selection was made with some intentional bias so as to match the average number

of stops observed in the field. First, a random sample of 30 vehicle trajectories was selected and sorted by the number of stops. Based on personal judgment any outliers were replaced by trajectories with a similar number of stops as observed in the field until the average number of stops was statistically the same as the average number of stops from the field data. The t-test was used to confirm that the average number of stops was same as in field data. Automation of this selecting process is possible using optimization tools and is described in Appendix F.

VSP modal analysis was performed on the sample of 30 simulated trajectories at the route- and section levels. The details of the sample tested are presented in Table 13. The average travel time from each sample (T_s) is compared to the average travel time observed in field-collected trajectories (T_f) using the t-test. The distribution of travel times in simulated sample is compared to the travel time distribution in the field data using the KS-test. The sample's average travel time and travel time distribution were found to be different from the field tested samples.

Table 20 Details of the Sample with Same Average Numbers of Stops as Field Data

Sample	Avg. No. of Stops	Avg. Travel Time (min)	No. of Data points	P-value of t-test (H_0: $T_f = T_s$) *Hypothesis*	P-value of KS-test (H_0: Distribution of T_f = Distribution of T_s) *Hypothesis*
Field Data	3.86	6.12	5,119		
Simulated	3.90	5.05	9,222	0.0005 *Reject H_0*	0.001 *Reject H_0*

Route Level Analysis

For the sample of 30 vehicle trajectories from simulation with same average number of stops as the field sample, the VSP distributions were found using the equation and binning approach of North Carolina State University (2002). Figure 26 shows the distribution for the vehicle activity in the simulated sample with average number of stops controlled in comparison to the field sample and the sample tested in Section 5.3.2 where the travel time distribution was controlled.

The Chi square test with the same bin groupings as in Section 5.3.2 indicated that the simulated sample with same average number of stops as field data was not able to reproduce the VSP distribution observed in the field data. However, the travel times on the arterial between simulated sample and field data are statistically different and as such, the observation in Figure 26**,** that the average number of stops controlled sample is not close to field data, can be misleading. For instance, while the VSP distribution of the sample with the average number of stops controlled shows that the proportion of time spent in cruise modes is higher, the actual number of seconds of data observed in the cruise mode may in fact be fewer than in the travel time controlled sample, since its overall travel time is lower. As such, the differences in emission rates of the simulated samples with the field-based estimates are more important.

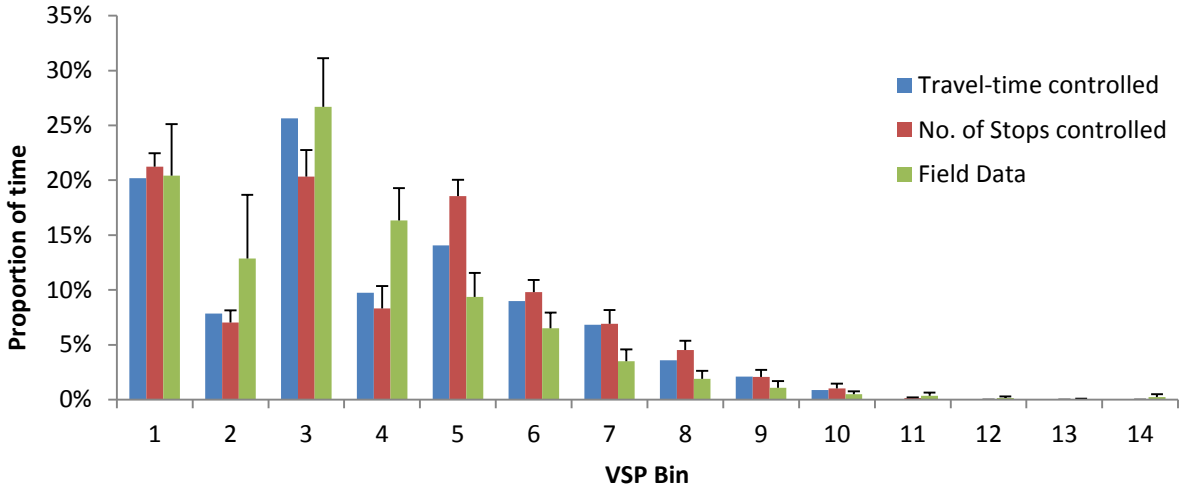

Figure 26 VSP distributions of travel time and no. of stop controlled simulated samples and field data

The VSP distributions of the 30 trajectories in the average number of stops controlled sample were coupled with the fleet average modal emission factors defined previously and the average emissions per unit distance of from the sample were obtained. Table 21 presents the results in comparison to field-based emissions estimates.

Table 21 Simulated Route-level Emissions of Samples Controlled for Average Numbers of Stops

Sample	NO_x (mg/mi) (Std. Error)	HC (mg/mi) (Std. Error)	CO (mg/mi) (Std. Error)	CO_2 (g/mi) (Std. Error)
Field	153 (*9.16*)	111 (*4.80*)	894 (*58.5*)	420 (*18.3*)
Simulated – 1	145 (*7.10*)	91 (*4.99*)	793 (*37.0*)	346 (*18.8*)
% Diff.	-5%	**-18%**	-11%	**-17%**

*Bolded figures indicate differences that are statistically significant at the 5% significance level

Table 21 shows that the differences between field-based and simulation-based estimates of all pollutants are negative. The absolute differences in emissions are within 20% across all pollutants. The absolute differences in emissions per unit distance of NO_x and CO are lower than for HC and CO. These differences in estimates of may be due to the lower average travel time of trajectories in the stop controlled sample, compared to the field-based vehicle activity.

To investigate the relationship between stops and travel time, 10 samples of 30 trajectories each were selected from the calibrated simulation model. 5 samples, each containing 30 trajectories, had the same average number of stops as the field data. The remaining 5 samples were selected to match the travel time distribution as field observed data. The 10 samples are plotted in Figure 27.

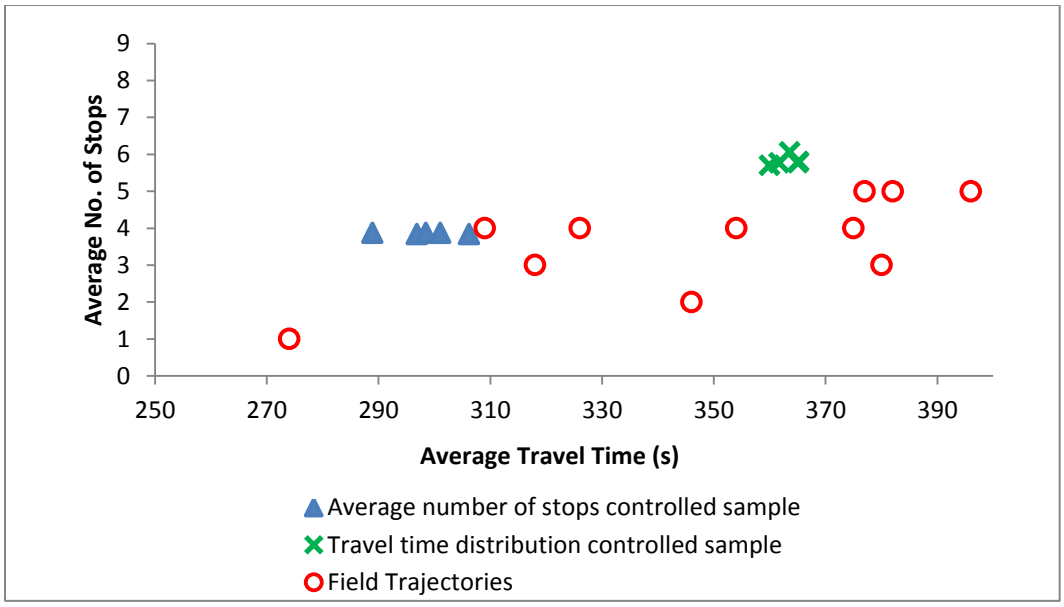

Figure 27 Relationship between average number of stops and average travel time for travel time distribution controlled and average number of stops controlled samples compared to field data

The average number of stops from field trajectories is 3.86 and the average travel time is 367. There is high inter-trajectory variability in the travel times of field trajectories as shown in Figure 27, although the trend is that as travel time increases, the number of stops increases. When the travel time distribution is controlled, the average numbers of stops in simulated trajectories is higher for all 5 samples than the average of all field trajectories. Conversely, for the average number of stops controlled samples, the average travel time is in much lower than the average travel time from field data. In simulation samples there is a positive correlation between the average number of stops and average travel time of samples. The field-collected sample of trajectories has a high average travel time, but a low average number of stops. Therefore, to match the average driving cycle observed in simulation with the average driving cycle in the field, it may be necessary to control for both the travel time and the average number of stops in the sample of selected trajectories. VSP modal approach is based on the combination of instantaneous speeds and accelerations, which vary between driving cycles. The emissions analysis on simulated vehicle activity may not produce results that are based on unrealistic driving cycles when either the travel time distribution or average

number of stops is controlled alone. As such the next section focuses on investigating the emissions from a selected sample of simulated trajectories which have both the same travel time distribution and average number of stops as field data.

5.3.4 Controlling for both travel time and avg. no. of stops

In order to control for both the travel time distribution and the average number of stops in a sample of 30 trajectories, the Latin Hypercube method in Section 5.3.3 was employed to identify stratifications at 0.2 intervals of the probability density of field-observed trajectory travel times. 6 trajectories were selected from each interval and the average number of stops was calculated. To match the average number of stops, the outlier trajectories were replaced by other trajectories with closer number of stops to the field-observed trajectories from the same intervals. The details of the selected sample are presented in Table 22.

Table 22 Details of Simulated Sample with Same Average Number of Stops and Travel Time Distribution as Field Sample

Sample	Avg. No. of Stops	Avg. Travel Time (min)	Number of data points	P-value of t-test (H_0: $S_f = S_s$) *Hypothesis*	P-value of KS-test (H_0: Distribution of T_f = Distribution of T_s) *Hypothesis*
Field Data	3.87	6.11	5,119		
Calibrated Simulated	3.87	5.99	10,787	0.6314 *Fail to Reject H_o*	0.9134 *Fail to Reject H_o*

The VSP distribution of the sample with matching travel time distribution and average number of stops as field data was compared to the travel time distribution controlled sample from Section 5.3.2 and the field sample. The stop controlled sample from Section 5.3.3 was not included because the average travel time of the sample was lower than the other two simulated samples and the field sample. The distribution is shown in Figure 28.

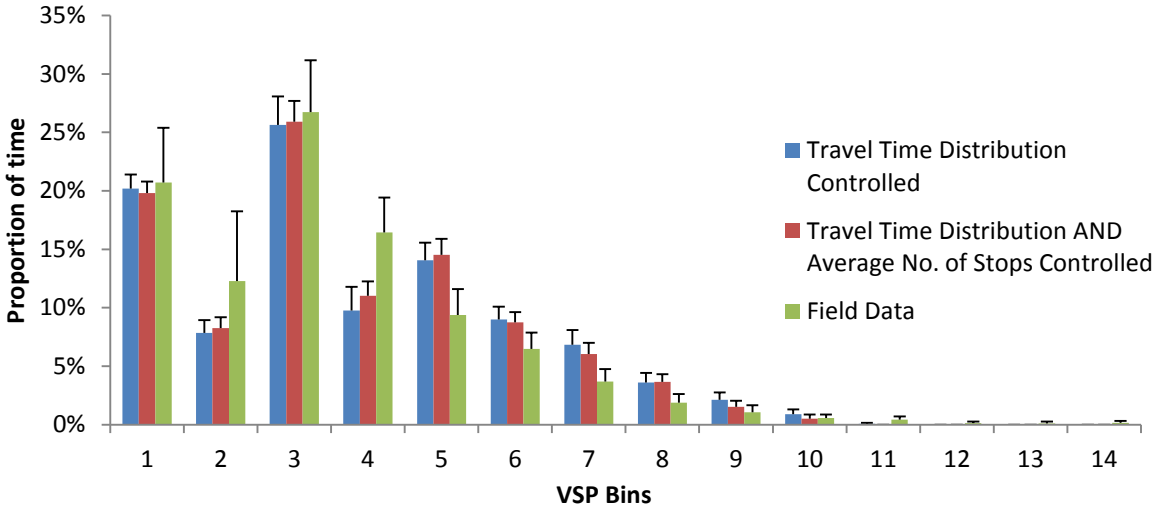

Figure 28 VSP distribution of travel time distribution and average number of stops controlled simulated samples and field data

There are very subtle differences between the VSP distributions of the two simulated samples. The sample with both travel time distribution and average number of stops matched with field data have more observations in Bins 5-6 and fewer observations in Bins 7, 9 and 10. The higher bins 7-10 represent accelerations at higher speeds than in Bins 4-6. A Chi-square test using the same bin grouping in Section 5.3.2 showed that the differences between the travel time distribution and average number of stop controlled sample is significantly different from the field-based VSP distribution although the test statistic was found to be smaller than the travel time distribution only controlled sample. The main differences between field-based and simulated vehicle activity were still observed in Bins 7-9. The results from applying the VSP modal approach to this sample is presented in Table 23.

Table 23 Route-level emissions from simulated sample with same travel time distribution and average number of stops as field data

		NO (mg/mi) (Std. Error)	**HC (mg/mi)** (Std. Error)	**CO (mg/mi)** (Std. Error)	**CO_2 (g/mi)** (Std. Error)
Field Data	Rate	153 (*9.16*)	111 (*4.80*)	894 (*58.5*)	420 (*18.3*)
Calibrated model: Travel time distribution controlled only	Rate	183 (*3.09*)	118 (*2.33*)	1031 (*20.3*)	448 (*8.53*)
	% Diff.	**20%**	**6%**	**15%**	7%
Calibrated model: Travel time distribution and average number of stops controlled	Rate	176 (*2.61*)	115 (*1.68*)	990 (*18.9*)	436 (*6.2*)
	% Diff.	**15%**	3%	11%	4%

*Bolded figures indicate differences that are statistically significant at the 5% significance level

Table 23 shows that when the simulated sample of trajectories was chosen based on having both the same travel time distribution and average number of stops as field trajectories, the emissions estimates were closer to the field-based estimates across all pollutants than when only the travel time distribution was controlled. The differences in emissions of CO_2 and HC per unit distance were below 5%, while the difference in estimates of NO and CO were at or below 15%. Only the estimation errors for NO_x were found to be were statistically significant. These emissions estimates are an improvement over the estimates from controlling only travel time distribution or average number of stops alone. Therefore at the route-level, vehicle activity of a sample of simulated vehicles from a calibrated model with travel time distribution and average number of stops same as in the field, may be used to accurate estimate emissions on an interrupted arterial road.

Section-level Analysis

The methodology in Section 5.3.2 was applied to the sample of 30 simulated trajectories with the same travel time distribution and average number of stops as field data to calculate emission rates for each of the 13 sections on the Hillsborough Westbound route. The results are presented in comparison to the section-level emissions from the sample of simulated trajectories with the same travel time distribution as field data. The section-level emissions estimates from field data are also presented in Figure 29.

Figure 29 Section Level Analysis comparing samples with varying average number of stops to empirical data

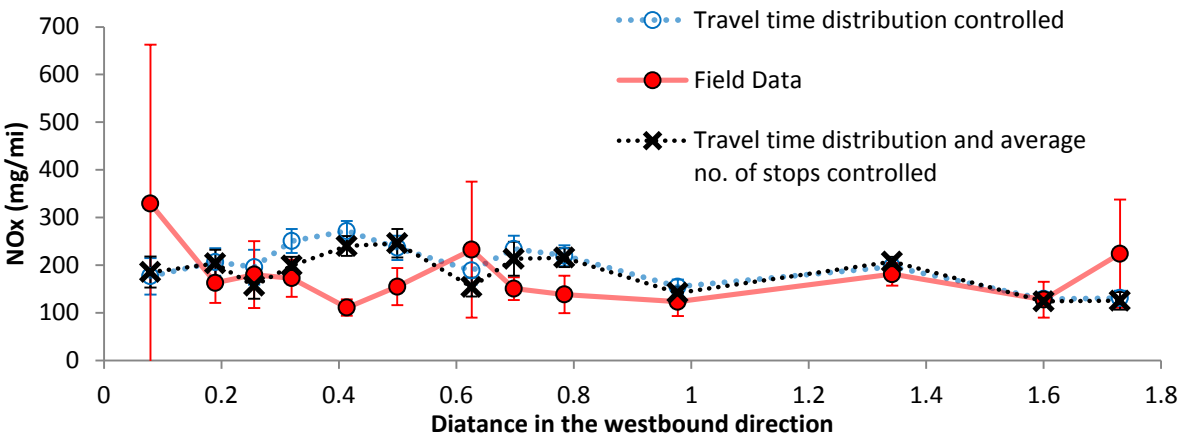

(a) Nitrogen Oxide (NO_x)

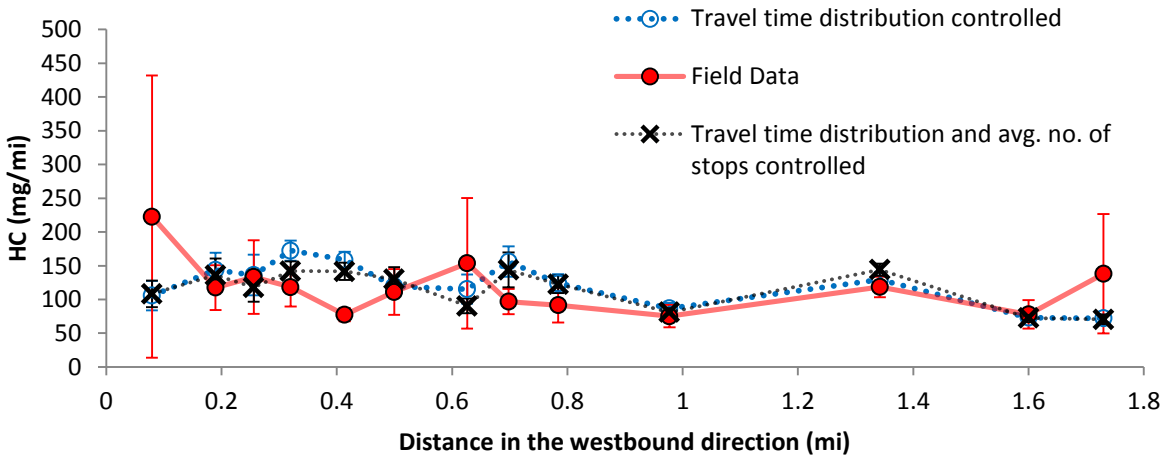

(b) Hydrocarbons (HC)

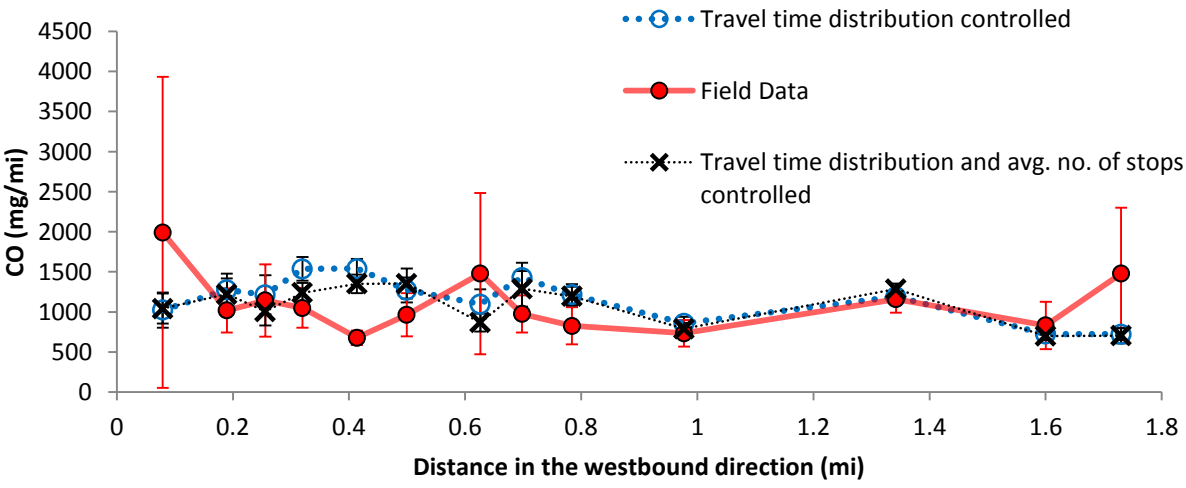

(c) Carbon Monoxide (CO)

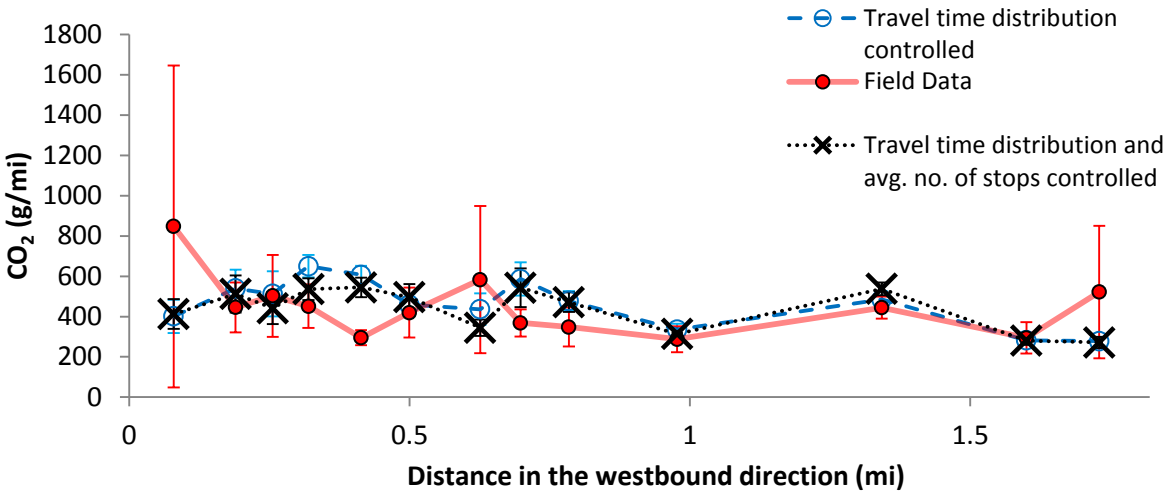

(d) Carbon Dioxide (CO_2)

A visual inspection of the results from the section level analysis shows that the emissions of NO, HC, CO and CO_2 per unit distance from the simulated sample with the travel time distribution and same number of average stops as field-tested vehicles produces lower emissions estimates at two sections than the travel time distribution controlled sample. This may be a due to fewer stops being made on average at the intersections contained in these sections. Both these sections are in the eastern end of the corridor where the spacing between intersections is small. It fails to capture the hotspot at section (7) Brooks and estimates lower emissions at this section than the travel time distribution controlled sample. As a result, the emission rates are closer to field-based estimates at some of the sections – (4) Horne, (5) Pogue, (8) Dan Allen (9) Dixie. It should be noted that the same emissions hotspots are captured or missed by both the samples from simulated data. Where the arterial has closely spaced intersections both simulation samples are not able to detect the exact locations of the emissions hotspots.

5.3.5 Summary of Calibration Results

Based on the results from Section 5.2, calibrating the parameters of internal behavioral models in the AIMSUN micro-simulator platform to generate more realistic vehicle activity on arterial segments improves the emissions estimates using the VSP modal approach. Under calibrated parameters, vehicle behavior on arterials is more realistic because the accelerations and speeds are constrained to the range of values observed in the field. The truncated normal distributions of three simulation parameters were defined using 95^{th} percentile values from each vehicle trajectory along the routes followed in the field.

Initially VSP modal based emissions estimates were compared between samples of simulated and real-world vehicles that have the same travel time distribution. Further analysis found that emissions estimates were sensitive to both the average number of stops and travel time distribution along a route and matching both these factors with observed field trajectories yielded better estimates of emissions from simulated vehicle activity. Table 24 summarizes the emissions estimations from calibrating the simulation model and comparing emissions estimates from simulated vehicle activity based on either the field-observed travel time distribution or the average number of stops and a combination of both factors.

Table 24 Summary route-level emissions on Hillsborough Westbound route from calibration of AIMSUN model and sample selection

Sample		**NO (mg/mi)** (Std. Error)	**HC (mg/mi)** (Std. Error)	**CO (mg/mi)** (Std. Error)	**CO_2 (g/mi)** (Std. Error)
Field Data	Rate	153 (*9.16*)	111 (*4.80*)	894 (*58.5*)	420 (*18.3*)
AIMSUN Default	Rate	221 (*3.52*)	128 (*2.77*)	1285 (*24.5)*	485 (*10.6*)
	% Diff.	**45%**	15%	**44%**	**16%**
Calibrated (Travel time distribution controlled)	Rate	183 (*3.09*)	118 (*2.33*)	1031 (*20.3*)	448 (*8.53*)
	% Diff.	**20%**	**6%**	**15%**	7%
Calibrated (Avg. no of stops controlled)	Rate	145 (*7.10*)	91 (*4.99*)	793 (*37.0*)	346 (*18.8*)
	% Diff.	-5%	**-18%**	-11%	**-17%**
Calibrated (Travel time distribution and avg. no of stops controlled)	Rate	176 (*2.61*)	115 (*1.68*)	990 (*18.9*)	436 (*6.2*)
	% Diff.	**15%**	3%	11%	4%

*Bolded figures indicate differences that are statistically significant at the 5% significance level

5.4 Application of Emissions Estimation Methodology on Eastbound Direction

In the previous section, vehicle activity data from a calibrated model of the AIMSUN micro-simulation software were coupled with Vehicle Specific Power-based modal emission factors to predict emissions along an arterial. Testing the effect of sampling simulated vehicle activity based on field-observed travel time distribution or the average number of stops showed that simulated driving cycles are better matched with field driving cycles when both these factors are the same as in field data. Subsequently the estimate emissions from the simulated activity on the arterial are closer to field-based estimates. This methodology was applied to the peak direction of traffic during the afternoon peak period in the previous section. This section demonstrates the robustness of the proposed methodology by applying it to the non-peak direction of traffic flow in the same peak hour period in the afternoon.

The eastbound traffic starts at the off-ramp from I-440 in the western end of Hillsborough Street in the study area heads east towards the downtown area of the City of Raleigh. Figure 30 shows the Hillsborough Eastbound route in marked in blue.

Figure 30 Hillsborough Street corridor and routes

During the afternoon peak period (5-6pm), the traffic volumes in the eastbound direction are lower than in the westbound direction. In addition, progression is maintained on in the direction of peak traffic (i.e. westbound traffic) rather than on the eastbound direction. As a result, more variation in travel time can be expected for the Hillsborough Eastbound route in the afternoon peak hour.

Vehicle activity data from 9 field-tested vehicles were collected on the Hillsborough Eastbound route in the afternoon peak hour. Following the methodology in Section 5.3.4, the travel time distribution and average number of stops from field-data were identified and used as factors to control the selection of a sample of 30 trajectories from the simulation model. Samples of 30 simulated trajectories were thus selected from the calibrated and default AIMSUN models. The details of the samples from Hillsborough Eastbound Route on which route level, section-level and second-by-second level analysis were then performed are shown in Table 25.

Table 25 Details of field and simulated-data samples on Hillsborough Eastbound Route

	No. of trajectories	No. of seconds	Avg. No. of Stops	Avg. Travel Time/min (Std. Error)	P-value of T-test (H_0: $T_f = T_S$)	P-value of KS-Test (H_0: Distribution of T_f = Distribution of T_S)
Field	9	3,201	3.89	5.93 (*0.48*)		
Calibrated Simulation	30	10,591	3.87	5.91 (*0.21*)	0.9853 (Fail to Reject H_0)	0.99 (Fail to Reject H_0)
Default Simulation	30	10,760	3.90	5.95 (*0.22*)	0.9618 (Fail to Reject H_0)	0.99 (Fail to Reject H_0)

5.4.1 Route level analysis for Eastbound Direction

The route level analysis was completed for the field-collected and simulated samples of vehicle activity data. The VSP distributions are presented in Figure 31. Chi-square tests based on the bin grouping used in the previous section were performed to check if the VSP distributions of the simulated trajectories came from the same population as the VSP distribution from the field data. It was found that neither of the distributions from simulated vehicle activity were the same as the VSP distribution, although the test statistic for the calibrated distribution was much smaller. For the default model, the biggest differences were for VSP bins 10-14 and bins 4-6. It is clear from Figure 31 that under default parameters there are more observations in the higher VSP bins 10-14and fewer observations in the lower bins 4-6 than in the empirical distribution. The differences in the distribution under calibrated parameters were most pronounced for VSP bins 4-6 and 7-9. There were more observations in the VSP 7-9 while slightly fewer observations in Bins 4-6.

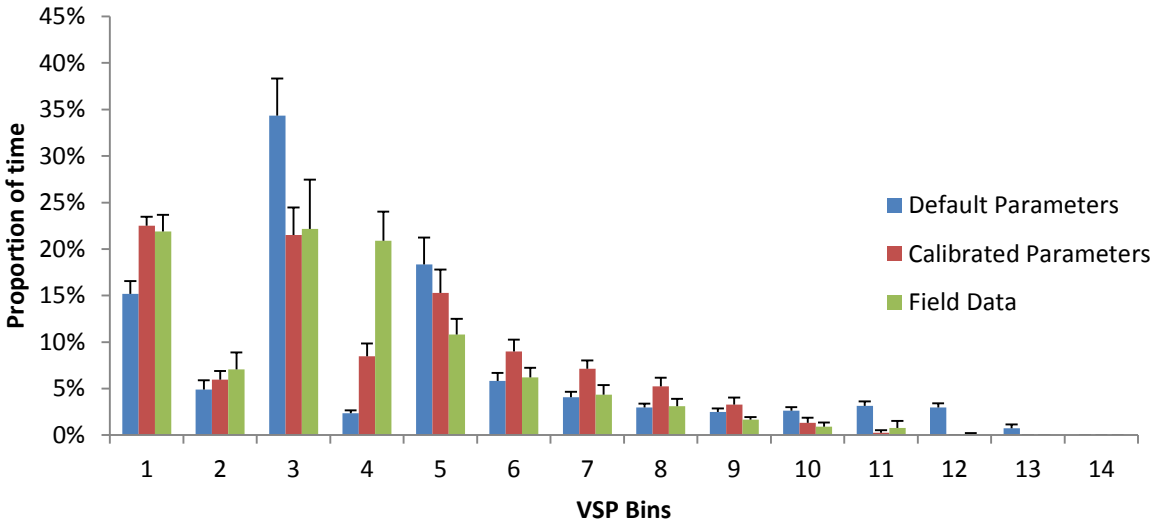

Figure 31 VSP Distributions from simulated and field data on Hillsborough Eastbound Route

The VSP modal approach was followed to calculate the emissions per unit distance using the fleet average modal emission factors developed by Anya et al (2013). The results are shown in Table 26.

Table 26 Route Level Emission Rates per unit Distance from Empirical and Simulated Vehicle Activity on Hillsborough Eastbound Route Based on Samples Controlled for Travel Time Distribution and Average Number of Stops

	Avg. No. of Stops	Avg. Travel Time/min (Std. Error)		**NO (mg/mi)** (Std. Error)	**HC (mg/mi)** (Std. Error)	**CO (mg/mi)** (Std. Error)	**CO_2 (g/mi)** (Std. Error)
Field Data	3.89	5.93 (*0.48*)	Rate	139 (*5.17*)	102 (*3.55*)	745 (*26.5*)	383 (*13.4*)
AIMSUN Default	3.87	5.91 (*0.21*)	Rate	209 (*4.36*)	119 (*1.73*)	1241 (*36.8*)	447 (*6.23*)
			% Diff.	**50%**	**17%**	**67%**	**17%**
Calibrated	3.90	5.95 (*0.22*)	Rate	182 (*3.57*)	112 (*2.01*)	1011 (*27.0*)	422 (*7.27*)
			% Diff.	**31%**	10%	**36%**	10%

*Bolded figures indicate differences that are statistically significant at the 5% significance level

The emissions analysis shows that the vehicle activity data from the both the simulation models cause the overestimation of the emissions per unit distance across all pollutants. The emissions estimates from the simulation model under calibrated parameters are closer to the field-based estimates for NO_x, HC, CO and CO_2 by 7-31%. The differences between the calibrated model and field based model estimates of HC and CO are both 10% and statistically significant at the 5% significance level. Thus it is demonstrated that calibrating the simulation model and applying the proposed methodology of selecting simulation trajectories based on both the travel time distribution and the average number of stops can lead to improved estimates of pollutant emission rates on arterial roads.

5.4.2 Section level analysis for Eastbound Direction

The section level analysis showed that the simulated vehicle activity data led to the overestimation of emissions per unit distance at most sections on the Hillsborough Eastbound route. The calibrated model clearly produced closer estimates at several sections, even when the intersections were spaced at smaller distances towards the eastern end of the corridor. Both sets of simulated data captured the sections with the peak emission rates or the hotspots along the corridor. Under default simulation conditions, some of the rates were highly over-predicted, particularly for the sections Brooks and Faircloth. Figure 32 shows the section-level emissions analysis of the Hillsborough Eastbound route.

Wilcoxon Rank Sum tests indicated that there was enough evidence to suggest that the section-level emissions estimates of NO_x and CO from simulated activity under default parameters are higher than the field-based section level emissions. Under the calibrated parameters, none of the differences in emissions estimates are statistically significantly different from field-based estimates. The results are summarized in Table 27.

Table 27 Summary of Wilcoxon Rank Sum test for Section Level Emissions Estimates on Hillsborough Eastbound Route

Pollutant	Sample 1	Sample 2	P-value of Wilcoxon Rank-Sum Test	Hypothesis (at the 5% significance level)
NO	Default Simulation	Field Data	0.016	Reject H_0
	Calibrated Simulation	Field Data	0.880	Fail to Reject H_0
HC	Default Simulation	Field Data	0.448	Fail to Reject H_0
	Calibrated Simulation	Field Data	0.448	Fail to Reject H_0
CO	Default Simulation	Field Data	0.019	Reject H_0
	Calibrated Simulation	Field Data	0.4793	Fail to Reject H_0
CO_2	Default Simulation	Field Data	0.4483	Fail to Reject H_0
	Calibrated Simulation	Field Data	0.4483	Fail to Reject H_0

Figure 32 Section-level analysis of emissions on Hillsborough Eastbound Route

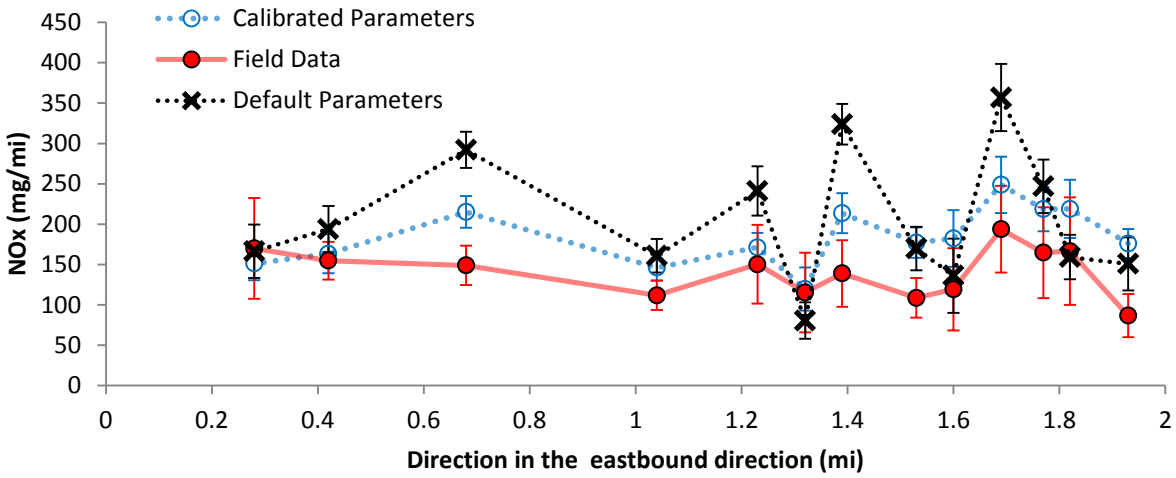

(a) Nitrogen Oxide (NO_x)

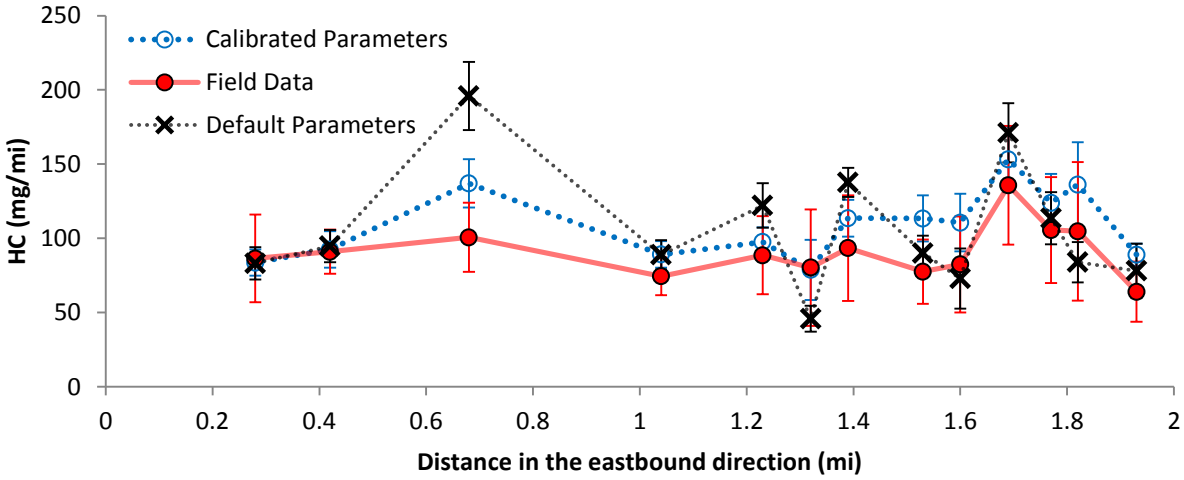

(b) Hydrocarbons (HC)

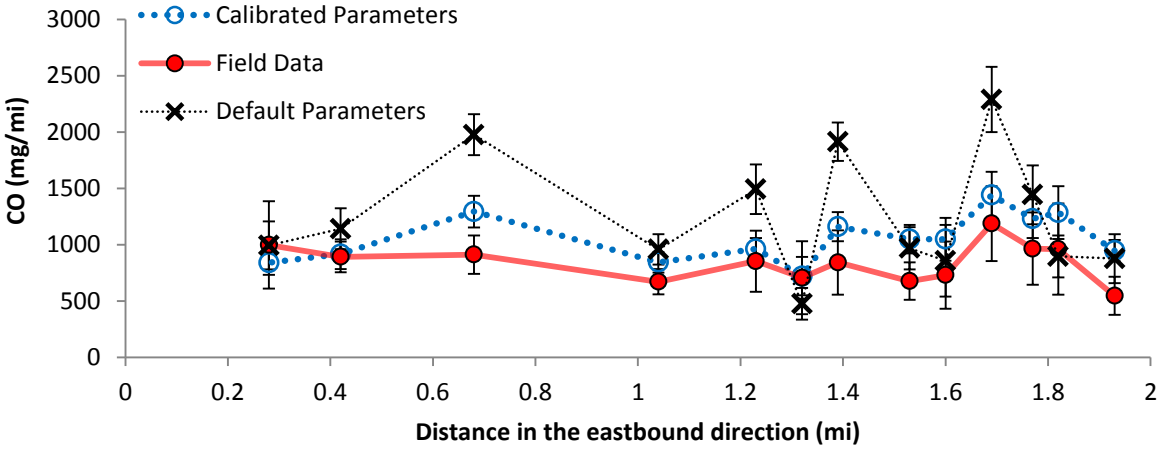

(c) Carbon Monoxide (CO)

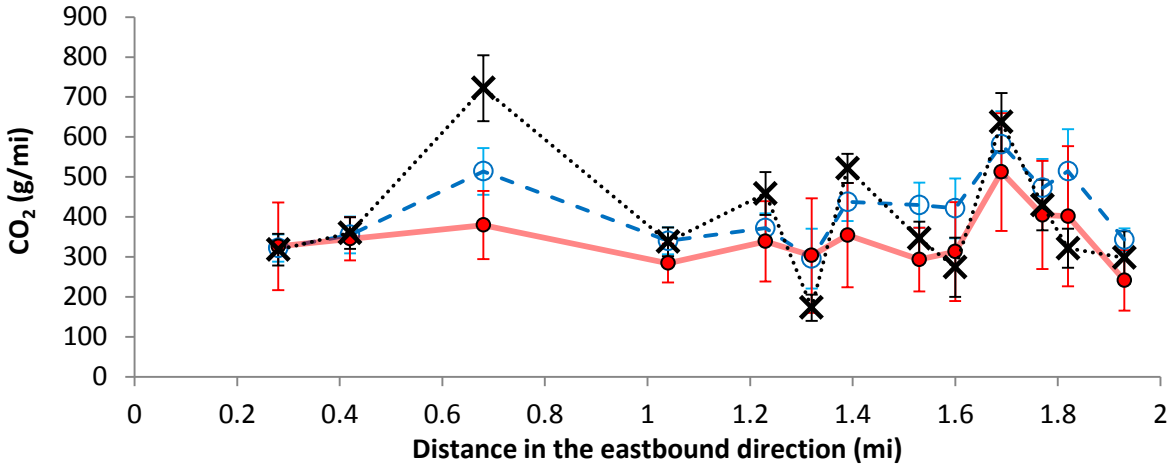

(d) Carbon Dioxide (CO_2)

5.4.3 Second-by-second Level Analysis for Eastbound Vehicle Activity

In the second-by-second analysis of vehicle activity on the Hillsborough Westbound route, it was shown that distributions of simulated accelerations within 10 mph speed bins were significantly different from that of field-observed accelerations. The distributions of instantaneous acceleration within 10mph bins from vehicle activity on the Hillsborough Eastbound route were found to exhibit similar differences as shown in Figure 33.

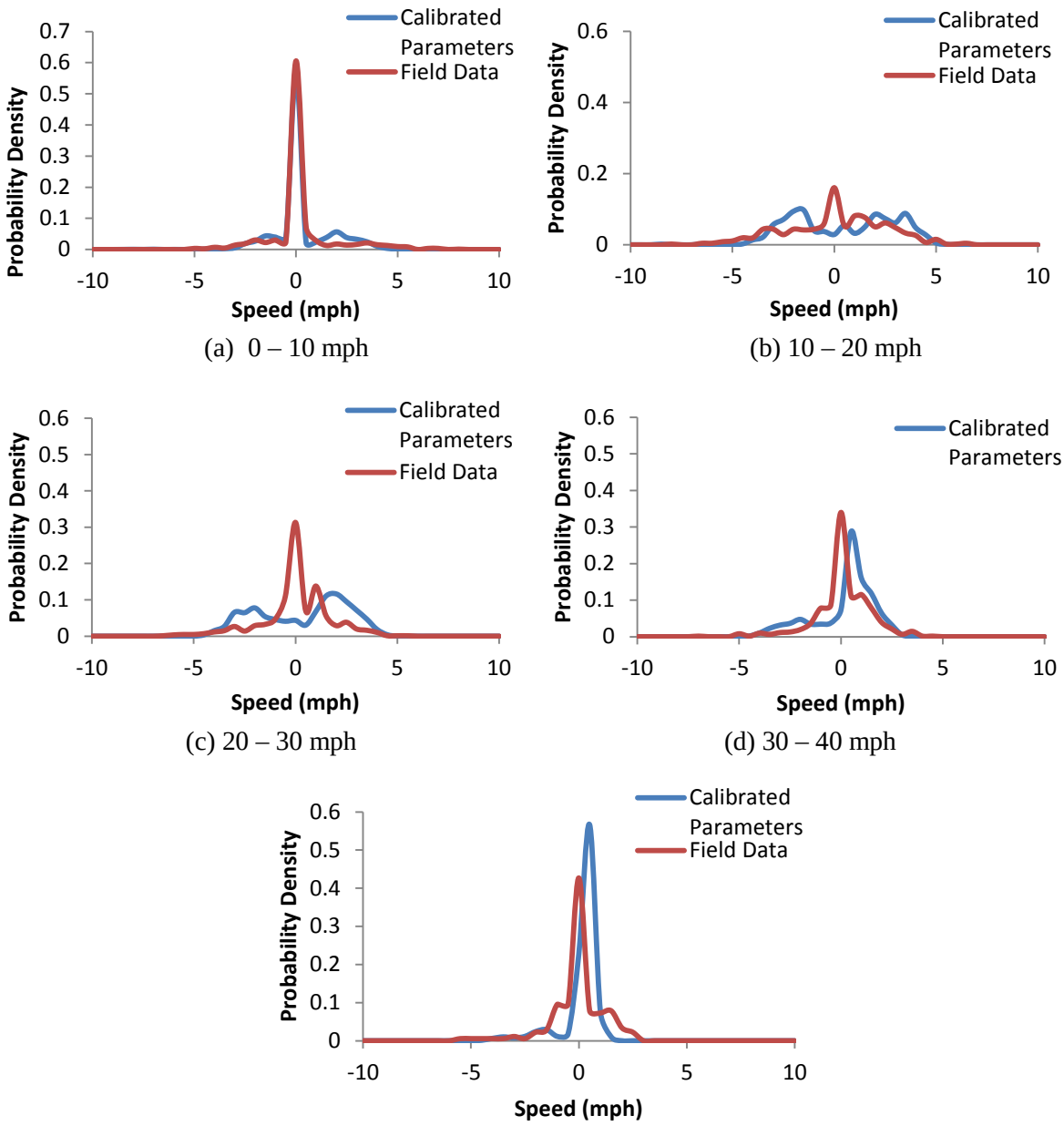

(a) 0 – 10 mph

(b) 10 – 20 mph

(c) 20 – 30 mph

(d) 30 – 40 mph

(d) 40 – 50 mph

Figure 33 Distributions of acceleration in 10 mph speed bins for the eastbound vehicle activity from calibration simulation and field data

In the 10-20mph speed bin, the field-collected vehicle activity shows fewer instances of acceleration or deceleration at a rate of more than 1 mph/s, than simulated vehicle activity.

The 10-20mph speed bin representing stop and go motion shows bimodal accelerations with few observations around 0 mph/s. The same is observed for 20-30mph. This indicates that when simulated vehicles travelling at low speeds between 10 and 30 mph, they accelerate and decelerate sharply in response to road geometry, other vehicles, route choice etc. Field observed vehicles experience lower accelerations and decelerations and more smooth trajectories at these low speeds. In the 30-40mph speed bin, simulated vehicles exhibit some accelerations and decelerations while field-observed vehicles appear to travel at constant speeds. In the higher speed bins, the shapes of the acceleration/deceleration distributions are similar, although the peaks of the simulated distributions are shifted to the right indicating more positive values of accelerations and fewer seconds of deceleration.

Figure 34 shows the distribution of speeds within each of the 10mph speed bins from simulated trajectories under calibrated model parameters and empirical trajectories. The 10-20mph, 20-30mph and 30-40mph speed bins show that there is more variation in the field-observed speeds that the simulated speeds. Simulated vehicles maintain the speed limit set on the corridor and do not go above 45mph while the field data shows some instances of higher speeds in the 40-50mph speed bin.

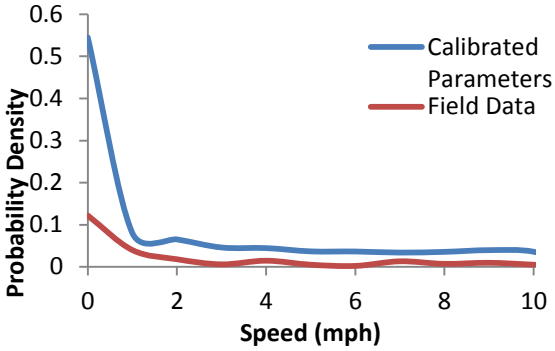

(b) 0 – 10 mph

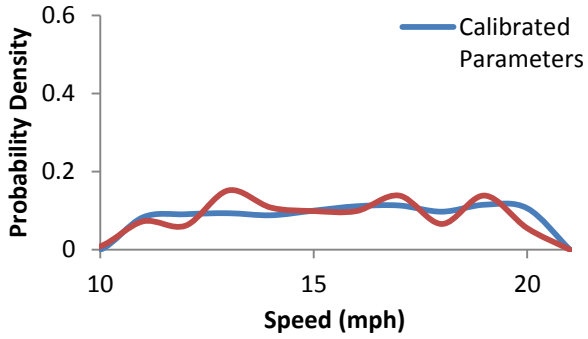

(b) 10 – 20 mph

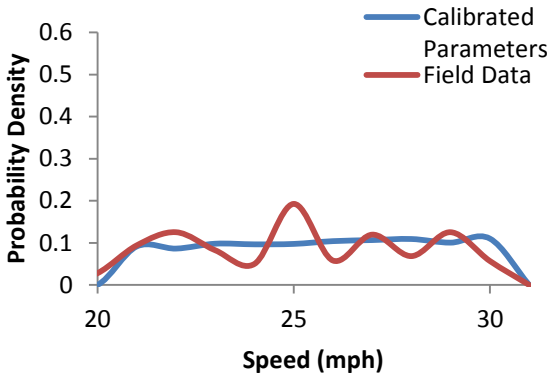

(c) 20 – 30 mph

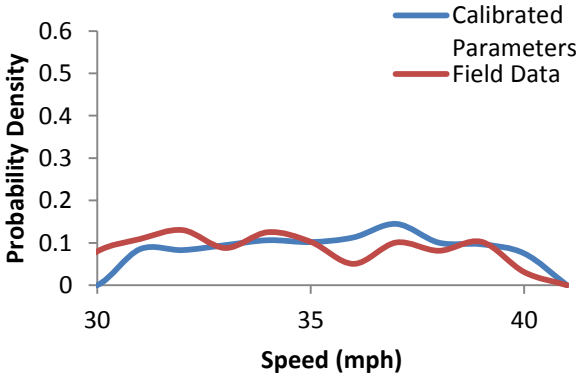

(d) 30 – 40 mph

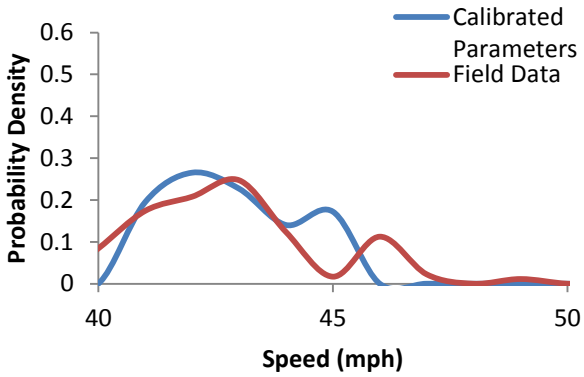

(e) 40 – 50 mph

Figure 34 Distributions of acceleration in 10 mph speed bins for the eastbound vehicle activity from calibration simulation and field data

The results of KS-tests which assessed whether the distributions of speeds and accelerations from simulated and calibrated data within each 10mph speed bin are equal are presented in Table 28. In most cases, there is enough evidence to conclude that the distributions of speeds or accelerations within the 10 mph speed bins are not same. It follows that these differences at the micro-scale vehicle activity lead to differences in estimates of pollutant emissions.

Table 28 KS-Test Results of Empirical vs. Simulated Speed and Acceleration Distributions on the Hillsborough Eastbound Route

	Speed		**Acceleration**	
Speed bin (mph)	**P-value** (H_0: S_{field} = $S_{simulation}$)	**Hypothesis**	**P-value** (H_0: A_{field} = $A_{simulation}$)	**Hypothesis**
0-10	0.003	Reject H_0	0.002	Reject H_0
10-20	0.174	Fail to Reject H_0	4.1E-07	Reject H_0
20-30	7.1E-06	Reject H_0	< 2.2E-16	Reject H_0
30-40	1.9E-12	Reject H_0	< 2.2E-16	Reject H_0
40-50	0.0001	Reject H_0	< 2.2E-16	Reject H_0

5.4.4 Summary of Methodology Application

This section utilized the methodology developed in Section 5.3 to confirm that calibrating selected internal behavioral parameters in AIMSUN simulation improves emissions estimation on arterial roads. The samples of simulated trajectories selected for comparison were based on the same number of stops as field-observed vehicles travelling in the eastbound direction and the distribution of their travel times. Although significant differences in emission rates from the calibrated simulation data were found at the route level for NO and HC and some differences with field-based estimates existed at the section-level, the calibrated vehicle activity and emissions were closer to the field observations than the output from the default AIMSUN model.

Close examination of the second-by-second speed and acceleration pairs from calibrated simulation data indicated that there are significant differences between the instantaneous operations of simulated and real-world vehicles. These differences are apparent

in the quantification of vehicle activity using the VSP binning approach and contribute to the discrepancy in the route and section-level emissions estimates. In the default model, the vehicles achieved higher speeds and accelerations, spending proportions of time in the higher VSP modes associated with higher emission rates.

Chapter 6 Conclusions

This thesis explored two main themes in using micro-simulation modeling tools to investigate the emissions from arterial corridors – (1) using measures of behavioral parameters from field-based vehicle trajectories to calibrate the modeling parameters in AIMSUN (2) demonstrating that individual trajectories from an AIMSUN model with calibrated behavioral parameters can be extracted based on having travel times and average number of stops that are close to field-observed values to estimate emissions accurately. In line with the objectives and scope of this thesis, the calibration process using the VSP modal approach is considered to be supplemental to the established methods of calibration already available in literature and used in practice, and is focused specifically in improving emissions estimates from a micro-simulation model.

In this thesis, the use of empirical vehicle activity data to calibrate the parameters of internal behavioral parameters in AIMSUN microscopic simulation software was demonstrated for a signalized arterial corridor in the Raleigh, North Carolina. The resulting improvement in emissions estimates from the VSP modal approach was validated against empirical vehicle activity-based emissions. However, some limitations of the calibrated simulation model in reproducing the vehicle activity observed in reality on a micro-scale were identified. The subsequent implications for integrating a micro-simulation model with a load-based emissions model are addressed in this chapter by providing the key conclusions from the research effort, recommendations based on the findings, and the scope for future work.

6.1 Major Findings

The AIMSUN micro-simulation software is capable of generating detailed trajectories of individual vehicles in a network. The simulated observations of second-by-second speed and acceleration data for each vehicle can be extracted using an API program that records observations on all physical parts of road network (sections and junctions). The car-following algorithm in AIMSUN is the main behavioral sub-model that computes and updates the instantaneous speed and position of every vehicle in the network during each simulation step.

Other internal behavioral models such as lane changing and gap acceptance play important roles in second-by-second vehicle activity, but due to the limitation of the scope of this thesis, only the car following model was studied in detail. Under the default parameters within the AIMSUN software package, simulated vehicle activity from a signalized arterial corridor at the micro-scale is not representative of real-world vehicle activity. The car following model in AIMSUN simulation directs vehicles such that they maximize their time at the desired speeds or at the speed limit if it is lower than the desired speeds. The simulated trajectories are characterized by sharp accelerations and decelerations and a tendency to remain at a constant speed that is often high. On a signalized arterial corridor, vehicles may need to frequently change speeds as a result of the inherent interruptions associated with an urban arterial road.

Load based emissions models such the VSP modal model used in this thesis rely on second-by-second speed and acceleration values of individual vehicles to determine emissions from transportation facilities. It is very important for the speed and positions of each vehicle in simulation to be updated realistically by the car following model in AIMSUN, such that subsequent emissions estimations are valid. Calibrating the values of the maximum desired speed, maximum desired acceleration and normal deceleration with data from empirical trajectories brought the simulated trajectories closer to what was observed in the field. This was quantified by Vehicle Specific Power distributions from simulated and field data. As such, in addition to other calibrating procedures for a road network in micro-simulation, it calibrating behavioral parameters based on trajectory data can help improve emissions estimates from micro-simulation models such as AIMSUN.

For the particular corridor studies in this thesis, the simulated vehicle activity on the was closer to field activity when the distributions of selected parameters – maximum desired acceleration and normal deceleration – were calibrated with the distribution of 95^{th} percentile values from field-observed trajectories and the maximum desired speed parameter was calibrated with a distribution of maximum values from the trajectories. It was assumed that the maximum speed from each field trajectory is the highest desired speed for the vehicle. For the distributions of the maximum desired acceleration and normal deceleration

however, it was found that the maximum values overestimated instantaneous in the simulation and yielded observations in high VSP bins which did not occur in the field. Conversely, for practical reasons, the 85th percentile parameters were discarded since they present the opportunity for simulation to underestimate the maximum desired accelerations and decelerations of a portion of vehicles from simulation.

Running multiple simulation replications provides an extensive database of vehicle trajectories. In order to draw a fair comparison between the VSP distribution and emissions rates of simulated and field-observed trajectories, trajectories from simulation should be chosen such the simulated vehicles encountered a sequence of events similar to the vehicles in the field. Controlling for the average number of stops as well as the travel time distribution to reflect field-observed trajectories when selecting the simulated sample of trajectories yielded closer estimates of emissions to the field-based estimates at the route level, than when either factor is controlled on its own.

When a sample of 30 trajectories from the default AIMSUN model had the same travel time distribution as field observed trajectories in on the Hillsborough Westbound route, the emissions of NO_x, HC, CO and CO_2 differed by 45%, 15%, 44% and 16% from the respective field based estimates. Under calibrated parameters, a sample of 30 trajectories lowered the errors in estimates to 20%, 6%, 15% and 7% for emissions per unit distance of NO, HC, CO and CO_2. When a sample was selected based on matching average number of stops observed in field trajectories, the emissions estimates were lower across all pollutants by up to 18% for HC and 17% for CO_2. A sample of 30 simulated trajectories which had the same travel time distribution and average number of stops as field trajectories resulted in the emission rates of NO_x, HC, CO and CO_2 having differences of 15%, 3%, 11% and 4% with the field-based estimates respectively. These errors are lower than the other two samples tested and are statistically not significant for all pollutants except NO_x. The methodology of selecting trajectories based on travel time distribution and average number of stops was used on the Hillsborough Eastbound route, calibrating the parameters reduced the error in emissions estimates by 19% for NO_x, 7% for HC, 31% for CO and 7% for CO_2. The differences between field observed HC and CO_2 emissions rates were at 10%.

One of the objectives of this thesis was to demonstrate the application of the VSP modal approach to analyzing emissions at different spatial scales and investigating if the method is able to capture the emissions "hotspots" along a route. Section level analysis showed that the emissions hotspots along the route were not effectively captured calibrated model in the westbound direction but captured reasonably well in the eastbound direction. However, the calibrated model produced estimates that were closer to the empirical emission rates at the section level, than the default model. This indicates that at although calibration may improve the emissions estimates from simulated vehicle activity, at smaller spatial scales the estimates may not be highly accurate.

Although calibrated simulation-based emission rates estimated at the route level were found to be reasonably accurate for samples of trajectories that had the same average number of stops and travel time distribution as field-observed trajectories, there exist differences in the vehicle activity between field and simulation, as shown by differing VSP distributions. An investigation of the second-by-second speed and accelerations from simulated and field data showed systematic differences in the distribution of positive and negative accelerations within 10 mph speed bins in the simulated and field data. In the low speed bins of 0 – 10 mph or 10 – 20 mph, the differences in the distribution of simulated and field-based accelerations are less pronounced than in the speed bin of 20 – 30 mph. In the 20 – 30 mph bin, the simulated accelerations and decelerations are higher. This implies that that vehicles travelling at speeds within the bin are accelerating to higher desired speeds at their maximum desired acceleration rate or rates that are closer to their maximum desired rate. On the other hand, the field vehicles do not accelerate or decelerate at high rates as much while travelling between 20 – 30 mph. Essentially, the calibration of car following model parameters reduces the magnitude of the accelerations or decelerations observed in simulated data, but the trajectories still contain sharp acceleration and decelerations compared to the smoother field trajectories. The more realistic values of acceleration, deceleration and speeds on the arterials lead to better estimates of emissions at the route-level.

The initial motivations for AIMSUN being the micro-simulation software of choice include- (1) AIMSUN has been used to model freeways in the Research Triangle Park in

North Carolina by Swidan (2011), who showed that emissions estimates from simulated activity and the VSP modal approach are within 10% of field-based estimates on freeways; (2) AIMSUN internal behavioral models have fewer parameters than other common micro-simulation software. In the process of investigating the car-following model within AIMSUN, a few limitations of AIMSUN micro-simulation platform have been identified. First, the vehicle attributes in AIMSUN may be set for individual vehicle type. However, these attributes, which include maximum desired speeds and accelerations and normal decelerations are not link-specific and apply to all vehicles in a network of that vehicle type. Therefore, in a road network that includes freeways and arterials, it may be very difficult to determine distributions for these vehicle attributes that are applicable to both road types. This will be especially difficult when using the network for estimating emissions since the work presented in this thesis shows that calibrating internal behavioral model parameters (vehicle attributes) influence emissions estimates from trajectories. Another limitation of AIMSUN is that acceleration or deceleration capabilities of a vehicle may not related to the desired speeds of the vehicles. The user is able to define truncated normal distributions of the maximum desired speeds and accelerations separately. However, when a value for desired speed or acceleration is assigned to a vehicle as its attribute, there is no way to ensure that a vehicle with a high maximum desired speed will also have a high maximum desired acceleration. The psycho-physical model in VISSIM is able to address issues such as these.

6.2 Recommendations and Future Work

The results from this research effort indicate that emission rates at the route level can be estimated reasonably well from a calibrated model of an arterial network in AIMSUN, given that the travel time distribution and average number of stops from simulated trajectories are consistent with the field. One of the key recommendations from this research is that further investigation be done to establish methods for which the trajectory travel times and average number of stops observed in the field are reflected in all simulated trajectories under calibrated parameters. In this thesis, not all simulated trajectories from the calibrated model were suitable for use in the VSP modal emissions analysis approach because on average simulated trajectories had longer travel times and more stops.

To utilize the capabilities of simulation to the fullest and produce a large number of vehicle trajectories for emissions analysis, an arterial road network modeled in AIMSUN should also be calibrated with regard to travel time and average number of stops. Methods to calibrate the model based on demand, capacity and route choice may help bring the average number of stops and trajectory travel times from the simulation closer to field-observed values of these factors. The calibration of maximum desired speeds, accelerations and normal decelerations using field data as proposed in this thesis can further ensure than emissions are predicted accurately from simulated trajectories.

There is a wide variety of traffic congestion management methods that may be applied to arterial corridors that address both transportation demand and supply sides (Rouphail, 2008). From the calibration and emissions estimation procedures presented in this thesis, simulated trajectories from AIMSUN can be used effectively to test the impacts on local air quality of traffic management strategies. This is especially useful because simulation allows the modeling of various infrastructure and traffic conditions that are new to an area or are altogether newly developed and non-yet-implemented solutions to traffic congestion or safety issues on arterial roads.

The work presented here contributes to the growing field of integrating micro-simulation models with emissions models. There remains a wide scope for future work in this, especially in the effective use of micro-simulation models to evaluate different traffic control scenarios and transportation facilities. A few suggestions are outlined below regarding future research:

- The AIMSUN micros-simulator is made up of several sub-models, only one of which is the car following model. The parameters associated with the other sub-models such as the gap acceptance model, may be calibrated to continue the efforts to match simulated vehicle activity with real-world activity. The challenge with this is the need for targeted field data collection. Conversely, in some cases, the model parameters may not be quantifiable from field data. In this case sensitivity analysis may be done to observe the impact of parameters such as reaction time.

- PEMS data is available to the research team at NC State University and to other institutions with access to equipment for on-road emissions measurements. It is necessary to continue enriching the PEMS database. This thesis showed that the average number of stops and trajectory travel time are suitable factors that help determine emissions accurately at the route level from simulated data. Further work needs to be done to calibrate the AIMSUN model such that the distribution of travel time and average number of stops of all simulated vehicle trajectories on a route matches the field data for the same route. To do this, a much larger number of vehicle trajectories on a route will be required from field data in addition to further calibration efforts on the simulation model.
- The VSP modal approach is an effective and simple emissions modeling approach. However, it requires extracting simulated data from AIMSUN. Of the two embedded emissions models in AIMSUN, Swidan (2011) explored the QUARTET emissions model and concluded that it was not possible to fit PEMS based emissions data into the QUARTET model. Further work needs to be done to investigate the second embedded model in AIMSUN – the model by Panis et al. (2006). The PEMS data may be used to calibrate the model by Panis et al. or identify the source of any systematic differences between the model estimates and the PEMS field data. An embedded emissions model in AIMSUN that estimates emissions accurately from the simulated vehicle activity will create a platform to seamlessly integrate traffic simulation and emissions models and provide greater flexibility and ease in assessing various traffic facilities conditions directly from the micro-simulator.

Chapter 7 References

Ahn, K. (1998). *Microscopic fuel consumption and emission modeling.* (M.S., Virginia Polytechnic Institute and State University).

Ahn, K., Kronprasert, N., & Rakha, H. (2009). Energy and environmental assessment of high-speed roundabouts. *Transportation Research Record: Journal of the Transportation Research Board, 2123*(1), 54-65.

Ahn, K., Rakha, H., Trani, A., & Van Aerde, M. (2002). Estimating vehicle fuel consumption and emissions based on instantaneous speed and acceleration levels. *Journal of Transportation Engineering, 128*(2), 182-190.

Anya, A., Rouphail, N., Frey, H. C., & Liu, B. (2013). Method and case study for quantifying local emissions impacts of a 3 transportation improvement project involving road re-alignment and 4 conversion to a multi-lane roundabout. *TRB 2013 Annual Meeting,*

Barth, M., Malcom, C., & Scora, G. (2001). *Integrating a comprehensive modal emissions model into ATMIS transportation modeling frameworks.* (No. UCB-ITS-PRR-2001-19).California Path Program.

Boriboonsomsin, K., & Barth, M. (2008). Impacts of freeway high-occupancy vehicle lane configuration on vehicle emissions. *Transportation Research Part D: Transport and Environment, 13*(2), 112-125.

Brockfeld, E., Kühne, R. D., Skabardonis, A., & Wagner, P. (2003). Toward benchmarking of microscopic traffic flow models. *Transportation Research Record: Journal of the Transportation Research Board, 1852*(1), 124-129.

Chamberlin, R., Swanson, B., Talbot, E., Dumont, J., & Pesci, S. (2011). Analysis of MOVES and CMEM for evaluating the emissions impacts of an intersection control change. *Proceedings of the Transportation Research Board (TRB) 2011 Annual Meeting,*

Cheng, J., & Druzdzel, M. J. (2000). Latin hypercube sampling in bayesian network. *Proceedings of the 13th International Florida Artificial Intelligence Research Symposium Conference,*

Cheu, R., Tan, Y., & Lee, D. (2003). Comparison of PARAMICS and GETRAM/AIMSUN microscopic traffic simulation tools. Paper presented at the *TRB 2004 Annual Meeting,*

Chu, L., Liu, H., Oh, J., & Recker, W. (2003). A calibration procedure for microscopic traffic simulation. *Proceedings of the 2003 Intelligent Transportation Systems Conference, 2*, 1574.

Clean Air Technologies International. (2003). *OEM-2100 montana system operational manual*. Buffalo, NY:

Coelho, M., Farias, T., & Rouphail, N. (2006). Effect of roundabout operation on pollutant emissions. *Transportation Research Part D: Transport and Environment,* (11), 333-343.

Dowling, R., Skabardonis, A., Halkias, J., McHale, G., & Zammit, G. (2004). Guidelines for calibration of microsimulation models. *Transportation Research Record: Journal of the Transportation Research Board,* (1876), 1.

Duran, A., & Earleywine, M. (2012). GPS data filtration method for drive cycle analysis applications. Paper presented at the *Proceedings of SAE 1012 World Congress & Exhibition,* doi:10.4271/2012-01-0743.

Fang, C. (2010). Traffic simulation study of lead vehicle behavior. *Integrated Transportation Systems, ICCTP 2010,* 2001.

Franco, V., Kousoulidou, M., Muntean, M., Ntziachristos, L., Hausberger, S., & Dilara, P. (2013). Road vehicle emission factors development: A review. *Atmospheric Environment, 70*, 84-97.

Frey, H. C., Rouphail, N. M., & Zhai, H. (2006). Speed-and facility-specific emission estimates for on-road light-duty vehicles on the basis of real-world speed profiles. *Transportation Research Record: Journal of the Transportation Research Board, 1987*(1), 128-137.

Gardes, Y., May, A. D., Dahlgren, J., & Skabardonis, A. (2002). Freeway calibration and application of the paramics model. Paper presented at the *81st Annual Meeting of the Transportation Research Board, Washington, DC,*

Gipps, P. G. (1986). A model for the structure of lane-changing decisions. *Transportation Research Part B: Methodological, 20*(5), 403.

Hollander, Y., & Liu, R. (2008). The principles of calibrating traffic microsimulation models. *Transportation, 35*, 347. doi:10.1007/s11116-007-9156-2

Jiménez-Palacios, J. L. (1999). *Understanding and quantifyinf motor vehicle emissions with vehicle specific power and TILDAS remote sensing.* (Ph.D, Massachusetts Institute of Technology (MIT)). Retrieved from http://hdl.handle.net/1721.1/44505

Jost, P., Hassel, D., Weber, F. J., & Sonnborn, K. S. (1992). *Emission and fuel consumption modelling based on continuous measurements.* (No. DRIVE project V 1053).

Koupal, J., Landman, L., Nam, E. K., Warila, J., & Scarbro, C. (2005). *MOVES2004 energy and emissions inputs draft report.* (No. EPA420-P-05-003).US EPA.

Kun, C., & Lei, Y. (2007). Microscopic traffic-emission simulation and case study for evaluation of traffic control strategies. *Journal of Transportation Systems Engineering and Information Technology, 7*(1), 93.

Li, M., Boriboonsomsin, K., Wu, G., Zhang, W., & Barth, M. (2009). Traffic energy and emission reductions at signalized intersections: A study of the benefits of advanced driver information. *International Journal of ITS Research, 7*(1), 49.

Ma, T., & Abdulhai, B. (2002). Genetic algorithm-based optimization approach and generic tool for calibrating traffic microsimulation parameters. *Transportation Research Record: Journal of the Transportation Research Board,* (1800), 6.

May, A. D. (1990). *Traffic flow fundamentals*. University of Michigan: Prentice Hall.

Moore, D. S., & McCabe, G. P. (2006). *Introduction to the practice of statistics* (4th ed.) W.H. Freeman & Company.

Nam, E. K., Gierczak, C. A., & Butler, J. W. (2003). A comparison of real-world and modelled emissions under conditions of variable driver aggressiveness. Paper presented at the *82nd Annual Meeting of the Transportation Research Board, Washington, DC,*

National Institute for Standards & Technology. (2012). *E-handbook of statistical methods* SEMATECH. doi:http://www.itl.nist.gov/div898/handbook/

National Research Council. (2000). *Modeling mobile source emissions*. Washington, D.C.: National Academy Press.

North Carolina Department of Transportation. (2012). *Traffic volume maps* doi:http://www.ncdot.gov/travel/statemapping/trafficvolumemaps/

North Carolina State University. (2002). *Methodology for developing modal emission rates for EPA's multi-scale motor vehicle and equipment emission system.* (No. EPA 420-R-02-027).US EPA.

Olstam, J. J., & Tapani, A. (2004). *Comparison of car-following models.* (No. VTI meddelande 960A). Linköping, Sweden: Swedish National Road Administration.

Panis, L., Broekx, S., & Liu, R. (2006). Modeling instantaneous traffic emissions and the influence of traffic speed limits. *Science of the Total Environment, 371*(1-3), 270.

Park, B., & Qi, H. (2005). Development and evaluation of a procedure for the calibration of simulation models. *Transportation Research Record: Journal of the Transportation Research Board,* (1934), 208.

Park, B., & Schneeberger, J. D. (2003). Microscopic simulation model calibration and validation case study of VISSIM simulation model for a coordinated actuated signal system. *Transportation Research Record: Journal of the Transportation Research Board,* (1856), 185. doi:http://dx.doi.org/10.3141/1856-20

Park, B., Won, J., & Yun, I. (2006). Application of microscopic simulation model calibration and validation procedure: Case study of coordinated actuated signal system. *Transportation Research Record: Journal of the Transportation Research Board, 1978*(1), 113-122.

Park, J. Y., Noland, R. B., & Polak, J. W. (2001). Microscopic model of air pollutant concentrations: Comparison of simulated results with measured and macroscopic estimates. *Transportation Research Record: Journal of the Transportation Research Board,* (1750), 64.

Pronello, C., & André, M. (2007). Pollutant emissions estimation in road transport models. *Report INRETS-LTE,*

Punzo, V., & Simonelli, F. (2005). Analysis and comparison of microscopic traffic flow models with real traffic microscopic data. *Transportation Research Record: Journal of the Transportation Research Board, 1934*(1), 53-63.

Qu, T., Rilett, L., & Zietsman, J. (2003). Estimating the impact of freeway speed limits on automobile emissions. Paper presented at the *82nd Annual Meeting of Transportation Research Board, Washington DC,*

Rakha, H., & Ding, Y. (2002). Impact of stops on vehicle fuel consumption and emissions. *Journal of Transportation Engineering, 129*(1), 23-32.

Rouphail, N. (2008). Traffic congestion management. In M. Kutz (Ed.), *Environmentally conscious transporation* (pp. 97). Hoboken, N.J.: John Wiley & Sons.

Sandhu, G. (2010). *Methods for quality assurance of portable emissions measurement system data and methods for field comparison of alternative fuels.* (M.S., North Carolina State University).

Servin, O., Boriboonsomsin, K., & Barth, M. (2006). An energy and emissions impact evaluation of intelligent speed adaptation. Paper presented at the *Intelligent Transportation Systems Conference, 2006. ITSC'06. IEEE,* 1257-1262.

Smit, R., Ntziachristos, L., & Boulter, P. (2010). Validation of road vehicle and traffic emission models–A review and meta-analysis. *Atmospheric Environment, 44*(25), 2943-2953.

Song, G., Lei, Y., & Zhang, Y. (2012). Applicability of traffic microsimulation models in vehicle emissions estimates: Case study of VISSIM. *Transportation Research Record: Journal of the Transportation Research Board,* (2270), 132.

Song, G., Yu, L., & Xu, L. (2013). Comparative analysis of car-following models for emission estimation. *Proceedings of the 92nd Annual Meeting of the Transportation Research Board,*

Song, Y., Yao, E., Zuo, T., & Lang, Z. (2013). Emissions and fuel consumption modeling for evaluating environmental effectiveness of ITS strategies. *Discrete Dynamics in Nature and Society, 2013*

Stathopoulos, F. G., & Noland, R. B. (2003). Induced travel and emissions from traffic flow improvement projects. *Transportation Research Record: Journal of the Transportation Research Board, 1842*(1), 57-63.

Stevanovic, A., Stevanovic, J., Zhang, K., & Batterman, S. (2009). Optimizing traffic control to reduce fuel consumption and vehicular emissions: Integrated approach with VISSIM, CMEM, and VISGAOST. *Transportation Research Record: Journal of the Transportation Research Board,* (2128), 105.

Swidan, H. (2011). *Integrating AIMSUN micro simulation model with portable emissions measurement system (PEMS): Calibration and validation case study.* (Master of Science, North Carolina State University).

Swidan, H. (Expected 2011). *Integrating AIMSUN micro simulation model with portable emissions measurement system (PEMS): Calibration and validation case study.* (Unpublished Masters of Science). North Carolina State University,

Toledo, T., Ben-Akiva, M., Darda, D., Jha, M., & Koutsopoulos, H. (2004). Calibration of microscopic traffic simulation models with aggregate data. *Transportation Research Record: Journal of the Transportation Research Board,* (1876), 10.

Transportation Research Board. (2010). *2010 highway capacity manual*. Washington, D.C.: Transportation Research Board.

TSS. (2012). *AIMSUN 7 dynamic simulators user's manual*

US EPA. (1994). Automobile emissions: An overview.*Fact Sheet OMS-5*

US EPA. (2003). *Ozone*. Washington, D.C.: Office of Air and Radiation.

US EPA. (2012). Six common air pollutants. Retrieved May 15, 2013, from http://www.epa.gov/airquality/urbanair/

Wang, J., Yu, L., & Qiao, F. (2013). Micro traffic simulation approach to the evaluation of vehicle emissions on one-way vs. two-way streets: A case study in houston downtown. Paper presented at the *Proceedings of the Transportation Research Board (TRB) 2013 Annual Meeting*,

Wee, S. H., Cheu, R., Lee, D., & Chan, W. T. (2002). Using GPS data to calibrate arterial speed profile in PARAMICS. *Applications of Advanced Technology in Transportation*, , 64.

Yazdani, B., & Frey, H. C. (2012). Quantification of roaf grade based on GPS receiver with barometric altimeter. *Proceedings Annual Meeting of the Air & Waste Management Association*,

Yue, H. (2008). *Mesoscopic fuel consumption and emission modeling.* (Ph.D., Virginia Polytechnic Institute and State University).

Zhai, H. (2007). *Regional on-road mobile source emissions characterization for conventional and Alternative vehicle technologies.* (Ph.D, North Carolina State University).

Zhang, J., Hounsell, N., & Shrestha, B. (2012). Calibrating of bus parameters in microsimulatio traffic modeling. *Transportation Planning and Technology*, *35*(1), 107.

Zhang, Y., Chen, X., Xiao, Z., Song, G., Yanzhao, H., & Lei, Y. (2009). Assessing effect of traffic signal control strategies on vehicle emissions. *Journal of Transportation Systems Engineering and Information Technology*, *9*(1), 150.

Zhizhou, W., Jian, S., & Xiaoguang, Y. (2005). Calibration of VISSIM for shanghai expressway using genetic algorithm. Paper presented at the *Proceedings of the 37th Conference on Winter Simulation*, 2645-2648.

APPENDICES

Appendix A Traffic Demand in the afternoon peak and off peak periods

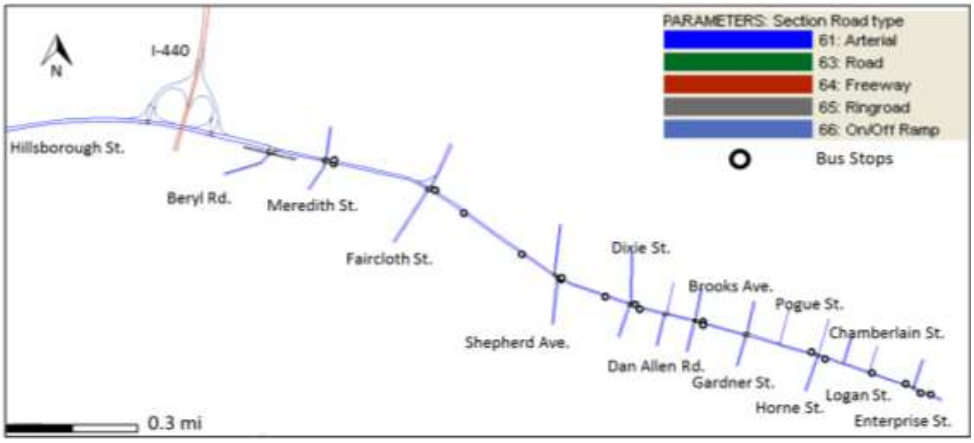

Figure A1 Schematic of Hillsborough Street Corridor modeled in AIMSUN

Turning movement counts were obtained from the City of Raleigh. These counts were performed on different dates and as such, the counts were balanced. The volume of traffic on the corridor was balanced by holding the counts at the intersections of the I440 E On-ramp, Gardner St. and Enterprise St. as references. The reference intersections were selected based on their location on the arterial and on the date on which the data collection at the intersections was completed.

Table A1 Input Flows at Each Intersection during Afternoon Peak Period (5pm – 6 pm)

Intersection		Approach Flow rate (vph)			
		North	South	East	West
1	I-440 W Off-ramp	493			615
2	I 440 E On-ramp	316			
3	Beryl Rd.		238		
4	Meredith Rd.	173	66		
5	Faircloth St.	331	374		
6	Shepherd Rd.	23	10		
7	Dixie Rd.	188	146		
8	Dan Allen Dr.		218		
9	Brooks Ave.	174	16		
10	Gardner St.	82	15		
11	Pogue St.				
12	Horne St.	79	101		
13	Chamberlain St.	2			
13	Logan St.				
13	Enterprise St.	95		652	

Figure A2 Turning movement counts at each intersection during afternoon peak period

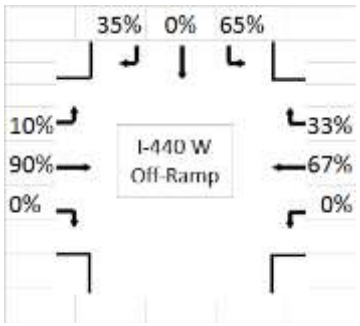
35% 0% 65%
10%
90%
0%
I-440 W Off-Ramp
33%
67%
0%

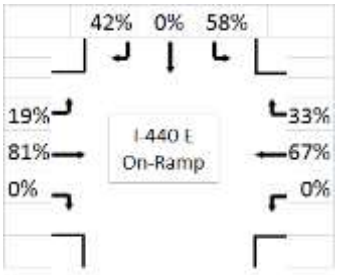
42% 0% 58%
19%
81%
0%
I-440 E On-Ramp
33%
67%
0%

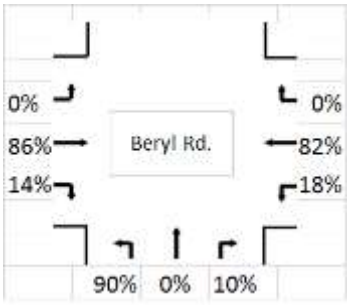
0%
86%
14%
Beryl Rd.
0%
82%
18%
90% 0% 10%

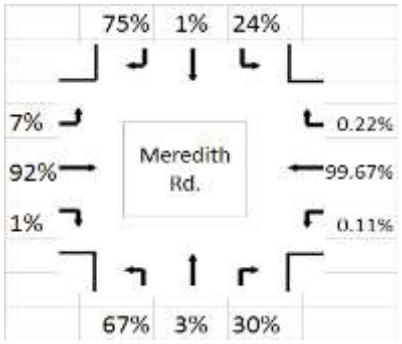
75% 1% 24%
7%
92%
1%
Meredith Rd.
0.22%
99.67%
0.11%
67% 3% 30%

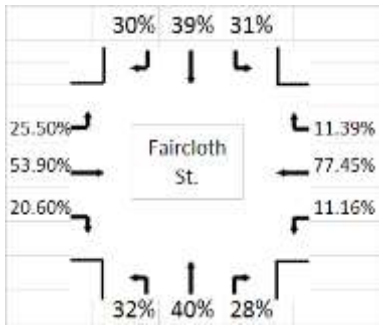
30% 39% 31%
25.50%
53.90%
20.60%
Faircloth St.
11.39%
77.45%
11.16%
32% 40% 28%

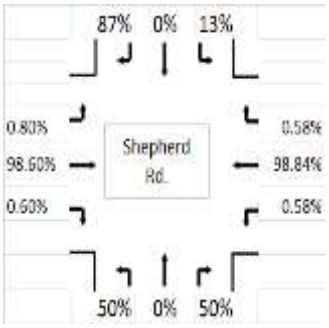
87% 0% 13%
0.80%
98.60%
0.60%
Shepherd Rd.
0.58%
98.84%
0.58%
50% 0% 50%

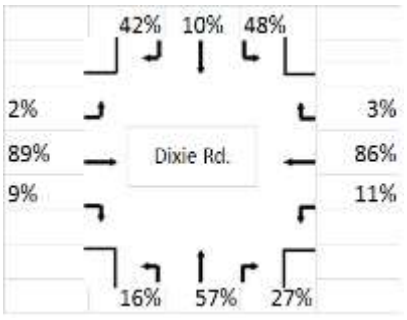
42% 10% 48%
2%
89%
9%
Dixie Rd.
3%
86%
11%
16% 57% 27%

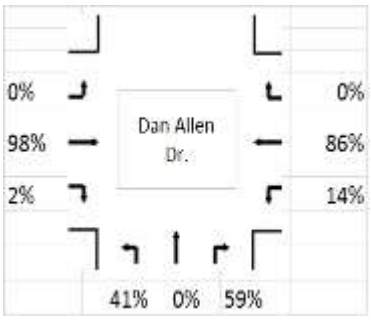
0%
98%
2%
Dan Allen Dr.
0%
86%
14%
41% 0% 59%

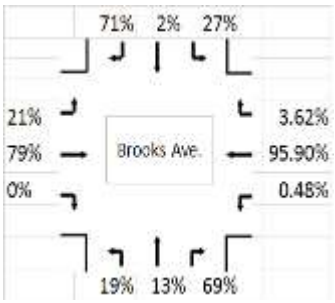
71% 2% 27%
21%
79%
0%
Brooks Ave.
3.62%
95.90%
0.48%
19% 13% 69%

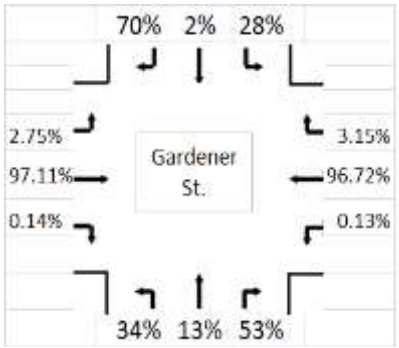
70% 2% 28%
2.75%
97.11%
0.14%
Gardener St.
3.15%
96.72%
0.13%
34% 13% 53%

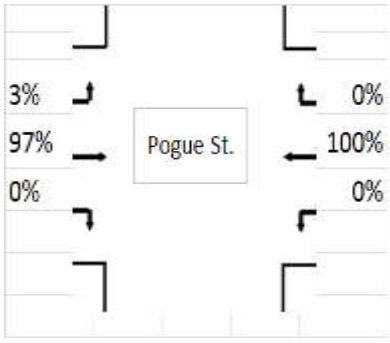
3%
97%
0%
Pogue St.
0%
100%
0%

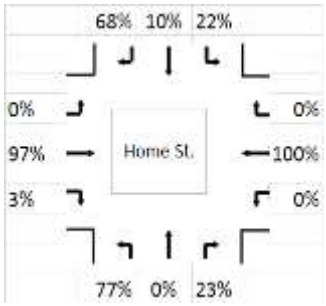
68% 10% 22%
0%
97%
3%
Home St.
0%
100%
0%
77% 0% 23%

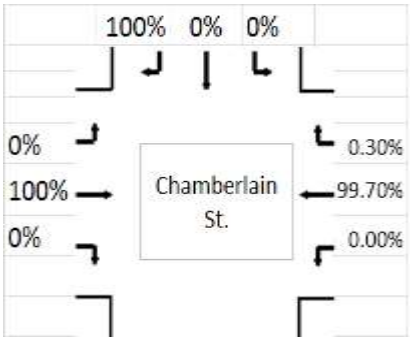
100%
0%
0%
0%
100%
0%
Chamberlain St.
0.30%
99.70%
0.00%

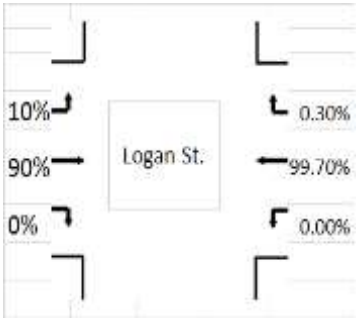
10%
90%
0%
Logan St.
0.30%
99.70%
0.00%

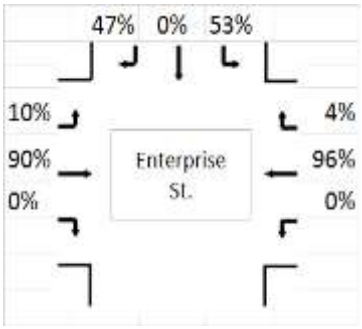
47%
0%
53%
10%
90%
0%
Enterprise St.
4%
96%
0%

Table A2 Input Flows at Each Intersection during Afternoon Off-Peak Period (1pm – 3.30 pm)

Intersection		Approach Flow rate (vph)			
		North	South	East	West
1	I-440 W Off-ramp	380			455
2	I 440 E On-ramp	246			
3	Beryl Rd.		195		
4	Meredith Rd.	140	58		
5	Faircloth St.	258	277		
6	Shepherd Rd.	19	8		
7	Dixie Rd.	151	132		
8	Dan Allen Dr.		169		
9	Brooks Ave.	141	13		
10	Gardner St.	66	12		
11	Pogue St.				
12	Horne St.	65	82		
13	Chamberlain St.	2			
13	Logan St.				
13	Enterprise St.	74		541	

Figure A3 Turning movement counts at each intersection during afternoon off-peak period

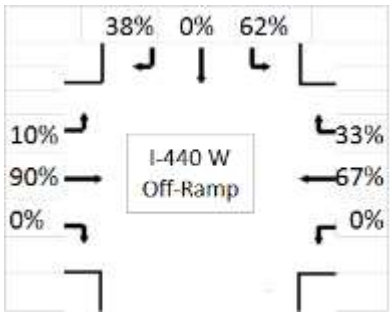
38% 0% 62%
10%
90%
0%
I-440 W
Off-Ramp
33%
67%
0%

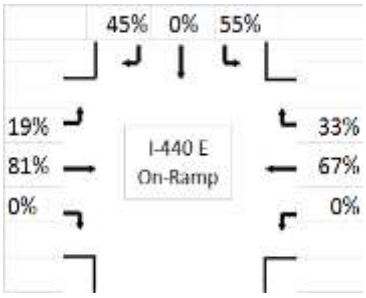
45% 0% 55%
19%
81%
0%
I-440 E
On-Ramp
33%
67%
0%

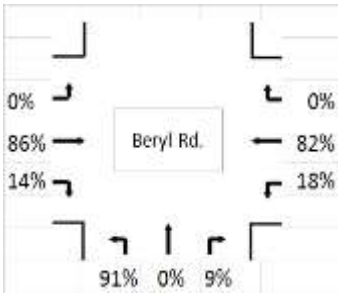
0%
86%
14%
Beryl Rd.
0%
82%
18%
91% 0% 9%

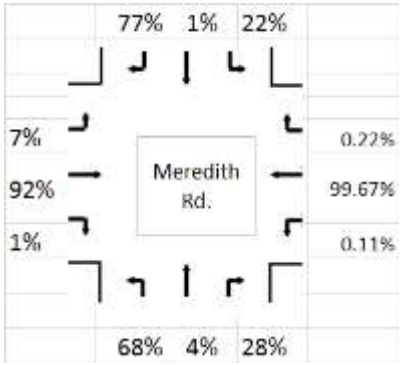
77% 1% 22%
7%
92%
1%
Meredith
Rd.
0.22%
99.67%
0.11%
68% 4% 28%

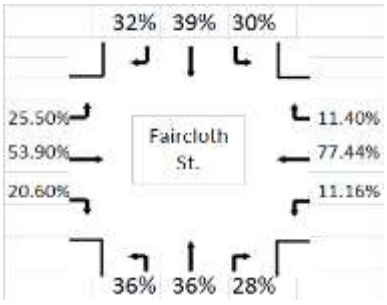
32% 39% 30%
25.50%
53.90%
20.60%
Faircloth
St.
11.40%
77.44%
11.16%
36% 36% 28%

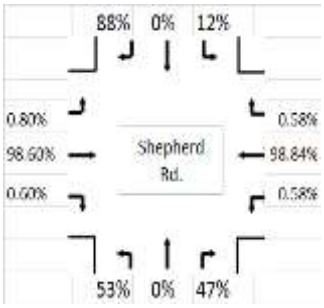
88% 0% 12%
0.80%
98.60%
0.60%
Shepherd
Rd.
0.58%
98.84%
0.58%
53% 0% 47%

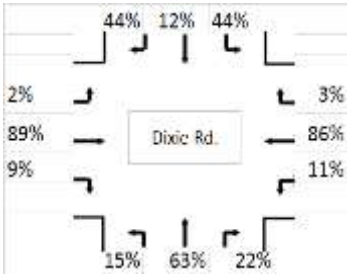
44% 12% 44%
2%
89%
9%
Dixie Rd.
3%
86%
11%
15% 63% 22%

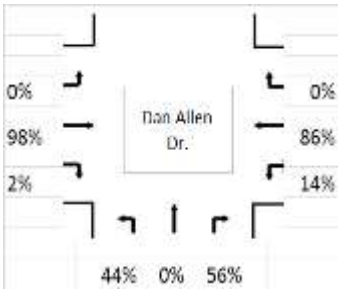
0%
98%
2%
Dan Allen
Dr.
0%
86%
14%
44% 0% 56%

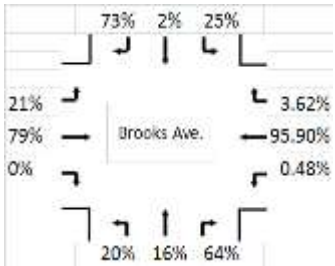
73% 2% 25%
21%
79%
0%
Brooks Ave.
3.62%
95.90%
0.48%
20% 16% 64%

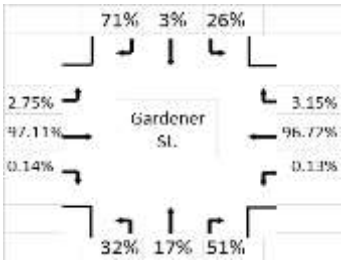
71% 3% 26%
2.75%
97.11%
0.14%
Gardener
St.
3.15%
96.72%
0.13%
32% 17% 51%

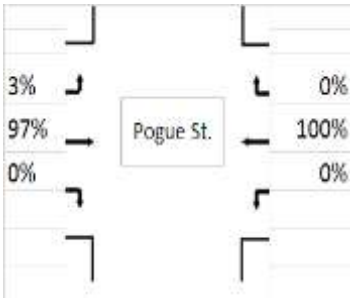
3%
97%
0%
Pogue St.
0%
100%
0%

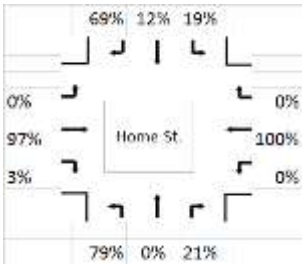
69% 12% 19%
0%
97%
3%
Home St.
0%
100%
0%
79% 0% 21%

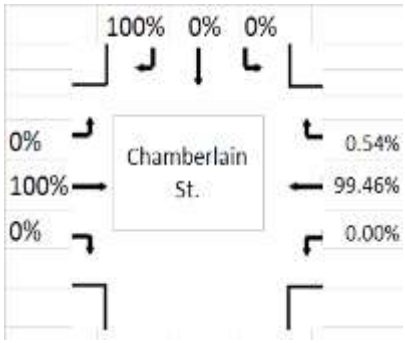
100% 0% 0%
0%
100%
0%
Chamberlain St.
0.54%
99.46%
0.00%

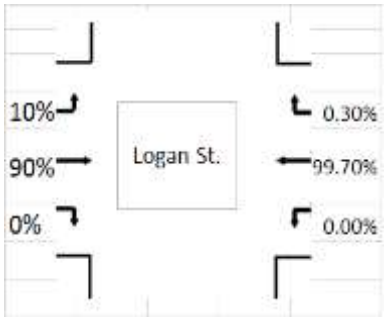
10%
90%
0%
Logan St.
0.30%
99.70%
0.00%

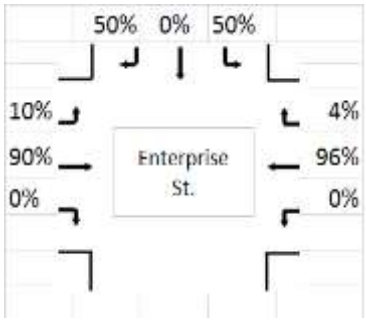
50% 0% 50%
10%
90%
0%
Enterprise St.
4%
96%
0%

Appendix B Field-tested Vehicles

Table B1 Details of all vehicles tested with PEMS

	Year	Make	Model	Displacement (L)	Mileage (mi)	Gross Weight (lbs)	Manual (M) or Automatic (A)
1	1997	Toyota	Camry	2.2	228,000	3,107	M
2	1997	Honda	Accord	2.2	228,780	3,705	A
3	1998	Buick	Century	3.1	69,736	3,335	A
4	1998	Chrysler	Sebring Lxi	2.5	132,507	3,204	A
5	1998	Honda	Accord	2.3	143,298	2,954	A
6	1998	Ford	Expedition	5.4	160,732	5,801	A
7	1998	Chevrolet	S10	4.3	141,957	3,238	A
8	1998	Volvo	S70T5	2.3	147,881	3,050	A
9	1999	Honda	Accord LX	2.3	83,918	3,990	A
10	2000	Honda	Civic	1.6	150,813	2,421	M
11	2000	Mitsubishi	Galant	2.4	139,146	4,205	A
12	2000	Nissan	Altima	2.4	161,560	3,990	A
13	2000	Chevrolet	Blazer	4.3	98,114	4,000	A
14	2001	Toyota	Camry	2.2	93,092	3,000	A
15	2001	Buick	LeSabre	3.8	108,868	3,766	A
16	2001	Honda	AccordV6	3	110,000	3,458	A
17	2002	Ford	Ranger	2.3	153,119	4,000	M
18	2002	Lexus	RX300	3	134,067	4,950	A
19	2002	Chevrolet	Silverado	4.8	153,021	5,000	A
20	2002	Jeep	Wrangler	4	89,705	4,450	A
21	2003	Chrysler	Pt Cruiser	2.4	84,493	4,087	A
22	2003	Chevrolet	Impala	3.4	129,969	3,308	A
23	2003	Toyota	Camry	2.4	163,266	4,244	A
24	2004	Honda	Civic	1.7	71,000	2,544	A
25	2004	Honda	Civic	1.7	91,967	1,720	A
26	2004	Toyota	Tacoma	3.4	89,590	4,250	A
27	2005	Mazda	3S	2.3	62,428	3,880	A
28	2005	Saab	9-2x	2.5	81,173	3,086	A
29	2005	Honda	Element	2.4	95,429	3,570	A
30	2005	Toyota	Camry SE	2.4	105,456	4,244	A
31	2005	Buick	LaCrosse	3.8	123,031	3,495	A
32	2005	Toyota	Tacoma	4	131,344	5,350	A

Table B1 CONTINUED Details of all vehicles tested with PEMS

	Year	Make	Model	Displacement (L)	Mileage (mi)	Gross Weight (lbs)	Manual (M) or Automatic (A)
33	2006	Scion	tC	2.4	17,400	2,970	A
34	2006	Mitsubishi	Eclipse	2.4	95,058	4,608	A
35	2006	VW	Jetta	2	114,930	3,300	M
36	2006	Honda	Civic Hybrid	1.4	84,944	2,875	A
37	2006	Chevrolet	Silverado	5.3	138,109	6,700	A
38	2006	Toyota	Tundra	4.7	84,234	6,600	A
39	2007	Honda	AccordEx	2.4	50,784	3,124	A
40	2007	Honda	Accord	2.4	66,122	3,124	A
41	2007	GMC	Sierra	5.3	122,588	6,400	A
42	2007	Jeep	Wrangler	3.8	30,647	4,640	M
43	2008	Toyota	Sienna	3.5	53,113	5,690	A
44	2008	Honda	Civic	1.8	36,800	2,640	A
45	2008	Honda	Fit	1.5	53,927	2,500	A
46	2010	Ford	F-150	4.6	282,206	6,450	A
47	2010	Toyota	Highlander	3.3	27,455	5,500	A
48	2011	Toyota	Camry	2.5	8,827	3,307	A
49	2011	Chevrolet	HHR	2.2	21,045	4,240	A
50	2012	Nissan	Versa	1.8	615	2,722	A
51	2012	Fiat	500	1.4	129,874	2,363	A
52	2012	Toyota	Camry	2.5	18,882	4,630	A
53	2013	GMC	Yukun	5.3	4,108	7,400	A

Appendix C Cumulative Probabilities of Field Data and Calibration Parameters

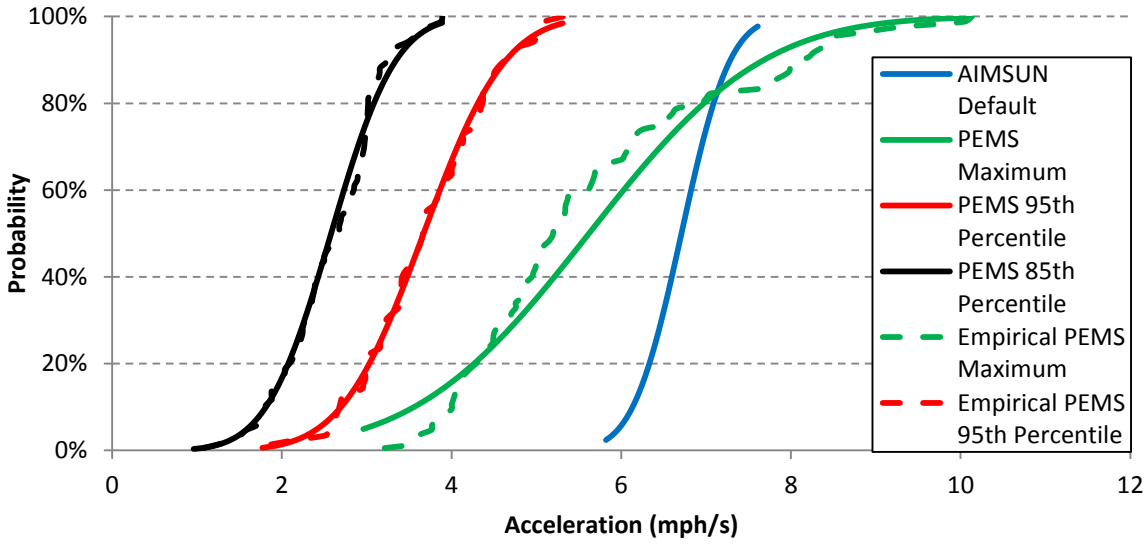

Figure C1 Cumulative probability distribution of maximum, 95th and 85th percentile accelerations from field observations and corresponding truncated normal distributions in AIMSUN

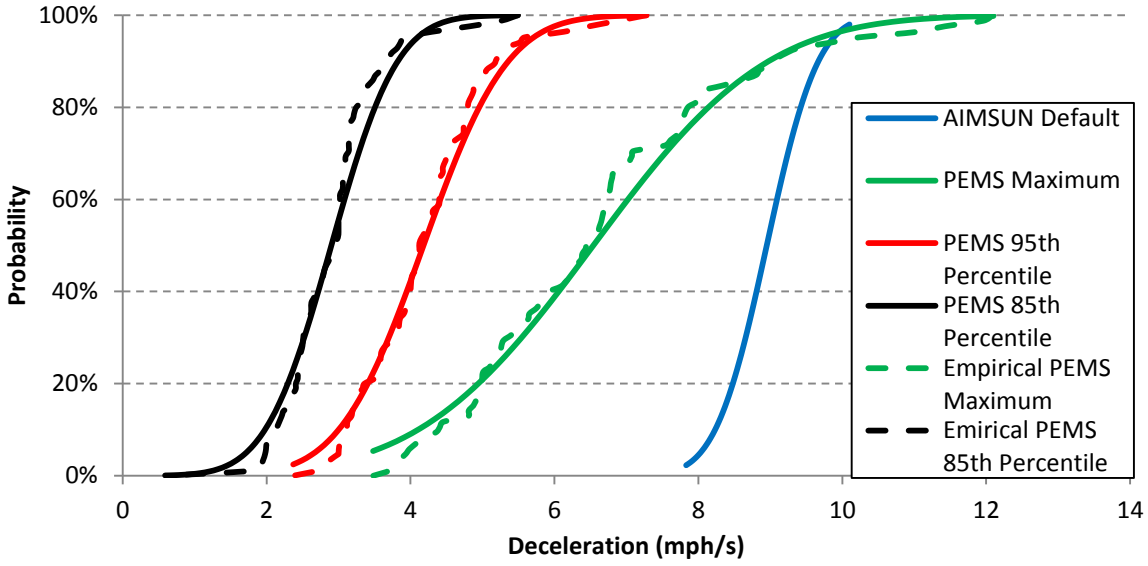

Figure C2 Cumulative probability distribution of maximum, 95th and 85th percentile decelerations from field observations and corresponding truncated normal distribution in AIMSUN

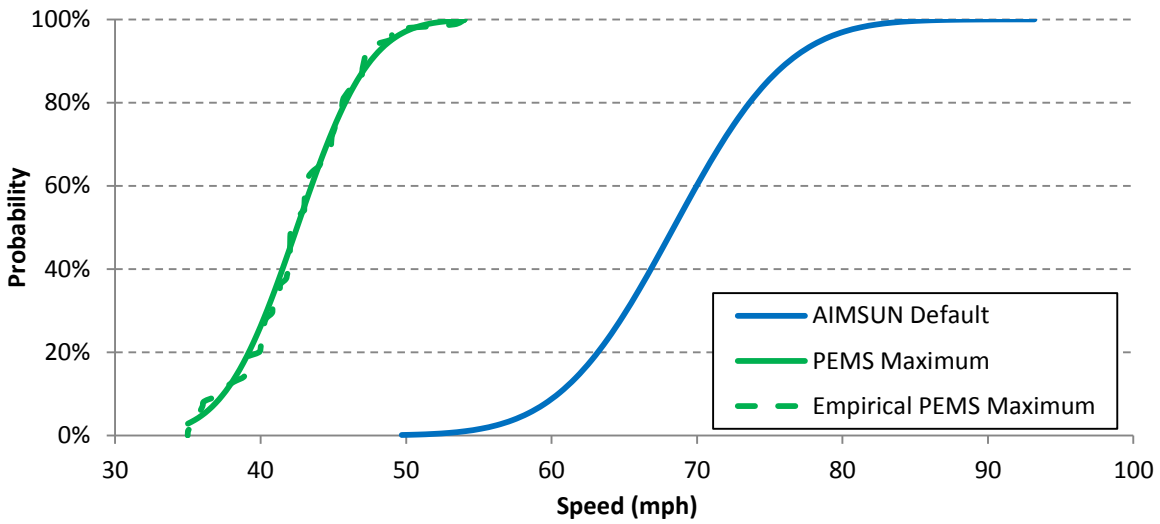

Figure C3 Cumulative probability distribution of maximum, 95th and 85th percentile speeds from field observations and corresponding truncated normal distribution in AIMSUN

Appendix D API Code for extracting second-by-second vehicle activity data

```
from AAPI import *
fileDir="c:/AIMSUN Output/"
def AAPILoad():

        AKIPrintString( "AAPILoad" )
        return 0

def AAPIInit():
        global f

        AKIPrintString( "Check: API is running" )
        rep=ANGConnGetReplicationId()
        if rep > 0 :
                filePath= '%sOutput_Rep_%d.txt' %(fileDir,rep)
                f=open(filePath,'w')
                if f != None:
                        f.write('Replication %d\n\n' %(rep))
        return 0

def AAPIManage(time, timeSta, timTrans, SimStep):
        global f
        nba = AKIInfNetNbSectionsANG()
        for i in range(nba):
                id = AKIInfNetGetSectionANGId(i)
                nb = AKIVehStateGetNbVehiclesSection(id,True)
                for j in range(nb):
                        infVeh = AKIVehStateGetVehicleInfSection(id,j)
                        string = str(time)+"\tVehicle\t" + str(infVeh.idVeh)
                        string=string + "\tSection\t" + str(infVeh.idSection)
                        string=string + "\tLane\t" + str(infVeh.numberLane)
                        string= string + "\tCurrentPos\t" + str(infVeh.CurrentPos)
                        string=string + "\tCurrentSpeed\t" + str(infVeh.CurrentSpeed)
                        string = string + "\n"
                        f.write(string)
                        f.flush()

        nbj = AKIInfNetNbJunctions()
        for i in range(nbj):
          id = AKIInfNetGetJunctionId(i)
          nb = AKIVehStateGetNbVehiclesJunction(id)
          for j in range(nb):
                infVeh = AKIVehStateGetVehicleInfJunction(id,j)
                string = str(time)+"\tVehicle\t" + str(infVeh.idVeh)
```

```
                        string=string + "\tNode\t" + str(infVeh.idJunction)
                        string=string + "\tFrom\t" + str(infVeh.idSectionFrom)
                        string= string + "\tCurrentPos\t" + str(infVeh.CurrentPos)
                        string=string + "\tCurrentSpeed\t" + str(infVeh.CurrentSpeed)
                        string = string + "\n"
                        f.write(string)
                        f.flush()

        return 0

def AAPIPostManage(time, timeSta, timeTrans, acycle):
        return 0

def AAPIFinish():
    global f
        AKIPrintString( "AAPIFinish" )
        f.close()
        return 0

def AAPIUnLoad():

        AKIPrintString( "AAPIUnLoad" )

        return 0

def AAPIPreRouteChoiceCalculation(time, timeSta):
        AKIPrintString( "AAPIPreRouteChoiceCalculation" )
        return 0
```

Appendix E MS Excel Code to identify total number of stops from second-by-second trajectory data

A sample of the second-by-second trajectory data extracted from AIMSUN micro-simulation software is presented in **Figure 1** followed by the macro code to extract the number of stops from each trajectory. The macro records the number of stops and the corresponding vehicle identification number in Sheet1.

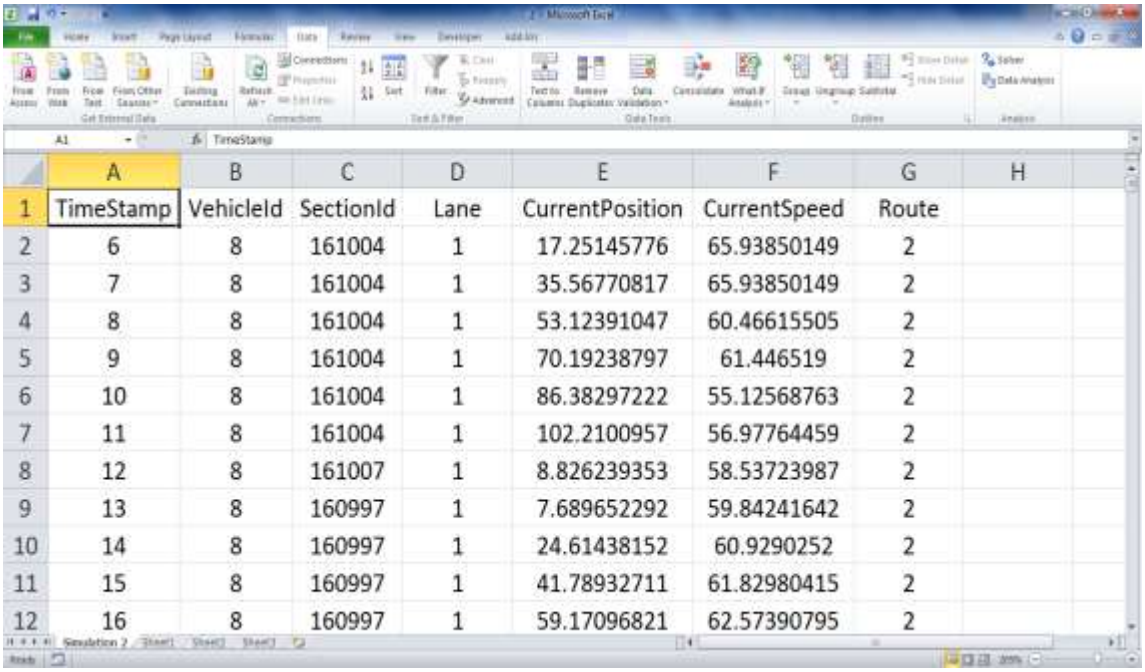

	A	B	C	D	E	F	G	H
1	TimeStamp	VehicleId	SectionId	Lane	CurrentPosition	CurrentSpeed	Route	
2	6	8	161004	1	17.25145776	65.93850149	2	
3	7	8	161004	1	35.56770817	65.93850149	2	
4	8	8	161004	1	53.12391047	60.46615505	2	
5	9	8	161004	1	70.19238797	61.446519	2	
6	10	8	161004	1	86.38297222	55.12568763	2	
7	11	8	161004	1	102.2100957	56.97764459	2	
8	12	8	161007	1	8.826239353	58.53723987	2	
9	13	8	160997	1	7.689652292	59.84241642	2	
10	14	8	160997	1	24.61438152	60.9290252	2	
11	15	8	160997	1	41.78932711	61.82980415	2	
12	16	8	160997	1	59.17096821	62.57390795	2	

FIGURE E.1 Sample of second-by-second trajectory data from Simulation Replication # 2

*NOTE that the CurrentSpeed is in km/h

MACRO CODE FOR IDENTIFYING NUMBER OF STOPS FROM SECOND-BY-SECOND TRAJECTORY DATA:

```
Sub Stops()

Dim VID(380000) As Integer
Dim VS(380000) As Double
Dim Stops(5000) As Integer
Dim countt As Integer
countt = 1

For i = 1 To 5000
Stops(i) = 0
Next

For i = 3 To 450000
   VID(i) = Sheets("Simulation 2").Cells(i, 2)
   VS(i) = Sheets("Simulation 2").Cells(i, 6)
Next

For i = 3 To 450000
If countt = 1 And VID(i) = VID(i - 1) And VS(i) < 8 And VS(i - 1) >= 8 Then
   Stops(VID(i)) = Stops(VID(i)) + 1
   countt = 0
End If

If VS(i) > 25 Then countt = 1
Next
For i = 1 To 5000

Sheets("Sheet1").Cells(3 + i, 2) = i
Sheets("Sheet1").Cells(3 + i, 3) = Stops(i)
Next
End Sub
```

Key: VID = VehicleId; VS = CurrentSpeed;

Appendix F Automated Sampling Algorithm

Automated sampling of *n* number of trajectories from a dataset of simulated trajectories is based on matching the distribution of the number of stops in the simulated sample with the field sample. The first and second moments of a sample quantify the average values and shapes of the sample distributions. The minimization of differences between these moments of the simulated and field samples is presented in the following algorithm.

$$\boldsymbol{min} \quad \boldsymbol{y} = \left|\boldsymbol{\sigma_n} - \boldsymbol{\sigma_f}\right|$$

$$subject\ to\ the\ constraints:$$

$$\mu_n = \mu_f$$

$$\sum I_i = n$$

$$i = 1, 2, \ldots, k$$

Where:

$$I_i = \begin{cases} 0\ ; & Do\ not\ select\ trajectory \\ 1; & Seclect\ trajectory \end{cases}$$

$x_i = number\ of\ stops\ of\ trajectory\ i$

$n = desired\ sample\ size\ to\ be\ drawn\ from\ all\ simulated\ trajectories\ (i = 1, 2, \ldots, k)$

$\mu_f = average\ number\ of\ stops\ across\ field\ trajectories$

$\sigma_f = standard\ deviation\ of\ stops\ across\ field\ trajectories$

$$\mu_n = \left(\frac{1}{n}\right)\sum I_i \cdot x_i \quad ; average\ number\ of\ stops\ of\ selected\ trajectories$$

$$\sigma_n = \sqrt{\left(\frac{1}{n-1}\right)\sum I_i \cdot (x_i - \mu_n)^2}$$

The standard Excel Solver Add In can be used to solve the minimization problem. However, it has a limit of 200 decision variables. Several other tolls such as SAS or R are available to solve the algorithm when the number of decision variables exceeds 200.